

COMPRESSIVE SPECTRUM SENSING FOR COGNITIVE RADIO  
NETWORKS

By

UKASH NAKARMI

Bachelor of Engineering in Electronics and  
Communication  
Tribhuvan University  
Kathmandu, Bagmati, Nepal  
2008

Submitted to the Faculty of the  
Graduate College of  
Oklahoma State University  
in partial fulfillment of  
the requirements for  
the Degree of  
MASTER OF SCIENCE  
Dec, 2011

COMPRESSIVE SPECTRUM SENSING FOR COGNITIVE RADIO  
NETWORKS

Thesis Approved:

Dr. Nazanin Rahnavard

---

Thesis Adviser

Dr. Qi Cheng

---

Dr. Johnson P Thomas

Dr. Sheryl A. Tucker

---

Dean of the Graduate College

## TABLE OF CONTENTS

Chapter	Page
<b>1 INTRODUCTION</b>	<b>1</b>
1.1 Motivation: Spectrum Demand and Scarcity . . . . .	1
1.2 Cognitive Radio and Spectrum Sensing . . . . .	2
1.2.1 Cognitive Radio Challenges . . . . .	4
1.3 Outline of Thesis . . . . .	5
<b>2 BACKGROUND AND LITERATURE REVIEW</b>	<b>7</b>
2.1 Cognitive Radio . . . . .	7
2.2 Conventional Spectrum Sensing Techniques . . . . .	9
2.2.1 Matched Filter . . . . .	10
2.2.2 Cyclostationary Feature Detection . . . . .	11
2.2.3 Pilot and Radio Detection . . . . .	12
2.2.4 Waveform Based Sensing . . . . .	13
2.2.5 Energy Detector . . . . .	14
2.3 Introduction to Compressive Sensing . . . . .	17
2.3.1 Compressible Signals . . . . .	19
2.3.2 Compressive Sampling . . . . .	19
2.3.3 Compressive Sensing Reconstruction . . . . .	21
2.4 Conclusion . . . . .	22
<b>3 WIDE BAND SPECTRUM SENSING FOR COGNITIVE RADIO NETWORK USING DISTRIBUTED COMPRESSIVE SENSING</b>	<b>23</b>

3.1	Introduction . . . . .	23
3.2	Problem Definition . . . . .	24
3.3	System Model . . . . .	27
3.4	Proposed Compressive Spectrum Sensing . . . . .	28
3.4.1	Generation of Sensing Matrix $\Phi$ . . . . .	28
3.4.2	Compressed Measurements . . . . .	29
3.4.3	Compressive Decoding . . . . .	30
3.5	Simulation and Results . . . . .	32
3.6	Conclusion . . . . .	38
<b>4</b>	<b>JOINT WIDE BAND SPECTRUM SENSING IN FREQUENCY OVERLAPPING COGNITIVE RADIO NETWORK USING DISTRIBUTED COMPRESSIVE SENSING</b>	<b>39</b>
4.1	Introduction . . . . .	39
4.2	Proposed Wideband Compressive Spectrum Sensing in Frequency Overlapping Networks . . . . .	40
4.2.1	Sensing Matrix $\Phi$ . . . . .	41
4.2.2	Compressed Measurement $Y$ . . . . .	42
4.2.3	Compressive Sensing Decoding . . . . .	43
4.3	Simulation and Results . . . . .	46
4.4	Conclusion . . . . .	53
<b>5</b>	<b>BINARY COMPRESSIVE SENSING</b>	<b>55</b>
5.1	Introduction . . . . .	55
5.2	Related Work and Contribution . . . . .	57
5.3	Binary Compressive Sensing . . . . .	58
5.3.1	<b>The Sampling Matrix, <math>\Phi</math></b> . . . . .	<b>60</b>
5.3.2	<b>Compressed Measurements and the Check Nodes</b> . . . . .	<b>61</b>

5.3.3	<b>Compressive Sensing Decoding</b> . . . . .	61
5.4	An Alternative Approach . . . . .	65
5.4.1	Compressive Sensing Decoding . . . . .	66
5.5	Analysis and Discussion . . . . .	66
5.5.1	Choice of Row-Weight (L) . . . . .	66
5.5.2	Encoding and Decoding Complexity . . . . .	69
5.5.3	The Number of Measurements (M) . . . . .	69
5.5.4	The Error Rate (E.R) . . . . .	70
5.6	Simulation and Results . . . . .	71
5.7	Conclusion . . . . .	79
<b>6</b>	<b>CONCLUSIONS AND FUTURE WORKS</b>	<b>80</b>
6.1	Future Works . . . . .	82
	<b>BIBLIOGRAPHY</b>	<b>85</b>

## LIST OF FIGURES

Figure	Page
1.1 Spectrum demand and scarcity . . . . .	1
1.2 The NTIA frequency allocation chart . . . . .	2
2.1 Cognitive radio cycle . . . . .	9
2.2 Various aspects of spectrum sensing for cognitive radios . . . . .	10
2.3 Cyclostationary feature detection . . . . .	12
2.4 Pilot Signalling in Primary Radio . . . . .	13
2.5 Basic block diagram of the energy detector . . . . .	15
2.6 Implementation of FFT in energy detector . . . . .	16
2.7 Tradeoffs in complexity and accuracies of sensing methods . . . . .	17
2.8 Traditional sampling and data compression . . . . .	18
2.9 Compressive sampling/sensing . . . . .	18
2.10 Compressive sampling measurement process . . . . .	20
2.11 CS Reconstruction Geometry. (a) Sparse vector in $\mathbb{R}^3$ . (b) $l_2$ minimization. (c) $l_1$ minimization. . . . .	21
3.1 Primary and secondary users coexistence . . . . .	25
3.2 System Model . . . . .	28
3.3 Probability of Detection in Noiseless Measurements . . . . .	33
3.4 Error Of Reconstruction in Noiseless Measurements . . . . .	34
3.5 Probability of Detection in Noiseless Measurements using OMP . . . . .	34
3.6 Error Of Reconstruction in Noiseless Measurements using OMP . . . . .	35
3.7 Probability of Detection in Noisy Measurements . . . . .	36

3.8	Error of Reconstruction in Noisy Measurements . . . . .	36
3.9	Probability of Detection using Reweighted $l_1$ Minimization . . . . .	37
3.10	Error of Reconstruction using Reweighted $l_1$ Minimization . . . . .	37
4.1	Schematic of overlapping networks and overlapping spectrum bands .	41
4.2	Joint spectrum sensing schematic in frequency overlapping networks .	45
4.3	POD using individual and joint reconstruction . . . . .	47
4.4	EOR using individual and joint reconstruction . . . . .	48
4.5	POD using individual and joint reconstruction in noisy measurements	49
4.6	EOR using individual and joint reconstruction in noisy measurements	49
4.7	Measurement gain for varying SOF when POD=0.99 . . . . .	50
4.8	ROC performance for different SNR . . . . .	51
4.9	ROC performance comparison, For SNR=-5dB, S.R=0.6 and Spar- sity=40% . . . . .	52
4.10	EOR comparison, For SNR=-5dB, S.R=0.6 and Sparsity=40% . . . . .	52
4.11	Original time domain signal and reconstructed using individual recon- struction method . . . . .	53
4.12	Original time domain signal and reconstructed using joint reconstruc- tion method . . . . .	53
5.1	Representation of Compressive Sensing with Bipartite Graph . . . . .	59
5.2	Reduced Graph after the First cycle of First Phase Recovery and Edge Removal and Check Nodes Update . . . . .	64
5.3	Probability of zero and light check nodes for different row-weight . . .	68
5.4	Probability of Check Nodes Recovered in First Iteration (CNRP) . . .	72
5.5	Numbers of Check Nodes Recovered in First Iteration (CNRN) . . . . .	73
5.6	Error Rate for different Row Weight . . . . .	74
5.7	Row weight and Decode Time . . . . .	74

5.8	Error Rate for different Sampling Rate and Row weight . . . . .	75
5.9	Original and Reconstructed Signal using Binary l1 and Our Scheme .	76
5.10	Error Rate Comparison with Binary $l_1$ scheme with threshold . . . .	77
5.11	Decode Time comparision Binary $l_1$ scheme with threshold . . . . .	77
5.12	Maximum heavy node degree . . . . .	78
6.1	Spectrum occupancy state variation in spatio-temporal region . . . .	82
6.2	Wireless sensor network with dynamic and rapid event changes . . . .	83



# CHAPTER 1

## INTRODUCTION

### 1.1 Motivation: Spectrum Demand and Scarcity

New advancements in wireless technologies have created an excessive demand of the wireless spectrum and resources. Current spectrum usage paradigm reflects fixed spectrum allocation technique. The available wireless spectrum resources have been assigned to existing wireless technologies. The excessive use of wireless spectrum and regulations imposed by the Federal Communications Commission (FCC) have created spectrum scarcity. Fig. 1.1 shows the train of increase in spectrum demand. The spectrum allocation chart in United States (Fig. 1.2) by National Telecommunications and Information Administration's (NTIA) shows the overlapping spectrum allocation that clearly reflects the spectrum scarcity mindset. Figs. 1 and 2 clearly reflect

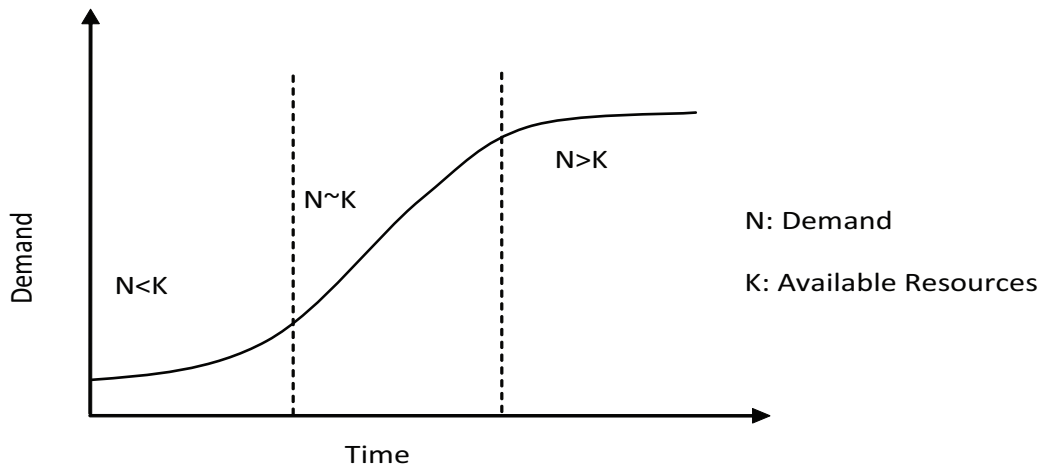


Figure 1.1: Spectrum demand and scarcity

the growing spectrum scarcity. FCC has shown its concerns regarding the excessive

spectrum demand at a rate faster than that can be made available. The demand of spectrum is out stripping supply and we are in the danger of *Spectrum Drought*. On

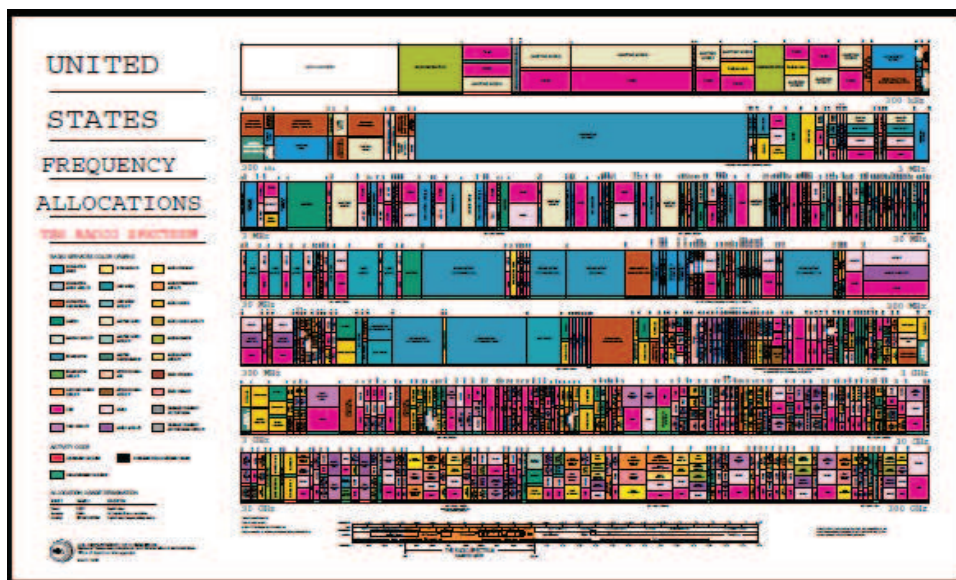


Figure 1.2: The NTIA frequency allocation chart

one hand, we are facing spectrum scarcity, whereas on the other hand, recent spectrum survey by spectrum policy task force (SPTF) shows that the wireless spectrum has been used inefficiently and the wireless resources are underutilized. The report shows the temporal and geographic variation in spectrum usage ranging from 15% to 85% [1]. A recent study by the Shared Spectrum [2] shows that over the spectrum band of 30 MHz to 3000 MHz over multiple locations, the spectrum usage is just 5.2% and maximum occupancy of 13% was recorded in New York city. These reports reflect the inefficient spectrum usage because of the spectrum distribution and licence and call for the new methods to tackle the spectrum bottleneck in wireless domain.

## 1.2 Cognitive Radio and Spectrum Sensing

The reports on spectrum usage clearly show that the problem of spectrum scarcity is not because of spectrum in-abundance but, it is because of inefficient usage and distribution. The spectrum reallocation and creating new spectrum allocation chart

is unfortunately not feasible as it is not possible to predict the future usage and demand of the spectrum, and also it is infeasible to create a uniform spectrum distribution policy that can meet the varying spatial temporal spectrum demand. Besides, any conflicts in spectrum reallocation will suffer opposition from the existing owners or users of the spectrum. Thus, unharmed and unaffected access of spectrum for the “primary users” is priority in development of any new efficient spectrum access scheme. These conflicts in spectrum scarcity and inefficient utilization call for the new technology which should be able to optimize the spectrum usage. The concept of Cognitive Radio (CR) was recently proposed in [3], which introduces a concept of secondary users (SR) or (CR) for efficient spectrum utilization. Mitola considered CR as the radio in which every possible parameter observed by wireless node/network is taken into account while making the decision on the transmission/reception. It is a system that sense, and is aware of, its operational environment and can dynamically and autonomously adjust its radio operating parameters accordingly. CR is: “A radio that employs the model based reasoning to achieve a specific level of competence in radio-related domains”. The primary objectives of a cognitive radio are two folds:

- Efficient utilization of wireless spectrum
- Reliable communications without affecting primary users

To achieve these objectives the primary task of CRs is to efficiently sense the primary users in the environment. A spectrum is said to be vacant when there are no primary users. The CRs should continuously monitor and sense the spectrum and efficiently use the vacant spectrum (Spectrum Holes) without disrupting the primary users. So, spectrum sensing is a mechanism of detecting presence or absence of primary users in the environment and hence find the available spectrum holes for the secondary communication purposes.

### 1.2.1 Cognitive Radio Challenges

The primary users or the current spectrum owners are not so receptive about the cognitive radios and the spectrum trade policies as they are likely to cause disruption to their access in the wireless spectrum and resources. The fundamental challenges in cognitive radio are efficiently identifying vacant bands over a wide band of spectrum over spatio temporal domain and maintaining Signal to Noise ratio (SNR) of secondary users communications [4] [5]. CRs have to be able to dynamically sense the radio spectrum and adapt its transmitter parameters according to the dynamic surrounding radio environment. The wideband spectrum sensing requires very fast digital sampler with high resolution to meet the dynamic and wide spectrum characteristics. Besides, the radio sensitivity of CRs have to be very precise with sensing interval as short as possible to meet the agility requirements. The implementation challenges in wideband spectrum sensing for Cognitive radios can be broadly seen under following categories.

- **Detection Capability:** The Primary users are not so receptive about the CR concept because of the harmful effects CR could cause them. A CR may not be able to correctly detect the spectrum and may start using it when primary user needs it and hence results in interference in the primary user communications. CRs not only have to sense the spectrum before beginning its transmission but also have to continuously sense during its transmission period so as to detect the reappearance of primary users anytime and vacate the spectrum for the primary users. Thus receiver sensitivity is also key factor in cognitive radio network. Besides, the dynamic fading and noisy communications channel makes finding the threshold for spectrum detection and decision process complex. Sensing time duration is also an important factor as C.Rs cannot afford spending long duration in spectrum sensing because it not only has to use the spectrum for its own communication purposes, but it should also be able to vacate the spectrum

immediately after a primary user reappears. The SNR margin for secondary communication creates the tradeoff between the receiver sensitivity and transmission power allocation. This requires CRs to have adaptive transmit power based upon the communications environment.

- **Wideband Sampling Circuitry:** Wideband spectrum sensing is a challenging task because of dynamic wide range of the frequency bands. It requires either discrete grouping of wide spectrum into the narrowbands and utilizes multiple narrowband sensing or use the digital signal processors to sample the wideband analog signal and then perform spectrum sensing. Unfortunately, the multiple narrowband sensing is not feasible and less attractive because of its complex structure in wideband model, whereas the DSP necessitates high speed ADCs.

A new sampling paradigm based upon sparse sampling named Compressive Sensing (CS) provides a sampling mechanism at rates lower than the Nyquist rates. The signal reconstruction scheme in compressive sensing is a norm optimization problem. In this thesis, we present a novel spectrum sensing mechanism for cognitive radio based upon the compressive sensing.

### 1.3 Outline of Thesis

The rest of the thesis is organized as follows. In the Chapter 2, we provide brief introduction to the spectrum scarcity and cognitive radio technique. A general outline of important spectrum sensing approaches is presented. A brief and quick introduction of compressive sensing and decoding approaches is also presented. In the Chapter 3, we propose wideband spectrum sensing for single network cognitive radio system using compressive sensing. Compressive sensing based joint spectrum sensing in frequency overlapping networks is proposed in the Chapter 4. We exploit the joint sparsity of the overlapped region to have better spectrum sensing performance at minimal cost. A

novel compressive sensing scheme for Binary signals is proposed in the Chapter 5. We implement the bipartite graphs to represent the binary compressive sensing process. A unique, but universal sampling matrix for binary signal is developed and graph and check-sum based decoding scheme for binary compressive sensing is proposed.

## CHAPTER 2

### BACKGROUND AND LITERATURE REVIEW

In this chapter, we present a brief introduction to cognitive radio and compressive sensing techniques. We will discuss about different stages of cognitive radio cycle and importance of spectrum sensing in cognitive cycle. We will present a critical viewpoint on different conventional spectrum sensing techniques and some new approaches to them. We shall also present an overview on new emergent sampling theory called compressive sensing for sparse signals.

#### 2.1 Cognitive Radio

The widespread acceptance of wireless technologies has created an unexpected demand of wireless bandwidths and is well expected to grow in future as well. Spectrum licensing has been the traditional approach to ensure the diverse wireless systems. However, due to the surplus demand, the frequency allocation have overlapped and left very small space for new emerging systems. On the contrary, the varying demand and utilization have created many of the allocated frequencies unused and vacant (spectrum holes) over spatio-temporal domain. The contrary in supply - demand and utilization have urged to look for new methods to accommodate secondary (unlicensed) wireless devices without disrupting the primary (licensed) users. Cognitive radio in a broad sense refers to various solutions that seek to overlay, underlay or interweave the secondary user's signals with the primary users.

Cognitive radio is an idea to take advantage of open spectrum policy. It should be designed to adapt dynamically to its environment and find the communication channel

ensuring minimal interference to the licensed users. The definition of cognitive radio is very broad as its functions are dynamic. FCC has defined cognitive radio as:

A radio frequency transmitter receiver that is designed to intelligently detect whether a particular segment of radio spectrum is currently in use, and to jump into (and out of) the temporary unused spectrum very rapidly without interfering with the transmission of other authorized users.

In [6], CR is defined as :

Cognitive radio is an intelligent wireless communication system that is aware of its surrounding environment and uses the methodology of ‘understanding by building’ to learn from the environment and adapt its internal states to statistical variations in the incoming RF stimuli by making corresponding changes in certain operating parameters (e.g. transmit power, carrier frequency, modulation strategy) in real time, with two primary objectives in mind: highly reliable communication whenever and wherever needed and efficient utilization of radio spectrum.

Basically, a cognitive radio has following capabilities:

- Sensors creating awareness in the environment
- Actuators enabling interaction with the environment
- Memory and a model of the environment
- Learning and modeling of specific beneficial adaptations
- Specific performance goals
- Autonomy



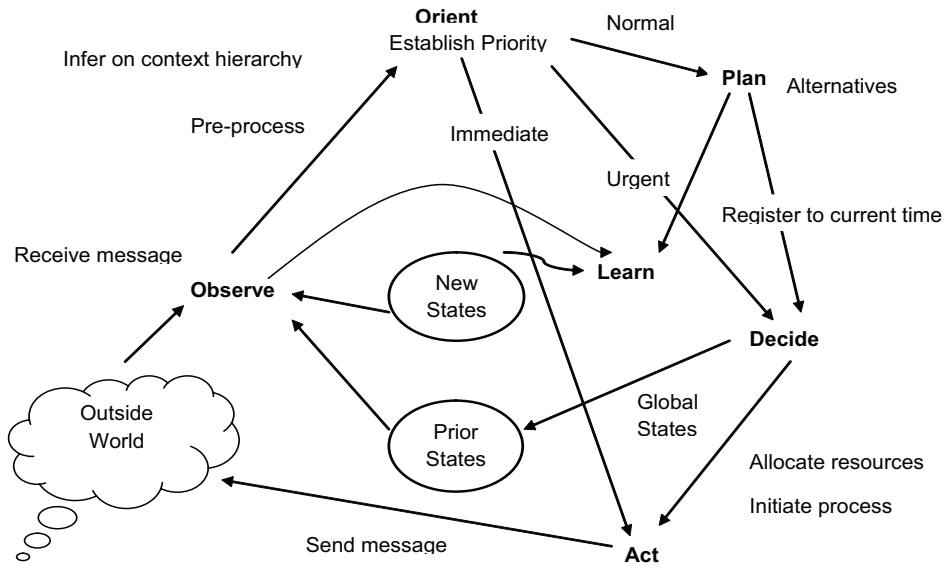


Figure 2.1: Cognitive radio cycle

In [7], cognitive radio cycle has been proposed as a top level loop for cognitive radio system. The cognitive cycle mainly consists of observe, orient, plan, decide and act (OOPDA). In cognitive cycle information about the communication environment is received by a cognitive radio through the direct observation or the stimuli signaling. In orient stage, based upon the received environment information a CR determines the importance and urgency. Planning, including negotiations with peers for best alternatives is considered in planning stage. Best decision is made based upon the alternatives and consequences and finally a CR acts by adjusting its resources and performs appropriate signaling. The cognitive cycle is shown in the Fig. 2.1.

## 2.2 Conventional Spectrum Sensing Techniques

Several factors make spectrum sensing practically challenging. Communication channel noise, multipath fading in environment makes spectrum sensing a complex problem. Receiver sensitivity of the spectrum detectors needs SNR of the signal to be above some threshold value to sense the signal. The SNR at the receiver may not

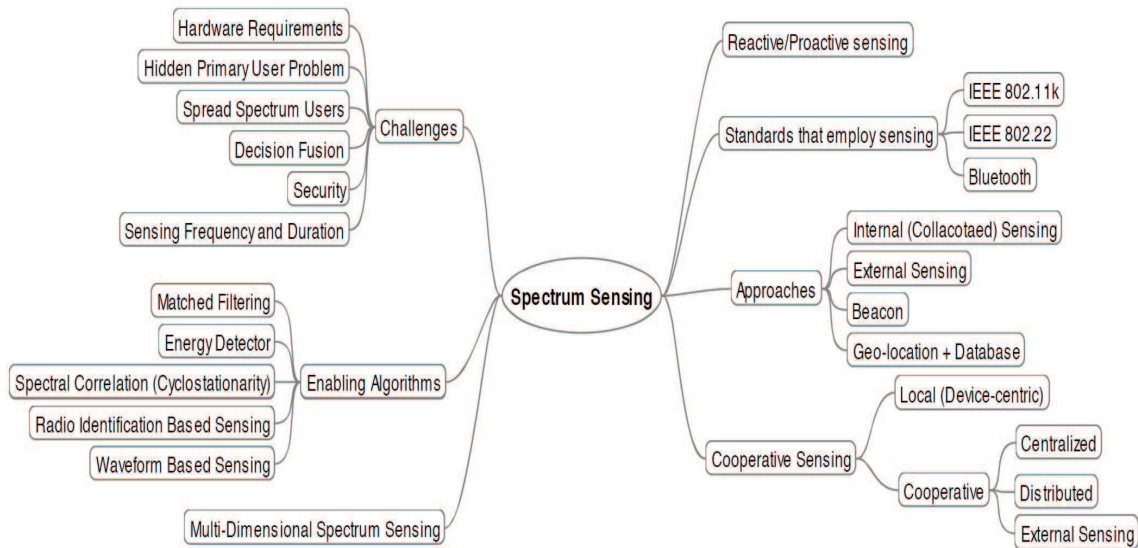


Figure 2.2: Various aspects of spectrum sensing for cognitive radios

be always greater than the threshold value because of noise and fading. Time dispersion of wireless signal makes coherent detection infeasible whereas the spatio-temporal varying noise interference characteristics yield power uncertainty issues in spectrum sensing [8, 9, 10]. Considering these facts, various aspects of spectrum sensing are taken into account while implementing efficient spectrum sensing method. Fig. 2.2 [11] reflects various aspects of spectrum sensing.

In the following section we will discuss about some of the most common approaches of spectrum sensing.

### 2.2.1 Matched Filter

A matched filter maximizes the signal to noise ratio, so when the information of the PU signal is known matched filter is an optimal method for any kind of signal detection [12]. Although, match filters are optimal and the coherency requires less time to achieve high processing gain, it is less attractive for practical purposes as it requires prior knowledge of the primary signal. Though information regarding a signal can be stored in memory, the synchronization and channel equalization remains

inevitable. Besides, a secondary user or spectrum detector requires extra circuitry to achieve carrier synchronization. So, in wideband spectrum sensing even though we have prior information regarding the signal, the dynamic signal characteristics in wideband communication makes it less feasible. Compressive detector using matched filters have been proposed in [13, 14]. Despite of its drawbacks matched filter is applicable to certain class of primary network with uniform signal characteristics and information about the signal is known in prior.

### 2.2.2 Cyclostationary Feature Detection

A signal is said to have a cyclostationary process if its statistical properties vary cyclically with time. Modulated signals are generally coupled with periodic carriers like sine wave, pulse trains, hopping sequences or cyclic prefixes which gives the periodicity to the signal. This periodicity helps in detecting and identifying the signal in noise dominant environment. Let  $x(n)$  be a discrete time series with mean  $\mu_x(n) := E\{x(n)\}$  and covariance  $c_{xx}(n; \tau) := E\{[x(n) - \mu_x(n)][x(n+\tau) - \mu_x(n+\tau)]\}$ . For  $x(n)$  complex valued, the covariance is a complex conjugate, and  $n$  and  $\tau$  are sets of integer  $Z$ , then from [15] :

Process  $x(n)$  is cyclostationary iff, there exists an integer  $P$  such that  $\mu_x(n) = \mu_x(n + lP)$ ,  $c_{xx}(n; \tau) = c_{xx}(n + lP; \tau)$ ,  $\forall n, l \in Z$ . The smallest of all such  $P$ s is called the period and its fourier coefficients called cyclic correlation are related by :

$$c_{xx}(n; \tau) = \sum_{k=0}^{P-1} C_{xx}\left(\frac{2\pi}{P}k; \tau\right) e^{j\frac{2\pi}{P}kn} \leftrightarrow C_{xx}\left(\frac{2\pi}{P}k; \tau\right) = \frac{1}{P} \sum_{n=0}^{P-1} c_{xx}(n; \tau) e^{-j\frac{2\pi}{P}kn} \quad (2.1)$$

The main advantage of spectral correlation in detection is that it differentiates the noise energy from signal energy because of the spectral correlation in modulated signal. A cyclostationary approach for signal detection is discussed in [16, 17]. Fig.

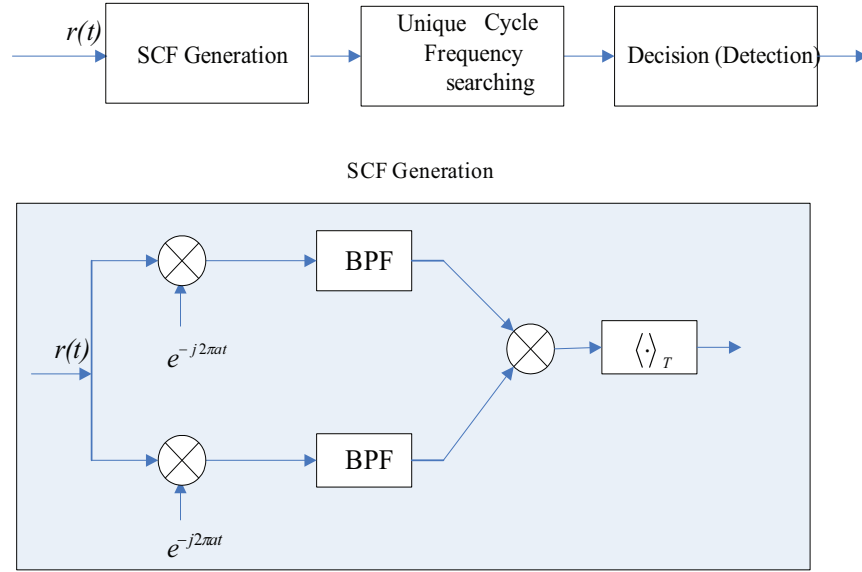


Figure 2.3: Cyclostationary feature detection

2.3 shows basic implementation of cyclostationary detection method using spectrum correlation function (SCF). In this method, signal information like phase, frequency and timing parameters are preserved for comparison. Though, this method is efficient for signal detection in noisy environment it requires longer sensing time to collect statistical parameters over long period of time. Moreover, it is computationally complex and requires prior knowledge about the signal.

### 2.2.3 Pilot and Radio Detection

Knowledge about the signal and its characteristics help in signal detection and identification. Such information enables cognitive radio with higher dimension knowledge and provides higher accuracy. For example, if it is known that the primary signal is a bluetooth signal, CR use this information for extracting information in space dimension. Radio identification techniques are used in European Transparent ubiquitous project (TRUST) [18]. In radio identification based sensing [19, 20], different features of signal are extracted and are classified using standard classification techniques and are compared with the primary signal prior information and decision is made accord-

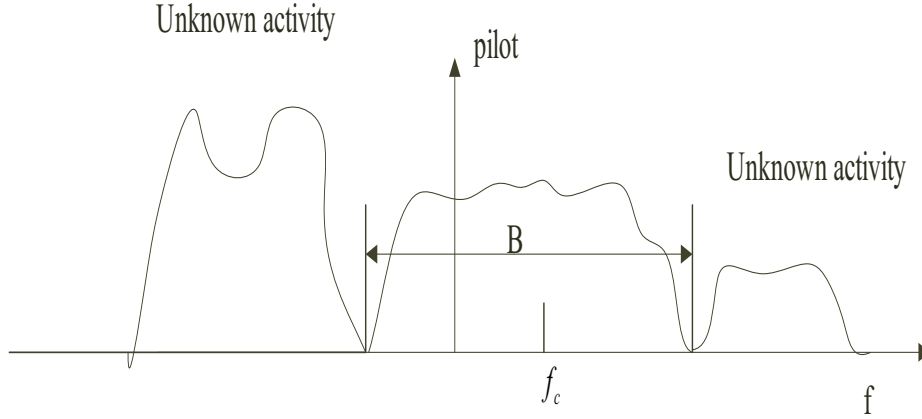


Figure 2.4: Pilot Signalling in Primary Radio

ingly. For example, in Pilot detection technique, the energy of the primary signal is confined inside a prior known bandwidth around the central frequency (Fig. 2.4) and activity outside it, is unknown. A primary signal sends periodic pilots and based upon the pilot sequences detection, a primary radio is identified. Signal detection in UWB impulse radio using pilot sequences is discussed in [21]. Radio identification suffers same drawbacks as the cyclostationary scheme, thus these schemes are not so attractive though they have better performance in discriminating against noise.

#### 2.2.4 Waveform Based Sensing

Waveform based sensing is not a complete spectrum sensing approach in itself. In this method, various characteristics of a signal are exploited. The metric so formed from those characteristics like preamble, spreading sequences etc is compared with the standard threshold and the decision is made accordingly. Let us consider a system as :

$$y(n) = s(n) + w(n) \quad (2.2)$$

where,  $y(n)$ ,  $s(n)$ ,  $w(n)$  are received signal, primary signal and noise, respectively.

The waveform based sensing metric is defined in [22] as:

$$M = Re \left[ \sum_{n=1}^N y(n)s^*(n) \right] \quad (2.3)$$

where, \* represents the conjugation. In absence of the primary signal the value of M becomes:

$$M = Re \left[ \sum_{n=1}^N w(n)s^*(n) \right] \quad (2.4)$$

whereas, in presence of the primary signal the decision metric becomes:

$$M = \sum_{n=1}^N |s(n)|^2 + Re \left[ \sum_{n=1}^N w(n)s^*(n) \right] \quad (2.5)$$

The metric thus obtained is compared with the standard threshold value  $\lambda_w$  and decision is made accordingly. Waveform based sensing using preambles is discussed in [23, 24]. Though waveform based sensing requires shorter sensing time [25] and can sense the signal at known environments they suffer from synchronization problems.

### 2.2.5 Energy Detector

Energy detector based techniques in spectrum sensing are most common approach in cognitive radio. Energy detection schemes, also known as radiometer or periodogram are widely used because of it's simple structure and computational gains [26, 27, 28]. When no information about the primary signal is known, and only the noise characteristics of channel are known, energy detector is the optimal solution for spectrum sensing. Basically, energy detector consists of a bandpass filter to out pass the out band noise and adjacent signals and is followed by a sampler, square law device and an integrator as shown in the Fig. 2.5. A band filtered signal is squared and integrated over the period to find the energy of the received signal and then compared with the threshold  $\lambda_e$  and decision is made accordingly. Let us consider a system defined as:

$$y(n) = x(n) + w(n) \quad (2.6)$$

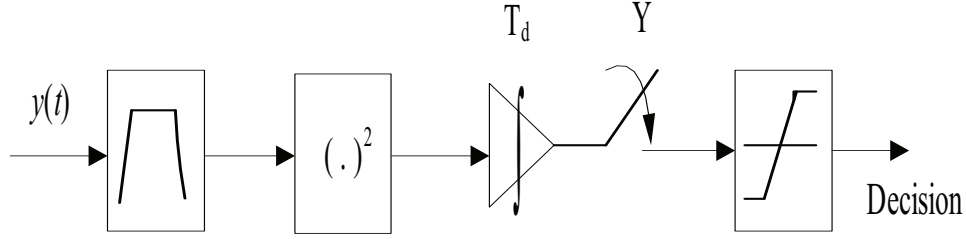


Figure 2.5: Basic block diagram of the energy detector

where,  $y(n)$ ,  $x(n)$  and  $w(n)$  are received signal, primary signal and the noise, respectively. Then for Energy detection scheme, test statistic is given by:

$$T = \sum_N (Y[n])^2 \quad (2.7)$$

The decision making process in energy detector is equivalent to distinguishing between the following two hypotheses:

$$H_0 : y(n) = w(n) \quad (2.8)$$

$$H_1 : y(n) = x(n) + w(n) \quad (2.9)$$

Expressions ( 2.8) and ( 2.9) are respectively cases of absence and presence of primary signal. The detection performance of energy detector can be seen under two parameters viz: probability of detection  $P_D$  and probability of false alarm  $P_F$  which can be formulated as:

$$P_{(D)} = Pr(T > \lambda_e | H_1) \quad (2.10)$$

$$P_{(F)} = Pr(T < \lambda_e | H_0) \quad (2.11)$$

So the goal in energy detector is always increasing  $P_D$  and decreasing  $P_F$ .

The time domain energy computation of a signal is inflexible in case of narrowband signals because of pre-filter matching problem. So energy computation in frequency

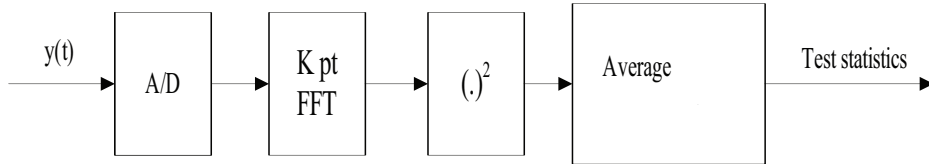


Figure 2.6: Implementation of FFT in energy detector

domain is another prevailing approach. Fourier coefficients of received signals are used to calculate the energy using Parseval's theorem. The frequency resolution of FFT increases with the number of points 'K' which is equivalent to increasing the sensing time of pre filter in time domain analysis. Fig. 2.6 shows the basic block diagram of energy detector in the frequency domain. The major challenge in energy detector scheme is estimating the appropriate threshold parameter. Though no information about the primary signal is required in this scheme, when the noise characteristics cannot be modeled, optimizing  $\lambda_e$  is a difficult challenge. In [29], the author has used decode and forward scheme in energy detectors to improve its performance in fading and noisy environment. For its simple implementation structure and computational gain energy detector is still one of the most feasible and commonly used approach in spectrum sensing.

Different spectrum sensing approaches have their own pros and cons based upon the communication environment. There is always a tradeoff between the complexity and the efficiency between different approaches of spectrum sensing. When noise characteristics are known energy detector outperforms other sensing approaches in terms of both accuracy and complexity. But when noise information are not known, other schemes like cyclostationary and waveform based approaches are preferred. Waveform based approach performs better when signal characteristics information are prior. So, for detection of known signals waveform and cyclostationary schemes are suitable. On the contrary, these approaches are very sensitive to hardware precession,



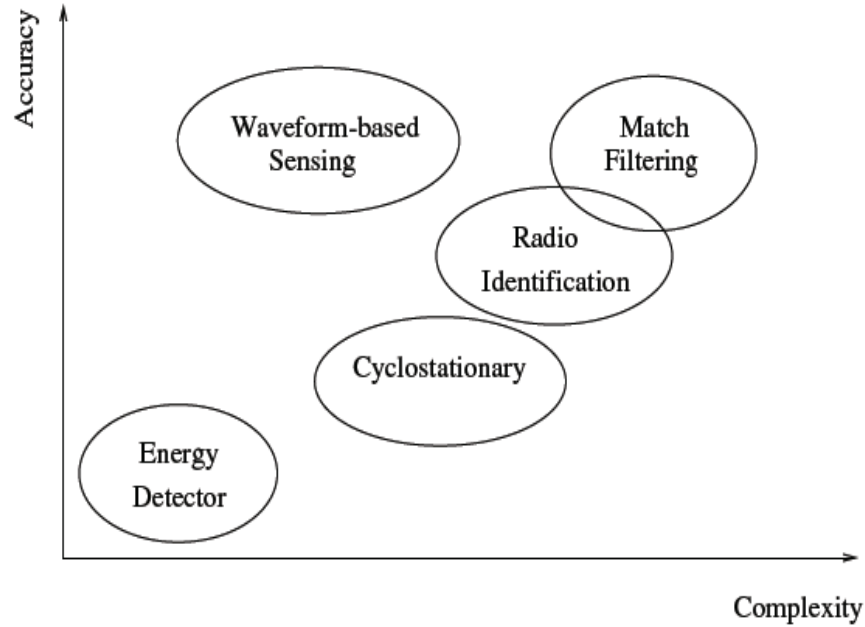


Figure 2.7: Tradeoffs in complexity and accuracies of sensing methods

clock synchronization and timing. Fig: 2.7 [11] provides a very broad comparison between different spectrum sensing approaches. Based upon the facts that energy detector is very simple to implement, computationally efficient and requires no any prior information about the signals, it is still most commonly used in spectrum sensing for cognitive radios.

### 2.3 Introduction to Compressive Sensing

Data acquisition and sampling is an important factor in digital systems. The Nyquist sampling theorem specifies that in order to recover a signal from its samples, the sampling process should be at least two times faster than the signal bandwidth. In many applications, including digital images, large communication networks the Nyquist rate is so high that it results too many samples, necessitates data compression, high-speed analog-to-digital converters, and makes the data acquisition very expensive. However, Compressive Sensing, (CS) a novel sensing/sampling paradigm goes against the

common wisdom in data acquisition. CS theory asserts that one can recover certain signals and images from far fewer samples or measurements than traditional methods [30, 31]. Compressive sensing is distinct from traditional single point sampling approaches and data compression in two very broad sense. In CS, each sample is linear functional of the original signal and, compression is carried in the data acquisition process itself rather than compressing the sampled data as in conventional data compression techniques. This difference is shown in the Figs. 2.8 and 2.9.

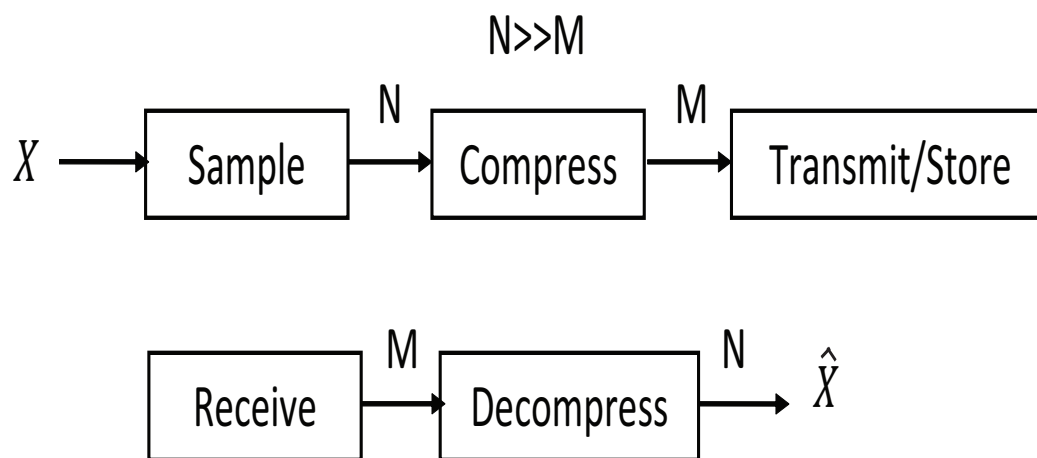


Figure 2.8: Traditional sampling and data compression

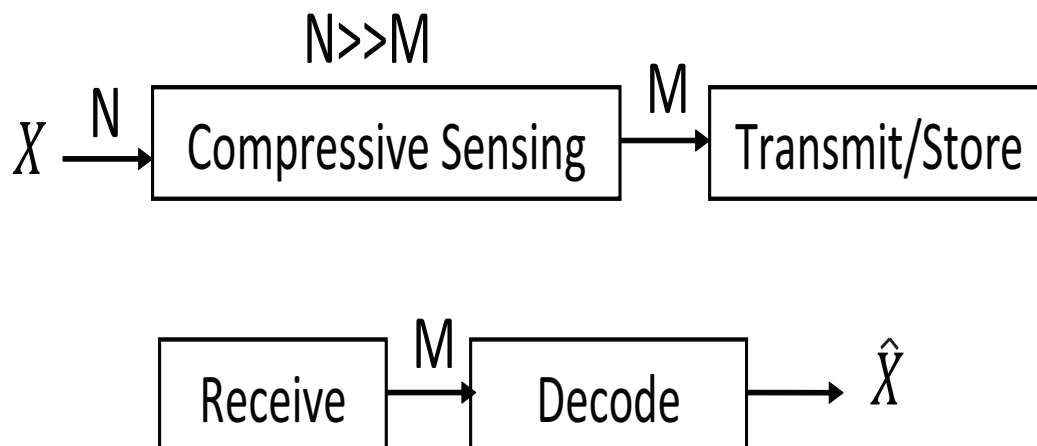


Figure 2.9: Compressive sampling/sensing

### 2.3.1 Compressible Signals

CS relies on two principles: sparsity, which pertains to the signals of interest, and incoherence, which pertains to the sensing modality. A signal is said to be sparse, if it contains few non-zero elements and other zeros. A real-valued, finite-length, one-dimensional, discrete-time signal  $X$ ,  $X \in \{\mathbb{R}\}^N$  with elements  $x[n], n = 1, 2, \dots, N$  can be represented in terms of a basis of  $N \times 1$  vectors  $\{\psi_i\}_{i=1}^N$ . Using  $N \times N$  basis matrix  $\Psi = [\psi_1 | \psi_2 | \dots | \psi_N]$  with the vectors  $\{\psi_i\}$  as columns, a signal  $X$  can be expressed as

$$X = \sum_{i=1}^N s_i \psi_i, \quad \text{i.e. } X = \Psi S. \quad (2.12)$$

The signal representation of  $X$  in  $\Psi$  domain is given by  $S$  and they are equivalent. The signal  $X$  is called  $K$  sparse in  $\Psi$  if it is linear combination of  $K$  basis vectors, i.e. only  $K$  elements of the  $S$  are non-zeros and other are zeros. In this special case, when a signal  $X$  is sparse in some domain and  $K \ll N$ ,  $X$  is said to be compressible.

### 2.3.2 Compressive Sampling

Let us consider, a real valued signal  $X \in \{R\}^N$  be a compressible signal in some domain  $\Psi$  as discussed in the Section 2.3.1. Let us consider a sampling/sensing matrix  $\Phi$  of dimension  $M \times N$ ,  $M < N$ . The sampling matrix  $\Phi$  is used to generate  $M$  linear measurements of signal  $X$ . Consider, a  $N$  length vector  $\phi_j, j = 1 : M$ , then the compressed measurements can be expressed as an inner products between  $X$  and  $\phi_j$ s as,  $y_j = \langle X, \phi_j \rangle$ . Arranging,  $y_j$ s in a  $M$  length vector  $Y$ , and measurement vectors  $\phi_j^T$  as rows of sampling matrix  $\Phi$ , the compressive sampling process can be expressed as:

$$Y = \Phi X = \Phi \Psi S = \Theta S. \quad (2.13)$$

The Compressive sampling measurement process is depicted in the Fig. 2.10.

The sampling matrix  $\Phi$  does not depend on the the signal  $X$ , however, it has to be *stable* and *incoherent* with the  $\Psi$  matrix. Some examples of suitable  $\Phi$  matrices

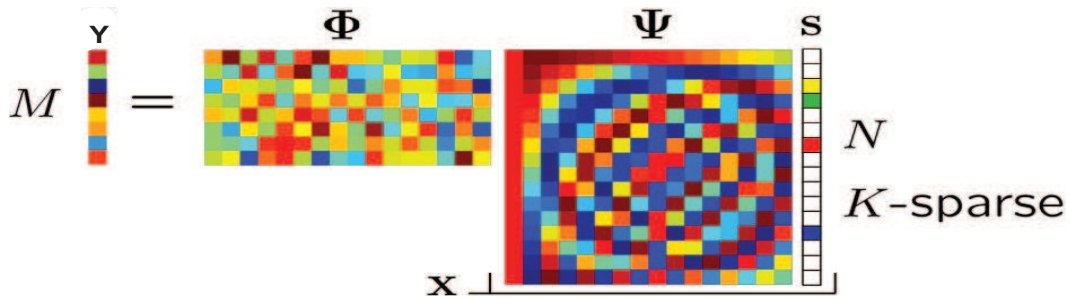


Figure 2.10: Compressive sampling measurement process

are:

- Gaussian :  $\Phi_{i,j} = N(0, \frac{1}{M})$
- Bernoulli/rademacher
- Sparse Gaussian
- Random orthoprojection

In [32, 30], the robustness of CS measurement matrix is studied and the so called *Restricted Isometry Property* (RIP) is proposed. For the matrix,  $\Theta = \Phi\Psi$ , the isometry constant  $\delta_s$ , is defined as the smallest number such that

$$(1 - \delta_s)\|S\|_2^2 \leq \|\Theta S\|_2^2 \leq (1 + \delta_s)\|S\|_2^2. \quad (2.14)$$

Then, the matrix  $\Theta$  is said to have RIP of order  $S$ , if  $\delta_s$  is not close to 1. The *mutual coherence* parameter  $\mu$  also represents the robustness of the sampling matrix in CS.

The mutual coherence between two matrix  $\Phi$  and  $\Psi$  is defined as

$$\mu(\Phi, \Psi) = \sqrt{N} \cdot \max_{k \leq M, j \leq N} | \langle \phi_k, \psi_j \rangle |. \quad (2.15)$$

$$\mu(\Phi, \Psi) \in [1, \sqrt{N}]. \quad (2.16)$$

A Gaussian measurement matrix has shown to have these properties necessary for the compressive sensing [32]

### 2.3.3 Compressive Sensing Reconstruction

The CS reconstruction is an under-determined system of linear equations. We have  $M$  equations given by  $Y = \Phi X$  and  $N$  variables of  $X$  have to be reconstructed. Given the RIP and *incoherent* property of sampling matrix  $\Phi$  is satisfied, a  $K$  - *sparse*,  $N$  long signal can be reconstructed from  $M$  linear equations, where  $M < N$ . Let us define, the  $p^{th}$  norm of vector  $S$  as

$$\|S\|_p := \left( \sum_{i=1}^N |s_i|^p \right)^{\frac{1}{p}}. \quad (2.17)$$

When  $p = 0$ , it gives the number of non-zeros entries in  $S$ . The CS reconstruction of  $K$  - *sparse* signal  $X$  can be obtained from  $l_0$  minimization process. However, it is computationally prohibitively complex.

The CS reconstruction approximation using least square solution is given by.

$$\hat{S} = \operatorname{argmin} \|S\|_2, \quad \text{such that } Y = \Theta S. \quad (2.18)$$

The CS reconstruction approximation using  $l_2$  minimization is not a good approximation. Fortunately,  $l_1$  norm minimization process relaxes the  $l_0$  optimization and gives approximate solution of the signal  $X$  as

$$\hat{S} = \operatorname{argmin} \|S\|_1, \quad \text{such that } Y = \Theta S. \quad (2.19)$$

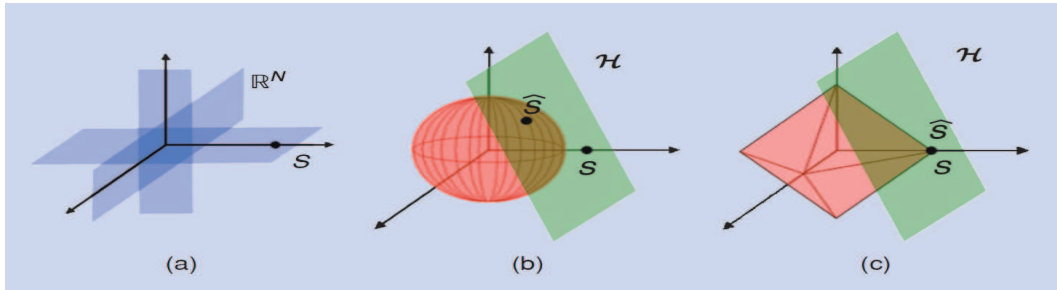


Figure 2.11: CS Reconstruction Geometry. (a) Sparse vector in  $\mathbb{R}^3$ . (b)  $l_2$  minimization. (c)  $l_1$  minimization.

Fig. 2.11 shows the basic geometry of CS reconstruction using norm minimization approach. Fig. 2.11 (b) shows pictorial representation of  $l_2$  minimization and why  $l_2$  minimization fails whereas from the Fig. 2.11 (c) we can see  $l_1$  minimization gives a good approximation of sparse signal  $S$ . Details of CS geometry can be found in [31, 30, 32].

Another class of CS reconstruction based on greedy pursuit such as Orthogonal Matching Pursuit, CoSaMP, have been discussed in [33, 34, 35, 36]. Model based compressive sensing decoding for special class of signals are discussed in [37, 38, 39]. There exists a tradeoff between different compressive sensing reconstruction and decoding algorithm in terms of their complexity, error rate, and signal model. However, we can list following important remarks about the compressive sensing process.

- Stable : The CS acquisition and recovery process is numerically stable.
- Universal: The CS sampling matrix is adaptive and universal to the signal models.
- Asymmetrical : Most of the processing is carried out at the decoder.
- Democratic : Each CS measurement carried equally important information.

## 2.4 Conclusion

In this chapter, we discussed about the spectrum scarcity and the cognitive radio technique. We presented a brief introduction to various spectrum sensing techniques and their tradeoffs. Spectrum sensing in cognitive radio for wideband network is an expensive approach in terms of data sampling and acquisition cost. Compressive sensing paradigm provides a new and efficient data acquisition and reconstruction approach for certain class of compressible signals. In the next chapter, we will model and discuss the application of compressive sensing in cognitive radio.

## CHAPTER 3

### WIDE BAND SPECTRUM SENSING FOR COGNITIVE RADIO NETWORK USING DISTRIBUTED COMPRESSIVE SENSING

#### 3.1 Introduction

The increasing demand for wireless resources and spectrum has created spectrum scarcity. However, spectrum utilization studies show that these scarce wireless spectrum has been distributed and used inefficiently [40], [41]. This bottleneck in spectrum scarcity and inefficient usage is addressed by the dynamic spectrum access policy [42, 43]. Cognitive radio (CR) with an ability to sense unused spectrum and opportunistically transmit over spectrum holes is proposed in [44], [6]. The fundamental challenge in the cognitive radio implementation is detection of the vacant spectrum (holes) [4]. Various spectrum sensing and detection mechanisms such as an energy detector [45], cyclo-stationary sensing [15] and pilot detection [46] have investigated the spectrum sensing problem under different wireless environment. The current trends in spectrum sensing and cognitive radios are well explained in many survey reports [47], [11]. Many of the spectrum sensing algorithms deal with the narrow band sensing which are tailored energy detector and power spectral density of the narrow band signal. Wideband spectrum sensing requires fast and dynamic spectrum analysis over larger spectrum band. Recent paradigm in sparse sampling, compressive sensing (CS) [30], [32] provides solution to sparse signal reconstruction as an optimization problem. In [48, 49], CS sampling, forward differentiation and singular value decomposition methods are used for wideband spectrum sensing purpose. These approaches provide wideband spectrum sensing in a simple individual network. To eliminate the

need of high speed analog to digital converters and digital signal processors in wide-band sensing, techniques such as random demodulators, parallel signal processing are proposed in [50, 51].

In this chapter, we build up basic compressive sensing model for the spectrum sensing in cognitive radio network. This model is then extended to the frequency overlapping jointly sparse networks in the Chapter 4. The rest of the chapter is organized as follows: In the Section 3.2, we formulate the spectrum sensing problem in single network for the cognitive radio. Section 3.3 presents the system model for our problem statement. Proposed spectrum sensing for cognitive radio using compressive sensing is discussed in the Section 3.4. Simulation results are presented in the Section 3.5 and finally Section 3.6, concludes the chapter.

### 3.2 Problem Definition

Let us consider a wideband communication model with primary and secondary (cognitive radios) users coexistence as shown in the Fig. 3.1. The total communication bandwidth of the system is divided into  $N$  subbands each centered at frequency  $f_n$ , where  $n = 1, 2, 3, \dots, N$ . Very few of the  $N$  subbands are occupied by the primary users at a given geographical and temporal region. Let us consider, out of  $N$  subbands,  $S \ll N$  are occupied by primary users during sensing time. The unoccupied channels by primary users over given spatio-temporal region called, *spectrum holes*, are opportunistically accessed by the cognitive users keeping the rights of the primary safe. The cognitive radios in the system need to detect these spectrum holes for secondary communication.

At time  $t$ , the received signal at  $m^{th}$  cognitive user can be expressed as:

$$y_m(t) = \sum_{n=1}^N x_n(t) * g_{nm}(t) + w_m(t), \quad (3.1)$$

where,  $*$  represents the convolution,  $x_n(t)$  is the signal of  $n^{th}$  primary user,  $g_{nm}(t)$



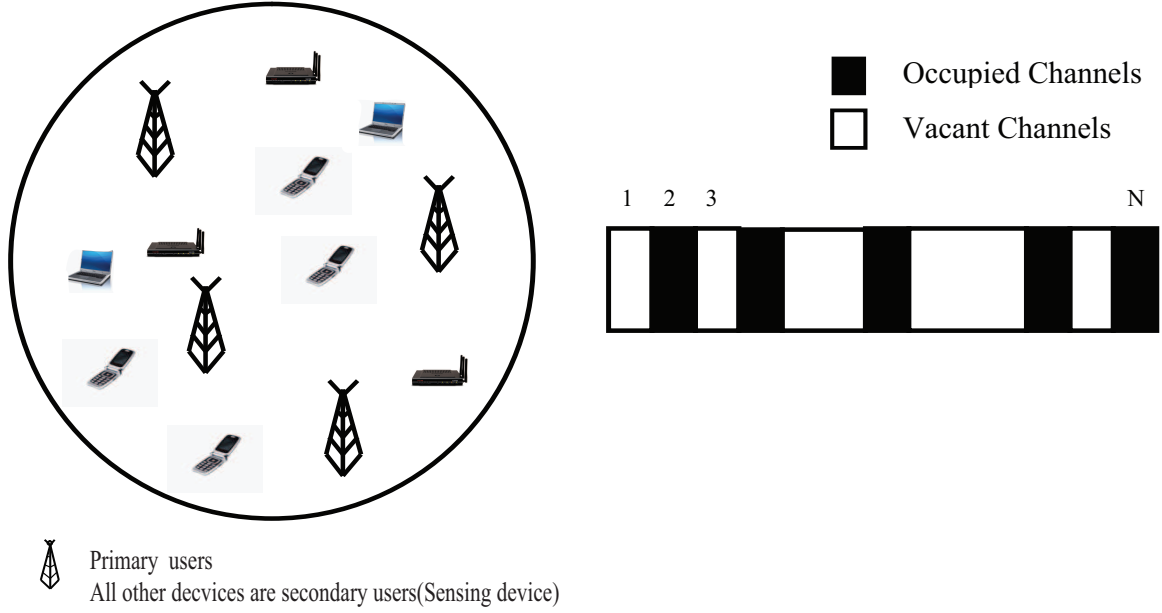


Figure 3.1: Primary and secondary users coexistence

denotes the channel gain response, and  $w_m(t)$  is additive white gaussian noise with zero mean and variance of  $\sigma_w^2$ . In frequency domain, (3.1) can be represented as:

$$y_f^{(m)} = \sum_{n=1}^N \mathbf{D}_g^{(nm)} x_f^{(n)} + w_f^m, \quad (3.2)$$

where  $\mathbf{D}_g^{(nm)}$  is a diagonal  $N \times N$  channel gain matrix between  $n^{th}$  primary and  $m^{th}$  CR.  $x_f$  and  $w_f$  represent corresponding frequency response of  $x(t)$  and  $w(t)$ , respectively and elements  $g_f^{(nm)}$  of  $\mathbf{D}_g^{(nm)}$  are given by:

$$g_{(i,j)} = 0; \quad i \neq j; \text{ and } i, j \in \{1, 2, \dots, N\}, \quad (3.3)$$

$$\text{and, } g_{(i,j)} = g_{f(i,j)}; \quad i = j; \text{ and } i, j \in \{1, 2, \dots, N\}. \quad (3.4)$$

However, we know that at any time  $t$ , only few of the  $N$  channels are occupied. Let  $\hat{S}$  be the set of occupied channels such that  $\hat{S} \subset \hat{N}$ .  $\hat{N}$  is the set of bands under consideration. Thus for all  $n : n \notin \hat{S}$

$$x_n(t) = 0. \quad (3.5)$$

From (3.5),  $\hat{N}$  is sparse. Accordingly, (3.1) and (3.2) reduce to,

$$y_m(t) = \sum_{s \in \hat{S}} x_s(t) * g_{sm}(t) + w_m(t), \quad (3.6)$$

$$\text{and, } y_f^{(m)} = \sum_{s \in \hat{S}} \mathbf{D}_g^{(sm)} x_f^{(s)} + w_f^m. \quad (3.7)$$

This sparseness of signal in the frequency domain makes CS possible for the spectrum sensing purposes in cognitive radio network. The frequency response of the channels occupied by the primary users are non-zero values, whereas, those of vacant channels are zero. Hence, the total frequency response of the signal under consideration is a sparse signal. In CS, instead of taking point by point samples as in conventional sampling, each sample taken is linear functional of the sparse signal. Consider the problem of reconstructing  $N \times 1$  length,  $S$  sparse signal  $X$ . Let us consider an  $M \times N$  dimension, where  $M < N$ , sensing matrix  $\Phi$ . We can obtain  $M$  compressed measurements,  $Y$ , using,  $Y = \Phi X$ . Since,  $M < N$ , the recovery of  $X$  from compressed measurements  $Y$  is ill-posed in general. Interestingly, provided  $X$  is sparse in some domain and the measurement matrix  $\Phi$  satisfies the restricted isometry property (RIP) [30], the signal  $X$  can be recovered from the measurement vector  $Y$ . The recovery of  $S$  non-zero elements of signal  $X$  is actually the solution of the  $l_0$  norm minimization problem.

$$\hat{X} = \arg \min \|X\|_{l_0}, \quad \text{s.t. } Y = \Phi X, \quad (3.8)$$

Unfortunately, solving  $l_0$  is prohibitively computationally complex. However, the approximate solution of  $X$  can be obtained using  $l_1$  minimization as:

$$\hat{X} = \arg \min \|X\|_{l_1}, \quad \text{s.t. } Y = \Phi X, \quad (3.9)$$

For secondary communication in the cognitive radio network, finding the set  $\hat{S}$  is the most important and first requirement. The complexity of spectrum sensing depends upon the requirements of an application. In cognitive radio spectrum sensing,

our primary concern is finding which of the  $S$  bands among  $N$  are occupied rather than the exact signal strength of the the occupied channels. In cognitive radio network, the problem of spectrum sensing using energy detector, at each  $m^{th}$  CR boils down to distinguishing between binomial hypotheses. The signal energy of each of the subband is compared with the threshold  $\lambda_e$  which is the function of noise and channel characteristics. If the received signal is greater than  $\lambda_e$  the channel is said to be occupied else it is taken as vacant. Finding an optimal  $\lambda_e$  is an agenda in the communication channel modeling research [52].

In conventional spectrum sensing, each secondary user senses and detects each of the band individually. This requires large number of measurements in the system and increases data acquisition cost [11, 48]. Besides, each sensing device/cognitive radio<sup>1</sup> needs to have sensing bandwidth entirely over the communication band making the sensing process more prone to noise.

### 3.3 System Model

We have  $N$  channels to detect, and  $M$  compressive sensing measurements, where,  $M \ll N$ . Out of  $N$  channels some of them are occupied by primary users (dark blocks in Fig.3.2) and some of them are empty (white blocks in Fig.3.2). Let  $S$  denotes the number of occupied channels and  $S \ll N$ . Hence in our system we assume  $N \gg M \gg S$ . We refer to  $S/N$  as sparsity. The sensing devices in our architecture can be seen as a unit having the combination of band-pass filters tapped at different bands.

---

<sup>1</sup>The terms sensing device and cognitive radio have been used interchangeably in this work

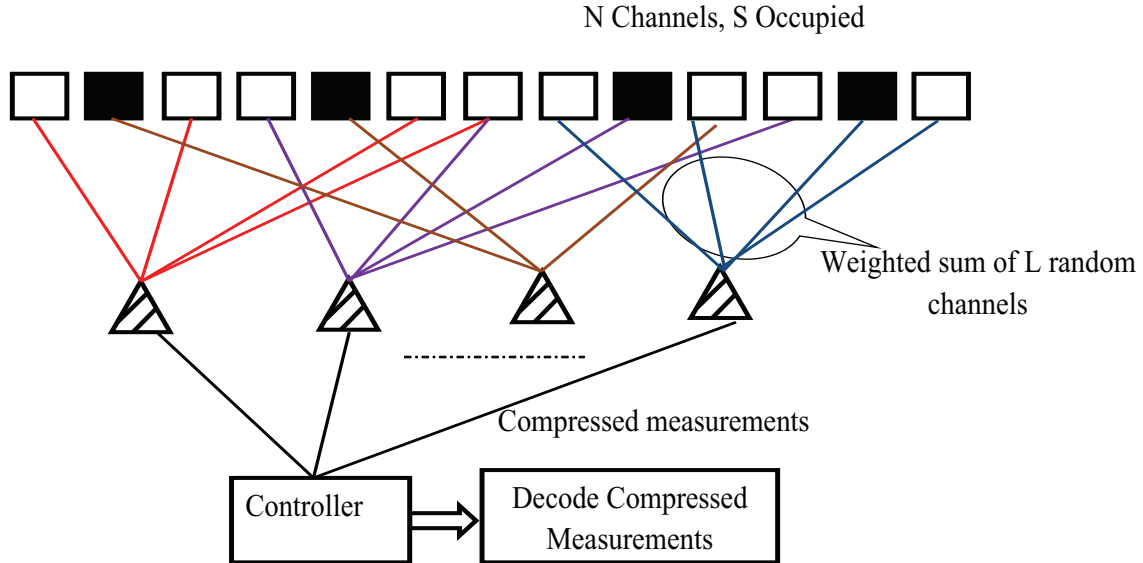


Figure 3.2: System Model

### 3.4 Proposed Compressive Spectrum Sensing

Let  $X = [x_i]_{N \times 1}$  be the signal component test statistics of  $N$  channels. If we denote the sensing matrix as  $\Phi_{M \times N}$  and  $Y = [y_i]_{M \times 1}$  as the compressed measurements, then,

$$Y = \Phi \times X. \quad (3.10)$$

#### 3.4.1 Generation of Sensing Matrix $\Phi$

In previous works [35, 30], the mathematical models of compressive sensing has been explained thoroughly. From the implementation point of view, the physical realization of sensing matrix  $\Phi$  is an important issue. The sensing matrix  $\Phi_{M \times N}$  in our model is the element-wise combination of the two matrices: Frequency selective matrix  $F_{M \times N}$  and channel response matrix  $H_{M \times N}$ . i.e

$$\Phi = F(\cdot \star)H, \quad (3.11)$$

where,  $(\cdot \star)$  represents element wise product. We consider each of the  $M_s$  sensing device/CR consists of  $m_s$  filter banks where each filter bank is collection of random

bandpass filter tapped at  $L$  random bands. For simplicity, we assume the filters are ideal with unity gain and zero phase. Hence,  $F$  is a binary matrix with constant row weight  $L$  and it is characterized by the following expressions:

$$\sum_{n=1}^N F_{m,n} = L \quad ; m = 1, 2, 3 \dots M, \quad (3.12)$$

Also, if  $L_m$  denotes the the set of band index of the filters in the  $m^{\text{th}}$  frequency selective filter bank, then:

$$F_{m,n} = 1 \quad ; \text{if, } n \in L_m, \quad (3.13)$$

$$\text{else, } F_{m,n} = 0. \quad (3.14)$$

Similarly, the channel response matrix is defined by:

$$H = |h_{m,n}|, \quad (3.15)$$

$$m = \{1, 2, \dots M\} \quad \text{and} \quad n = \{1, 2, \dots N\},$$

where,  $|h_{m,n}|$  is the channel response between  $m^{\text{th}}$  sensing device and the  $n^{\text{th}}$  primary signal, and is function of the channel modeling. In our simulations, we model the channel characteristics as the distance gradient model and assume we have complete channel state information (CSI) [49]. From (3.11) and (3.13), we can have :

$$\Phi_{m,n} = F_{m,n} \times H_{m,n} \quad ; \text{if } F_{m,n} = 1, \quad (3.16)$$

$$\text{else, } \Phi_{m,n} = 0. \quad (3.17)$$

Hence, the sensing matrix  $\Phi$  is a constant row weight matrix.

### 3.4.2 Compressed Measurements

Each element of measurement vector  $Y$  is the weighted sum of  $L$  elements of  $X$  as given by (3.18), where the  $i^{\text{th}}$  element of  $Y$ ,  $y_i$ , is given by:

$$\forall i = 1, 2, 3, \dots M, \quad y_i = \sum \Phi_{i,j} \times x_j, \quad j = 1, 2, 3 \dots N, \quad j \in L_i, \quad (3.18)$$

where,  $\Phi_{i,j} = 0$ , if  $F_{i,j} = 0$ , else,  $\Phi_{i,j} = F_{i,j} \times G_{i,j}$ , We know that the the Filter Matrix is constant row weight matrix with row weight  $L$  and accordingly,  $\Phi$  is a also a constant row weight matrix with row weight  $L$ . Hence, each compressed measurement is the weighted sum of the  $L$  elements of  $X$ .

If we consider the transmission channel from sensing device to controller is noisy, then the measurement  $Y$  is effected by noise as:

$$Y = \Phi \times X + W, \quad (3.19)$$

where,  $W$  is the additive gaussian noise of zero mean and variance  $\sigma_w^2$ .

### 3.4.3 Compressive Decoding

Compressive sensing (CS) decoding techniques based on optimization algorithms with  $l_1$  minimization (Basis Pursuit) is discussed in [30, 32]. We implement Basis Pursuit and Orthogonal Matching Pursuit in this problem to observe the performance in the spectrum detection. CS decoding based on  $l_1$  minimization is as follows:

$$\hat{X} = \underset{X}{\operatorname{argmin}} \|X\|_1, \quad \text{s.t. } Y = \Phi X. \quad (3.20)$$

In case of noisy measurements the constraint is modified as:

$$\|Y - \Phi X\|_2 \leq \delta, \quad (3.21)$$

where,  $\delta$  is the noise energy. We also implement the compressive decoding technique based upon the greedy pursuit called Orthogonal Matching Pursuit (OMP) [33, 34, 35]. A greedy algorithm computes the support of  $X$  iteratively. The steps in the OMP can be summarized in following procedure.

Given:  $M \times N$  measurement matrix  $\Phi$ ,  $M$ , length compressed measurements  $Y$  of  $N$  long vector  $X$ .

1. Normalize  $\Phi$  such that each column of  $\Phi$ ,  $(\Phi_i)$  has unit norm. i.e  $\|\Phi_i\|_2 = 1$ .

2. Initialize residual:  $r_0 = Y$ , Index set ( $Col$ ), count, ( $t = 1$ ) and empty set  $\Theta_0$ .
3. Find the index  $I_t$  that solves:

$$I_t = \underset{i}{\operatorname{argmax}} | \langle r_{t-1}, \Phi_i \rangle |, \quad i = 1 : N.$$

4. Modify Index set and empty set  $Col_{(t)} = Col_{(t-1)} \cup I_t$  and  $\Theta_t = [\Theta_{t-1} \dots \Theta_t]$ .
5. Solve least square problem to obtain signal estimate,

$$X_t = \underset{X}{\operatorname{argmin}} \|\Theta_t X - Y\|_2. \quad (3.22)$$

6. Calculate new residual,

$$r_t = Y - \Theta_t X_t \quad (3.23)$$

7. Increment count:  $t = t + 1$  and go to step 3.

OMP is an iterative based method. At each step, the residual is modified and new supports of the signal are determined. These steps are repeated until minimum residual value threshold is met or up to predefined numbers of iteration. In our simulations, we implement  $l_1$  minimization (Basis Pursuit) and the orthogonal matching pursuit for the spectrum detection. An improved version of  $l_1$  minimization termed as weighted  $l_1$  minimization is developed in [53, 54]. In weighted  $l_1$ , the weight to each component of the signal vector is introduced. The use of weights is to counter influence the signal magnitude on the minimization function. The large weights are used to discourage non-zero entries and vice versa. One of the possible weight functions for this case may be the inverse function of the signal component. The re-weighted  $l_1$  minimization scheme developed in [53] can be summarized as following.

1. Set the iteration count,  $l = 0$  and weight,  $v_i^0 = 1; i = 1, 2 \dots N$
2. Solve the  $l_1$  minimization problem,

$$x^l = \underset{X}{\operatorname{argmin}} \|V^{(l)} X\|_{l_1}, \text{ Subject to : } Y = \Phi X \quad (3.24)$$

3. Update weights,

$$v_i^{(l+1)} = \frac{1}{|x_i^l| + \epsilon} \quad (3.25)$$

where,  $\epsilon$  is small positive number slightly greater than the smallest sparse element in  $X$ .

4. If iteration count  $l = \text{maximum iteration}$ , Terminate, else go to step 2.

The re-weighted  $l_1$  process improves the reconstruction performance. However, it is an iterative  $l_1$  process, hence the performance gain is achieved at a cost of decoding time. The  $l_1$  minimization process has to be repeated in every iteration for every modified weight values. This accounts for the delay in reconstruction process and spectrum detection.

### 3.5 Simulation and Results

For our experimental simulation we take  $N = 1000$ . We take measurements at different rate from 10% to 40% of total signal length. The results provided are the average of 10000 simulations under different signal strength values and different random measurement matrices keeping sparsity (S/N) and other characteristics are same. We consider two different simulation scenarios with sparsity 5 % and 10%. Moreover, we observe the results in two different channels i.e. noiseless and noisy channels with noise energy of 20 dB. Following parameters are defined for the performance measurement.

- **Sampling Rate** ( $S.R = \frac{M}{N}\%$ ): Sampling rate is defined as the ratio of the number of compressed measurements to the total number of channels. S.R is represented in % as well.
- **Probability Of Detection (POD)**: It is the ratio of total number of hits to the sums of total hits and miss. Hit is an event when we decide the presence or



absence of primary user correctly, whereas, any other wrong decision is termed as miss event. For an illustration let us consider,  $B$  and  $E$  denote busy and empty state of channel respectively, and  $H$  and  $M$  denote Hits and Miss. The following table shows an example of Hit and a Miss detection.

$$\begin{bmatrix} B & E & B & E \\ B & B & E & E \\ H & M & M & H \end{bmatrix}$$

- **Error of Reconstruction (EOR):** EOR is the ratio of energy difference between reconstructed and original signal to the energy of the original signal.

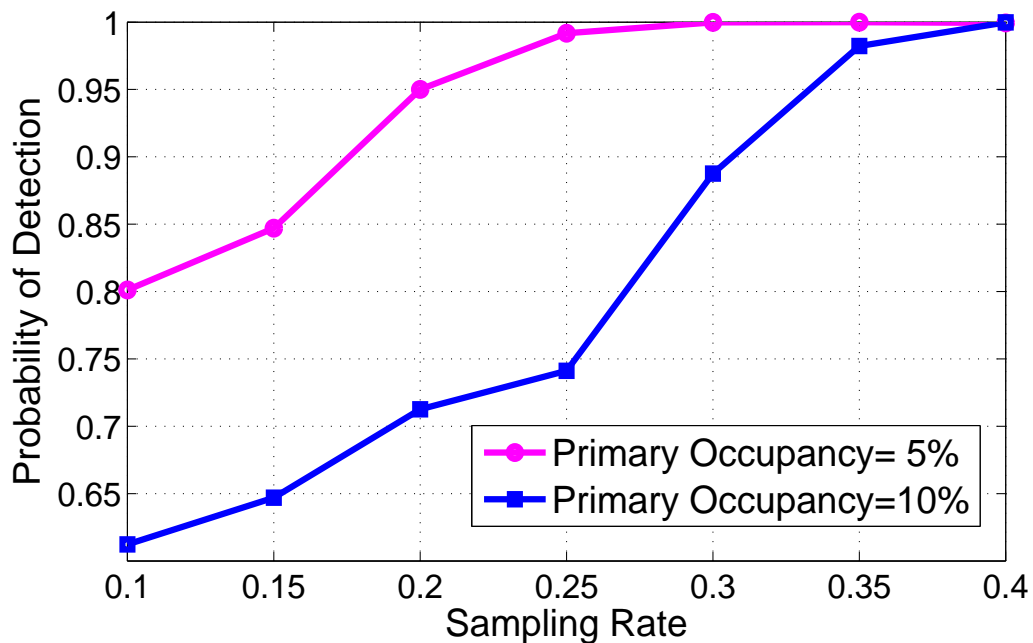


Figure 3.3: Probability of Detection in Noiseless Measurements

Figs. 3.3 through 3.6 depict our simulation results for  $l_1$  minimization and OMP method for different primary users occupancy rate. We can clearly see from our results for the noiseless measurements that different decoding algorithms provide different performance levels for our system. The POD using OMP for 5% primary occupancy

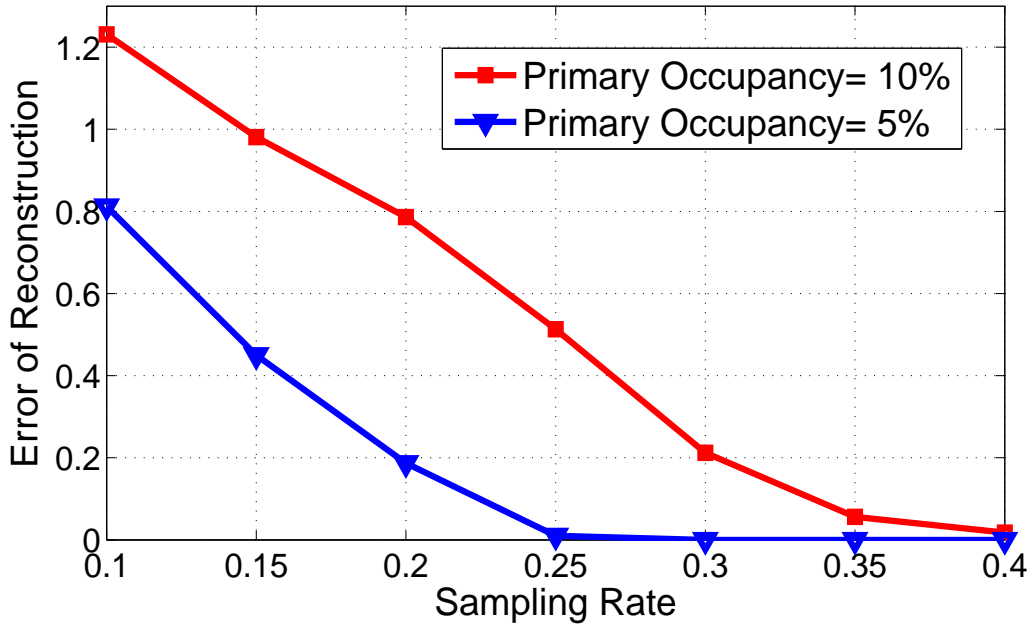


Figure 3.4: Error Of Reconstruction in Noiseless Measurements

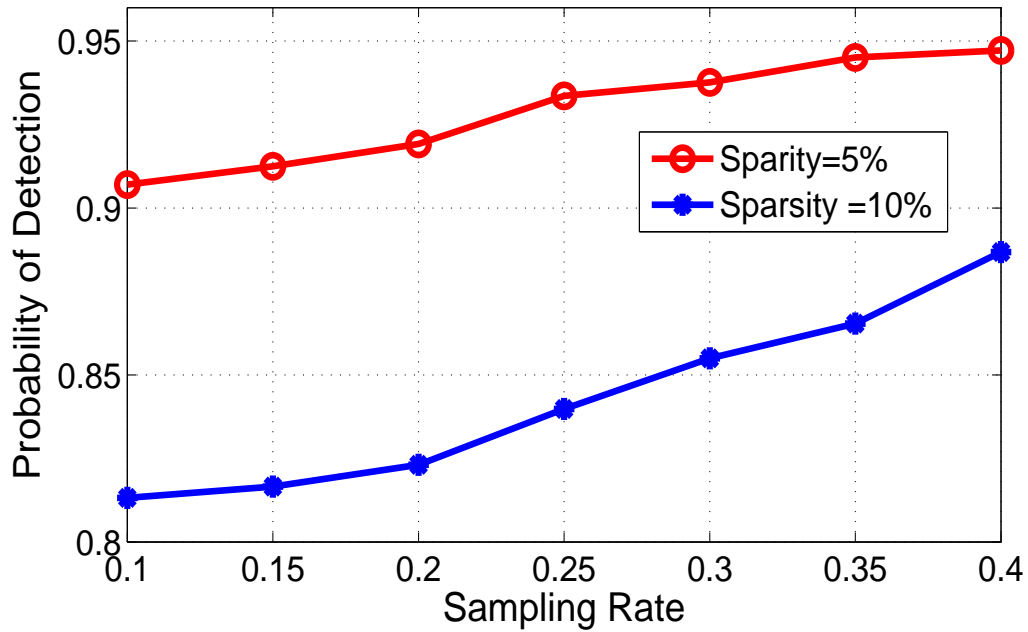


Figure 3.5: Probability of Detection in Noiseless Measurements using OMP

is about 0.95 at sampling rate of 40%. OMP is comparatively less efficient compared to  $l_1$  minimization.  $l_1$  method has high POD increase rate as we increase the sampling

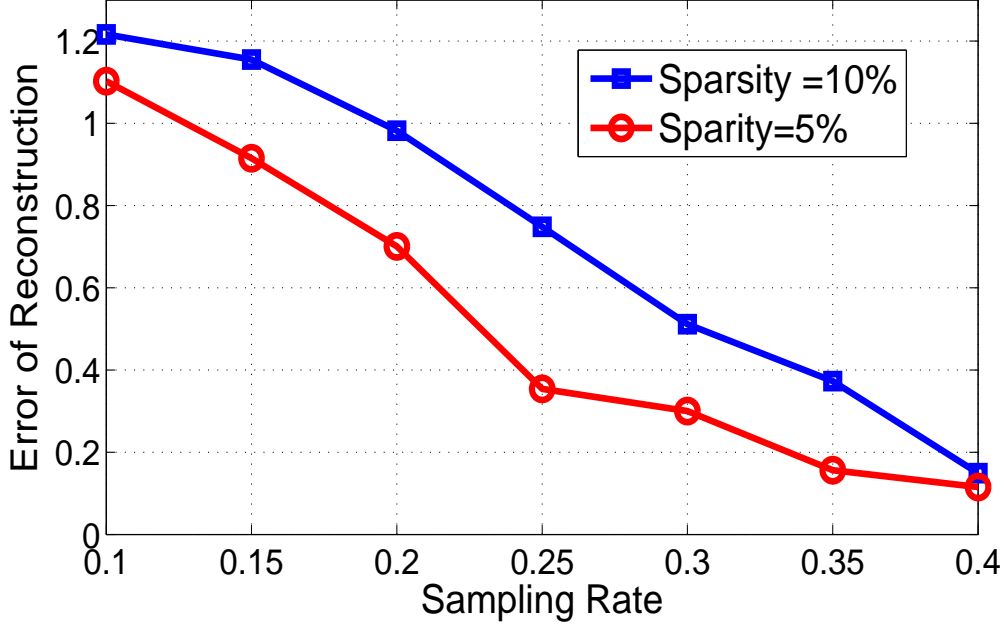


Figure 3.6: Error Of Reconstruction in Noiseless Measurements using OMP

rate. For sampling rate as low as 25%, we get POD close to 1. For a signal of 10% occupancy, the number of measurements required for successful decoding increases compared to that of 5% occupancy. Figs. 3.4 and 3.6 show the over all error in energy of the reconstructed signal using  $l_1$  and OMP, respectively.

Figs. 3.7 and 3.8 shows the performance measurement comparison for noisy and noiseless measurement in 10% primary occupancy, using  $l_1$  minimization method. We can clearly see that POD and EOR deteriorates in noisy measurements but still more than 90% of spectrum is detected with sampling rate as low as 40% and overall error in energy is about 0.1

In Figs. 3.9 and 3.10, we clearly see that the reweighted  $l_1$  minimization improves the performance in terms of both reconstruction detection probability and reconstruction energy error. The performance gain is achieved in reweighted scheme because in each iteration, the higher value of weight suppresses the zero components and lower value of weight estimates non zero components of the signal more closely to their

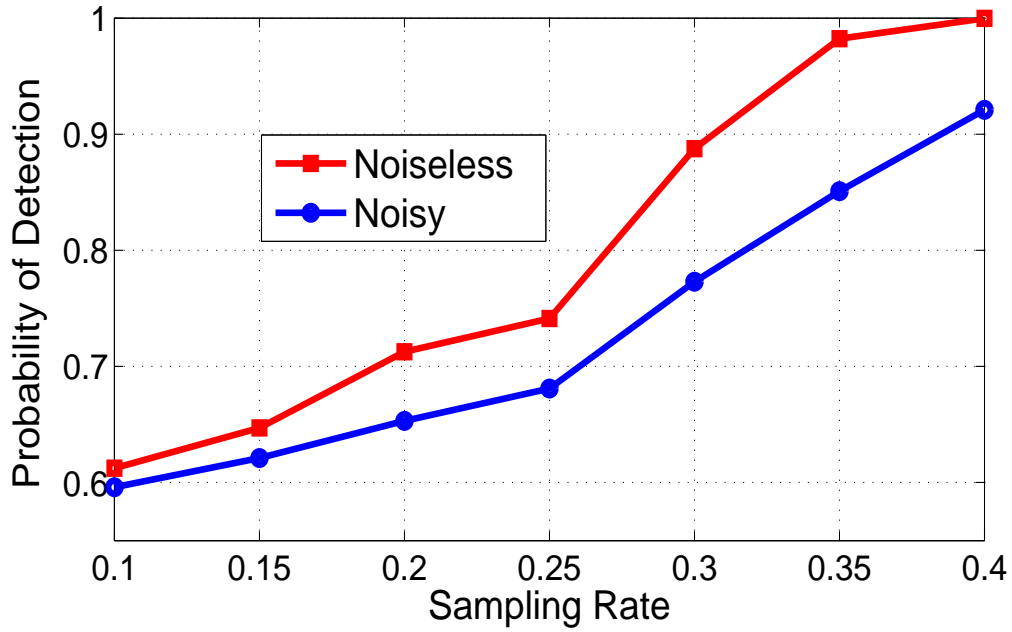


Figure 3.7: Probability of Detection in Noisy Measurements

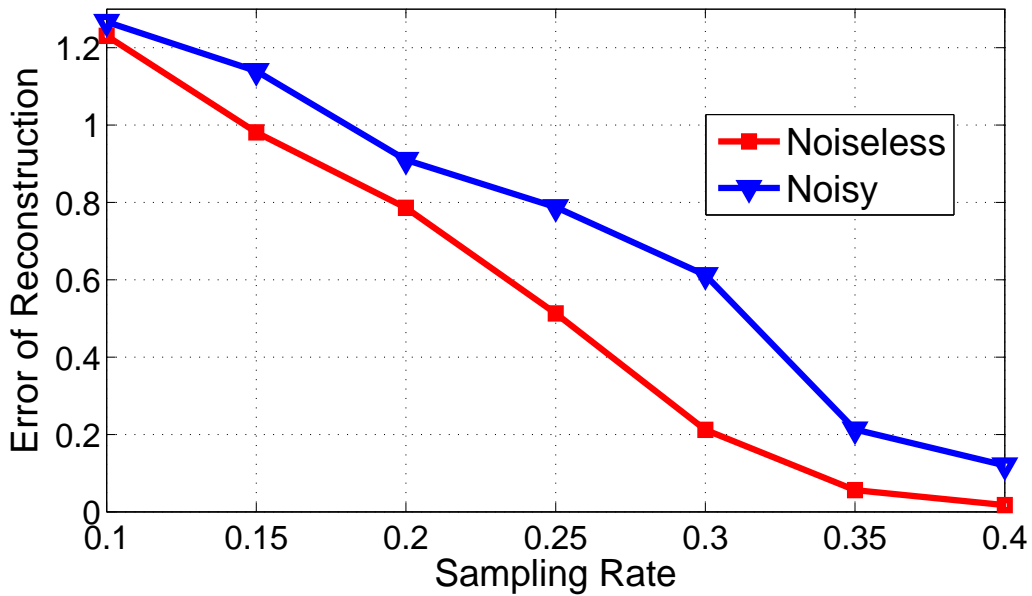


Figure 3.8: Error of Reconstruction in Noisy Measurements

actual value. For this reason we choose the weight of each element to be the inverse of its approximated value in each iteration. However, the reweighted  $l_1$  minimization requires more computational complexity and decoding time because the minimization

process has to be repeated at every iteration for the modified weights.

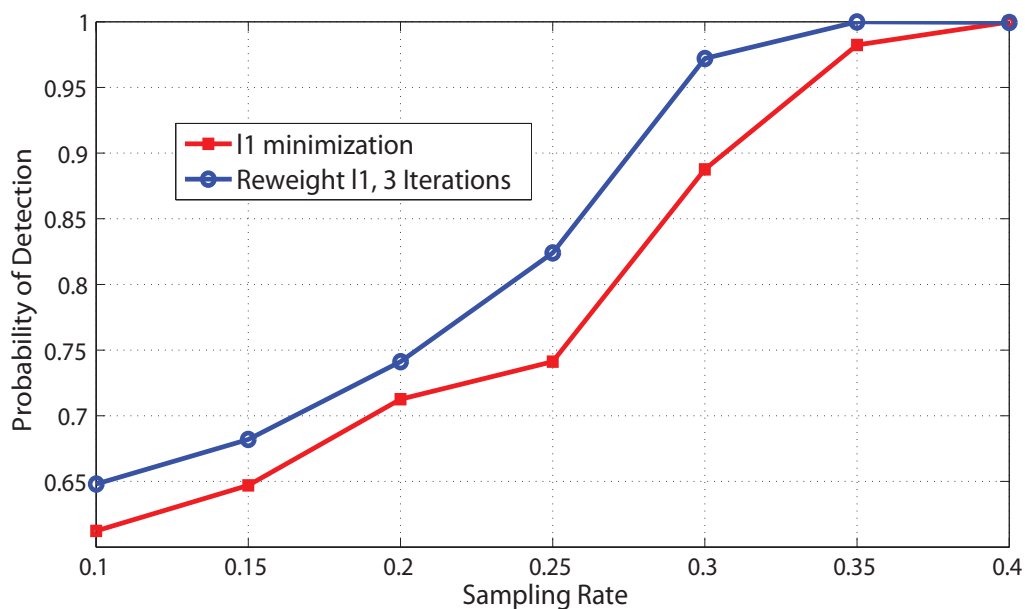


Figure 3.9: Probability of Detection using Reweighted  $l_1$  Minimization

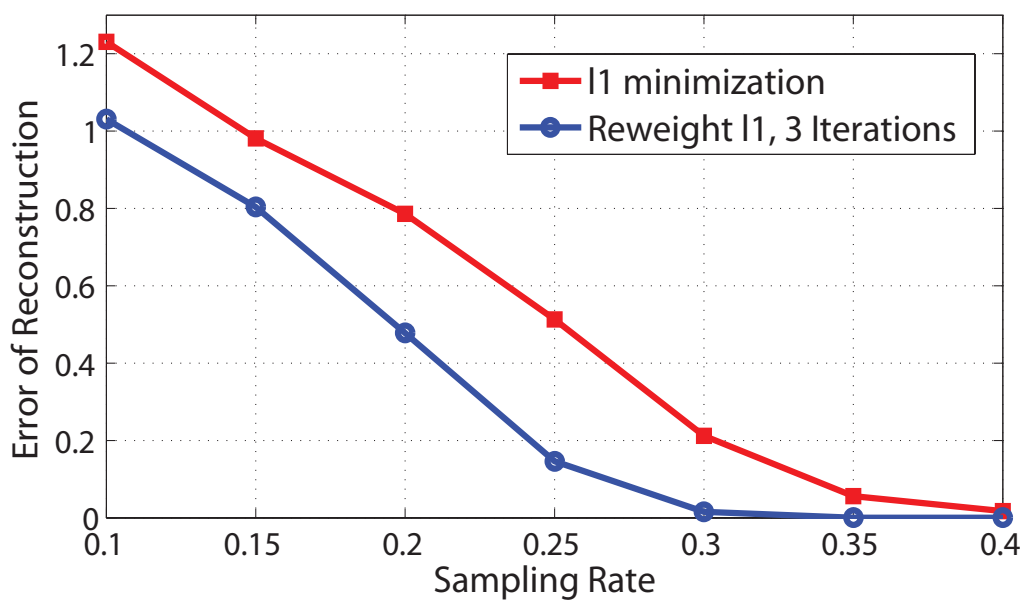


Figure 3.10: Error of Reconstruction using Reweighted  $l_1$  Minimization

### 3.6 Conclusion

In this chapter, we proposed a spectrum management architecture for cognitive radios using compressive sensing technique. We evaluated our scheme with different simulations using different decoding algorithms and channel cases. The advantage of our architecture is that, not only we reduce the total number of reports sent to the controller using compressive sensing but also show that the Probability of Detection (POD) at the controller is improved. We also showed that our architecture can also perform efficiently for spectrum sensing in noisy measurements by increasing the sampling rate. Reweighted  $l_1$  scheme is used to improve the performance in the spectrum sensing. In totality, the proposed architecture significantly enhances the spectrum sensing for cognitive radio networks. This chapter also lays the foundation for the concept of overlapping networks in the Chapter 4. The basic spectrum sensing scenario presented in this chapter is extended into the system where more than one network exists and networks overlap in their operating region in geo-spatial and frequency domain.

## CHAPTER 4

# JOINT WIDE BAND SPECTRUM SENSING IN FREQUENCY OVERLAPPING COGNITIVE RADIO NETWORK USING DISTRIBUTED COMPRESSIVE SENSING

### 4.1 Introduction

The NTIA's frequency allocation chart [55] shows many networks overlap in the frequency zone because of spectrum scarcity. The spectrum overlapping or jointly sparse frequency overlapping networks in cognitive radio network come into picture because of spatial diversity of primary and secondary transmission power [56]. In conventional spectrum sensing approaches, it is considered that all the CRs are silent and synchronized during the sensing period. In large overlapping networks, or in spatially distant CRs, synchronization cannot be guaranteed due to spatial diversity of primary transmission power [56]. This creates jointly sparse frequency overlapping networks over large spatial domain. In this chapter, we extend our work in the Chapter 3 and propose joint reconstruction for wideband spectrum sensing in such frequency overlapping networks using distributed compressive sensing. We extend our work in wideband compressive sensing for cognitive radios [57] into a frequency overlapping network and present joint reconstruction scheme for spectrum sensing in frequency overlapping networks.

The rest of the chapter is structured as follows. In the Section 4.2, we introduce the frequency overlapping network and formulate the spectrum sensing problem for it. We propose joint compressive sensing scheme for jointly sparse frequency overlapping cognitive radio networks. Individual reconstruction scheme and joint reconstruction

for the compressed measurement are presented and compared. Section 4.3 provides simulation results for the proposed joint wideband spectrum sensing in frequency overlapping networks and finally, Section 4.4 concludes the chapter.

## 4.2 Proposed Wideband Compressive Spectrum Sensing in Frequency Overlapping Networks

The NTIA's frequency allocation chart clearly shows the frequency overlapping over different system protocols to meet the band scarcity issue. Let us consider two network systems  $S_1$  and  $S_2$  with some overlapping operating bands as shown in Fig. 4.1. We call the networks  $S_1$  and  $S_2$  as the frequency overlapping networks and denote it with network  $H_N$ . The theoretical backgrounds on joint sparse signal can be found in literatures [58, 59]. Let  $B_{s1}$  and  $B_{s2}$  represent the spectrum band of  $S_1$  and  $S_2$  respectively, where  $|B_{s1}| = N_1$  and  $|B_{s2}| = N_2$ .  $B_{sc}$  denotes the frequency overlapping between  $S_1$  and  $S_2$  and  $|B_{sc}| = N_c$ . The total number of bands (channels) under consideration is :  $N_T = N_1 + N_2 - N_c$ . In jointly sparse frequency overlapping networks, for each of the network, (3.7), takes the form of:

$$y_{if}^{(m)} = \sum_{s \in \hat{S}_i} \mathbf{D}_{gi}^{(sm)}(x_{if}^{(s)} + x_{cf}^{(s)}) + w_f^m, \quad (4.1)$$

where,  $i = 1, 2$  refers to corresponding network,  $x_{if}^{(s)}$  and  $x_{cf}^{(s)}$ , denote the spectral innovation of  $i^{th}$  network and joint sparse portion, respectively, as illustrated in the Fig. 4.1, and all other notations have same meaning as in (3.7). We consider, each of the network consists of  $M_s$  sensing devices and each sensing device takes  $m_s$  compressed measurements. So total number of measurements taken in each network =  $M_s \times m_s = M$ .

Let  $X_1 = [x_i^{(1)}]_{N_1 \times 1}$  and  $X_{(2)} = [x_i^{(2)}]_{N_2 \times 1}$  represent the test statistic for the spectrum sensing in two networks  $S_1$  and  $S_2$  respectively and  $X_{(c)} = [x_i^{(c)}]_{N_c \times 1}$  represents that of overlapping portion. A vector  $V$  of length  $N$  is said to be  $K$  sparse if  $V$  contains



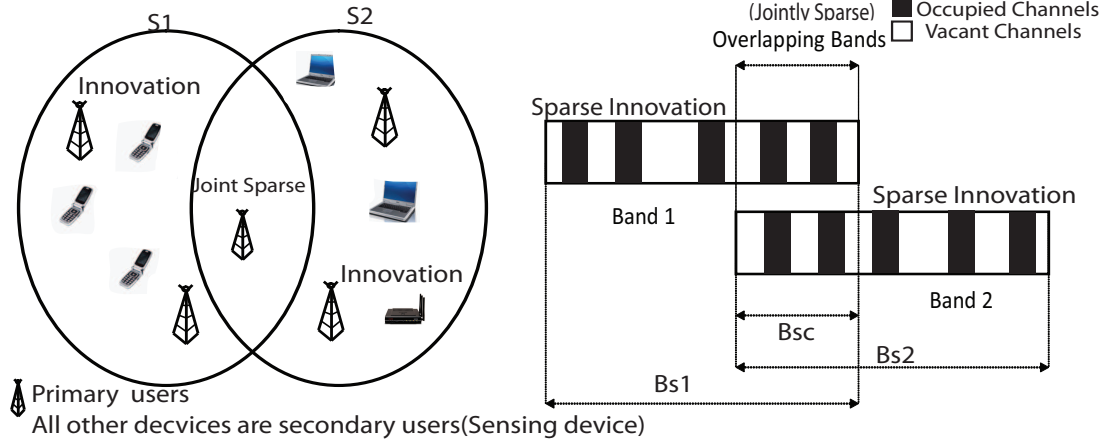


Figure 4.1: Schematic of overlapping networks and overlapping spectrum bands

only  $K$  non-zero elements, i.e.  $\|V\|_{l_0} = K$ , where,  $l_0$  denotes norm zero. Also, the support of a vector,  $V = [v_i]_{N \times 1}$  is defined as:  $supp(V) = \{i, v_i \neq 0, i = 1, 2, \dots, N\}$ . Let,  $|supp(X_1)| = K_1$  and  $|supp(X_2)| = K_2$ .  $K_1$  and  $K_2$  denote number of occupied channels in network 1 and 2, respectively. It should be noted that in spectrum sensing for cognitive radios, our objective is to find the  $supp(X_1)$  and  $supp(X_2)$  and hence detect primary users and find the spectrum holes.

In compressive sensing, it is the method of data acquisition which makes it distinct from conventional sampling approaches. In the following subsections, we describe the sampling approach, the structure of sparse sampling matrix  $\Phi$ , data acquisition techniques and decoding approaches.

#### 4.2.1 Sensing Matrix $\Phi$

In previous works [35, 30] the mathematical models of compressive sensing have been explained thoroughly. From the implementation point of view the physical realization of sampling matrix  $\Phi$  is an important issue. The sensing matrix  $\Phi_{M \times N}$  in our model is the element-wise combination of the two matrices: random frequency selective matrix

$F_{M \times N}$  and channel response matrix  $H_{M \times N}$ . i.e

$$\Phi = F(\cdot \star)H, \quad (4.2)$$

where,  $(\cdot \star)$  represent element wise product. We consider each of the  $M_s$  sensing device/CR consists of  $m_s$  filter banks, where  $M_s \times m_s = M$ . Each filter bank is collection of random bandpass filter tapped at  $L$  random bands. For simplicity, we assume the filters are ideal filters with unity gain and zero phase. Hence,  $F$  is a binary matrix with constant row weight  $L$ . Also, if  $L_m$  denotes the the set of band index of the filters in the  $m^{th}$  frequency selective filter bank, then:

$$F_{m,n} = 1 \quad ; \text{if, } n \in L_m, \quad (4.3)$$

$$\text{else, } F_{m,n} = 0. \quad (4.4)$$

Similarly, the channel response matrix is defined by:

$$H = h_{m,n}, \quad m = 1, 2, \dots M \quad \text{and} \quad n = 1, 2, \dots N, \quad (4.5)$$

where,  $h_{m,n}$  is the channel response between  $m^{th}$  sensing device and the  $n^{th}$  primary signal, and is function of the channel modeling. From (4.2) and (4.3), we can have :

$$\Phi_{m,n} = F_{m,n} \times H_{m,n} \quad ; \text{if } F_{m,n} = 1, \quad (4.6)$$

$$\text{else, } \Phi_{m,n} = 0. \quad (4.7)$$

Hence, the sensing matrix  $\Phi$  is a constant row weight matrix.

#### 4.2.2 Compressed Measurement $Y$

Let the sensing matrix  $\Phi$  for network systems  $S_1$  and  $S_2$  be represented by  $[\Phi_1]_{M_1 \times N_1}$  and  $[\Phi_2]_{M_2 \times N_2}$  respectively, with the characteristics as explained in Section 4.2.1. For ease in calculation, we assume  $M = M_1 = M_2$  and  $N_1 = N_2 = N$ . Each sensing device samples the spectrum bands in the corresponding network system in  $S_1$  and  $S_2$ .

Each sensing device gives  $m_s$  compressed measurements and each network consists of  $M_s$  sensing devices. For each system the total number of compressed measurements sent to the individual controller unit is then  $M = M_s \times m_s$ . The  $i^{th}$  compressive measurement at  $m^{th}$  sensing device is given by:

$$y_m^{(i)} = \Phi_{(m,:)} \times X, \quad (4.8)$$

$i = 1, 2 \dots m_s, m = 1 : \text{number of sensing devices } (M_s)$  Hence,  $Y_1$  and  $Y_2$ , denoting the compressed measurement at network system 1 and 2 respectively, can be written as:

$$Y_i = \Phi_i \times X_i; \quad i = 1, 2. \quad (4.9)$$

Similarly, in case of the noisy measurements, it is affected with additive white gaussian noise of zero mean and variance  $\sigma^2$ ,  $W(0, \sigma^2)$ .

$$Y_i = \Phi_i \times X_i + W_i; \quad i = 1, 2. \quad (4.10)$$

### 4.2.3 Compressive Sensing Decoding

The solution to the compressive sensing decoding is an optimization problem. CS decoding algorithm based upon the norm optimization like Basis pursuit ( $l_1$ ) minimization is discussed in [32, 30, 60].

In the followings, we first provide a quick reference to individual compressive spectrum sensing and individual reconstruction, and then we illustrate the joint reconstruction scheme for the frequency overlapping networks.

#### Individual Reconstruction

In individual reconstruction scheme, each network reconstructs its compressively sensed test statistics individually without cooperating with other networks and the decision about the spectrum occupancy is made accordingly using thresholding [52].

The reconstructed test vector in individual reconstruction is give by:

$$\hat{X}_i = \arg \min \|X_i\|_{l_1} \quad s.t. \quad Y_i = \Phi_i X_i \quad ; i = 1, 2, \quad (4.11)$$

where as in case of the noisy measurements the optimization constraint is minimized as:

$$\|Y_i - \Phi_i X_i\|_2 \leq \sigma^2, \quad (4.12)$$

### Joint Reconstruction

The number of required measurements for CS reconstruction is a function of the sparsity of the signal. It has been shown that the number of samples required for the CS reconstruction is in the order of  $CK \log\left(\frac{N}{K}\right)$  [30, 59]. In overlapping networks, the individual reconstruction requires redundant numbers of samples for reconstruction. In individual reconstruction, the number of measurements required depends on  $(K_1 + K_2)$ . In [56], the LASSO algorithm with iterative user consensus is used to detect the overlapped bands. However, the advantage of common sparse elements in joint reconstruction is not exploited, and individual reconstruction is required in each network. In joint reconstruction, the number of measurements required for reconstruction depends on  $(K_1 + K_2 - K_c = K_T)$ . It has been shown that the the number of required measurements for CS reconstruction depends upon the sparsity, hence the joint reconstruction will have the measurement gain. Moreover, only one joint optimization is performed for the reconstruction of the both networks. We implement joint reconstruction scheme for spectrum sensing in frequency overlapping networks and compare it with the conventional individual reconstruction scheme and the iterative LASSO consensus algorithm [56]. In joint reconstruction scheme, cognitive users in each network take the compressed measurements of spectrum in their network. The CS measurements are sent to a common controller unit. The schematic of joint spectrum sensing and reconstruction in frequency overlapping network is shown in the Fig. 4.2. The dark boxes represent the occupied channels whereas, white boxes

represent spectrum holes.

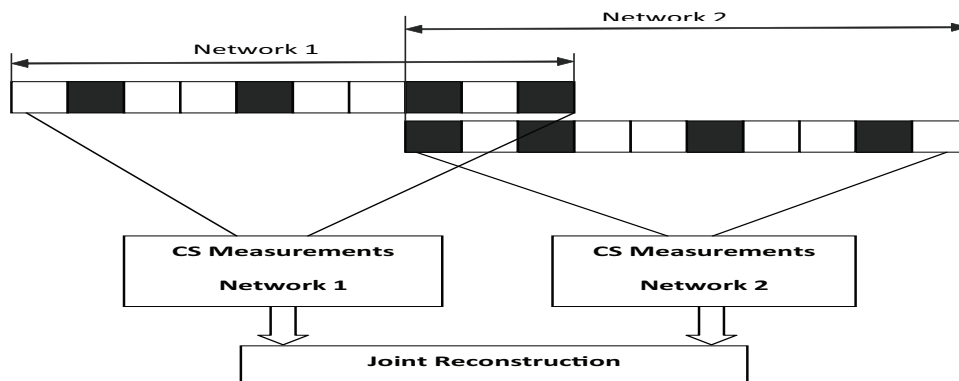


Figure 4.2: Joint spectrum sensing schematic in frequency overlapping networks

Let the measurements for the joint reconstruction be denoted by  $Y$  as,

$$Y = \begin{bmatrix} Y_1 \\ Y_2 \end{bmatrix}, \quad (4.13)$$

where,  $Y_1$  and  $Y_2$  are compressed measurements of networks  $S_1$  and  $S_2$ , respectively.

Joint reconstruction matrix  $\Phi_{joint}$  for reconstruction of the spectrum test statistics,

$$X := \begin{bmatrix} X_{i1} \\ X_c \\ X_{i2} \end{bmatrix},$$

be represented as:

$$\Phi_{joint} = \begin{bmatrix} \Phi_A & \Phi_{C_1} & \Phi_{null} \\ \Phi_{null} & \Phi_{C_2} & \Phi_B \end{bmatrix}. \quad (4.14)$$

If  $I_c$  denotes the set of the overlapping bands of two networks,  $\hat{X}_{i1}$  and  $\hat{X}_{i2}$  denote innovation bands of network 1 and 2 respectively, and  $(\phi)_j$  denotes the  $j^{th}$  column of

the  $\Phi$ , then :

$$\begin{aligned}
\Phi_A &= (\Phi_1)_j & j \in \hat{X}_{i1}, \\
\Phi_B &= (\Phi_2)_j & j \in \hat{X}_{i2}, \\
\Phi_{C_1} &= (\Phi_1)_j & j \in I_c, \\
\Phi_{C_2} &= (\Phi_2)_j & j \in I_c,
\end{aligned} \tag{4.15}$$

and  $\Phi_{null}$  are null matrices. Then the joint reconstruction optimization for  $X$  is performed as:

$$\hat{X} = \arg \min \|X\|_{l_1} \quad s.t. \quad Y = \Phi_{joint} \times X. \tag{4.16}$$

In case of noisy measurements the constraint of optimization is modified accordingly as in (4.12).

### 4.3 Simulation and Results

For evaluating our performance we define following performance measurement parameters.

#### Performance Measurement and Simulation Parameters

- **Sampling Rate** ( $S.R = \frac{2M}{N_T}$ ): Sampling rate is defined as the ratio of the number of compressed measurements to the total number of channels.
- **Probability Of Detection (POD)**: It is the ratio of total number of hits to the sums of total hits and miss. Hit is an event when we decide the presence or absence of primary user correctly, whereas, any other wrong decision is termed as miss event.
- **Error of Reconstruction (EOR)**: EOR is the ratio of energy difference between reconstructed and original signal to the energy of the original signal.

- **Sparse Overlapping Factor** ( $SOF = \frac{K_c}{K_T}$ ): SOF is the ratio of number of occupied channels in the overlapping bands to the total number of occupied channels in the network.
- **Measurement Gain (MG)**: For the given probability of detection, measurement gain is defined as:

$$MG = 1 - \frac{\# \text{ of measurements required in joint reconstruction}}{\# \text{ of measurements required in individual reconstruction}}$$

For simulation purpose we take total number of channels,  $N_T = 1000$ , out of which,  $N_c = 30\%$  are overlapping, the sparsity, ( $\frac{K_T}{N_T} = 10\%$ ), and  $SOF = 0.5$  unless stated otherwise. Compressed measurements at different sampling rate are obtained and reconstructed. The results provided are the average of 1000 simulations. Both noisy and noiseless measurement schemes are simulated.

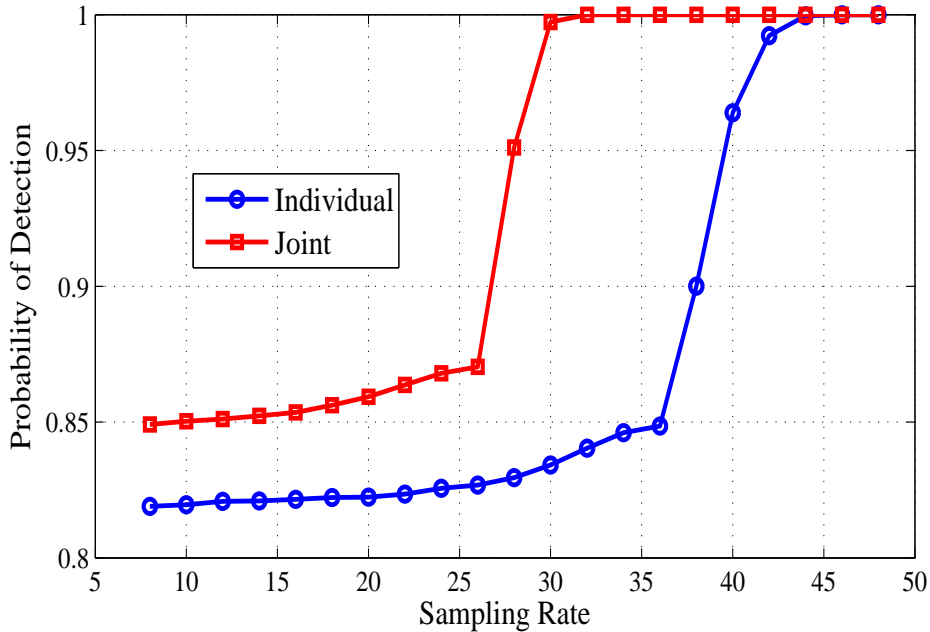


Figure 4.3: POD using individual and joint reconstruction

From Figs. 4.3 and 4.4, it is clearly observed that for the same number of compressed measurements, the joint reconstruction algorithm has better performance than the individual reconstruction. We see that the  $POD$  approaches 1 for joint

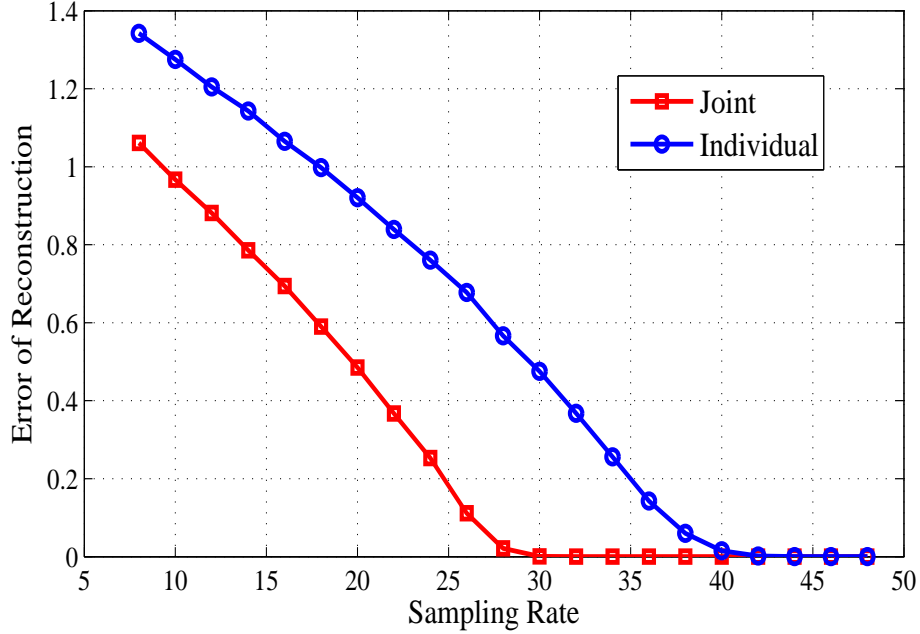


Figure 4.4: EOR using individual and joint reconstruction

reconstruction at sampling rate of 30% whereas it is at 44% for the individual reconstruction. This gain in measurements is the consequence of sparse overlapping elements and joint reconstruction. The *EOR* for joint reconstruction approaches to zero for the sampling rate of as low as 28% where as for that of individual reconstruction it occurs at 40%. We see that for same performance the joint reconstruction requires less number of samples. This reduces the data acquisition cost and the redundancies. Figs. 4.5 and 4.6 are the performance measurement under noisy measurements.



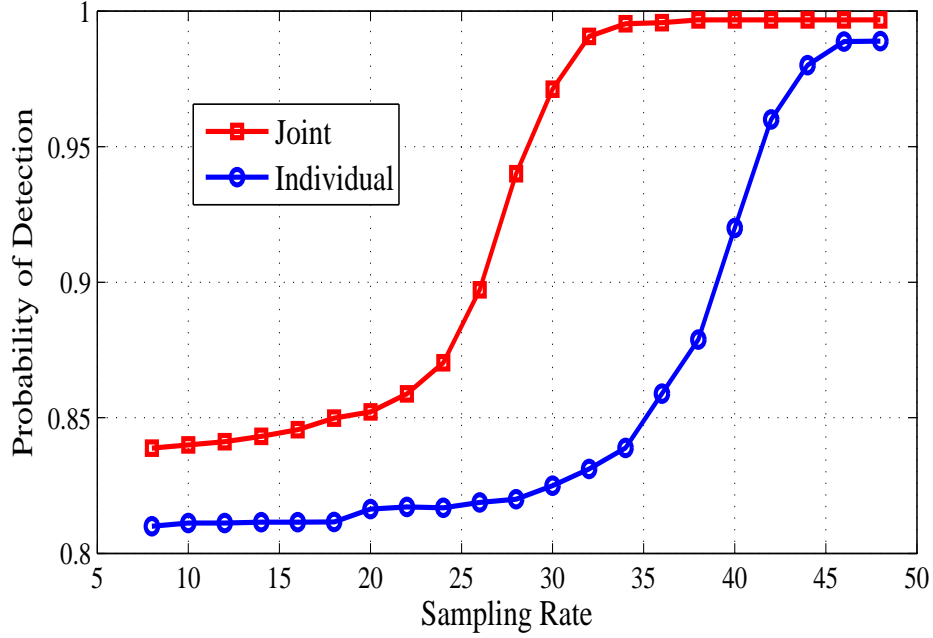


Figure 4.5: POD using individual and joint reconstruction in noisy measurements

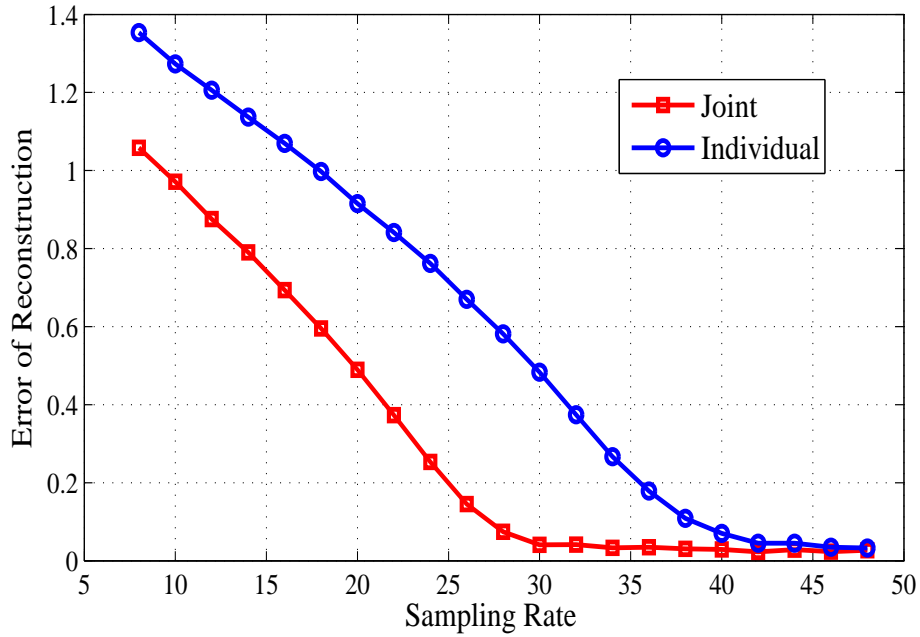


Figure 4.6: EOR using individual and joint reconstruction in noisy measurements

The performance under noisy measurements degrades both in terms of probability of detection and reconstruction error, however the joint reconstruction scheme still

performs better than the individual reconstruction. Fig. 4.7 shows the effect of the varying SOF on the measurement gain between the individual reconstruction and the joint reconstruction. It shows the measurement gain for  $POD = 0.99$ .

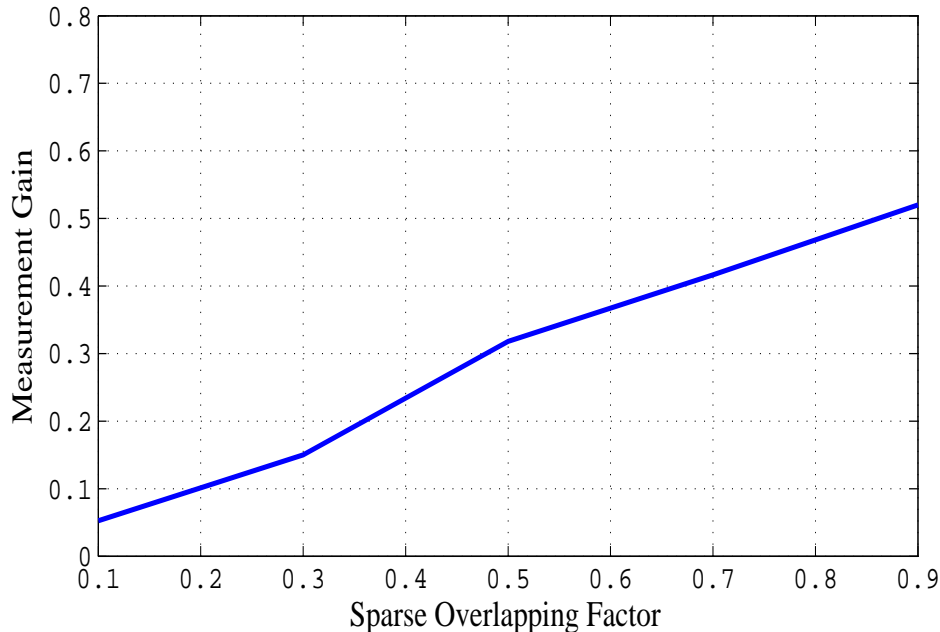


Figure 4.7: Measurement gain for varying SOF when  $POD=0.99$

We can clearly see that the measurement gain increases as the SOF increases. This implies that the number of measurements required in joint reconstruction for same performance decreases comparatively to individual reconstruction when there are more occupied channels in the overlapping region.

In the Fig. 4.8 we present the performance of joint reconstruction scheme in terms of probability of primary detection and false alarm rate. The Receiver Operating Characteristic (ROC) curve for different SNR is presented. It is clearly seen that the ROC have good performance for low false alarm rate and depends on the SNR. We compare our performance with the iterative LASSO consensus scheme in [56]. In [56], the frequency overlapping scheme is illustrated using multihop cognitive network. Fig. 4.9 is the *Receiver operating characteristics (ROC)* comparison and Fig. 4.10

shows the comparison of reconstruction error. We clearly observe that the joint reconstruction scheme has better receiver operating characteristics where as the error of reconstruction is comparable to that of in iterative LASSO consensus.

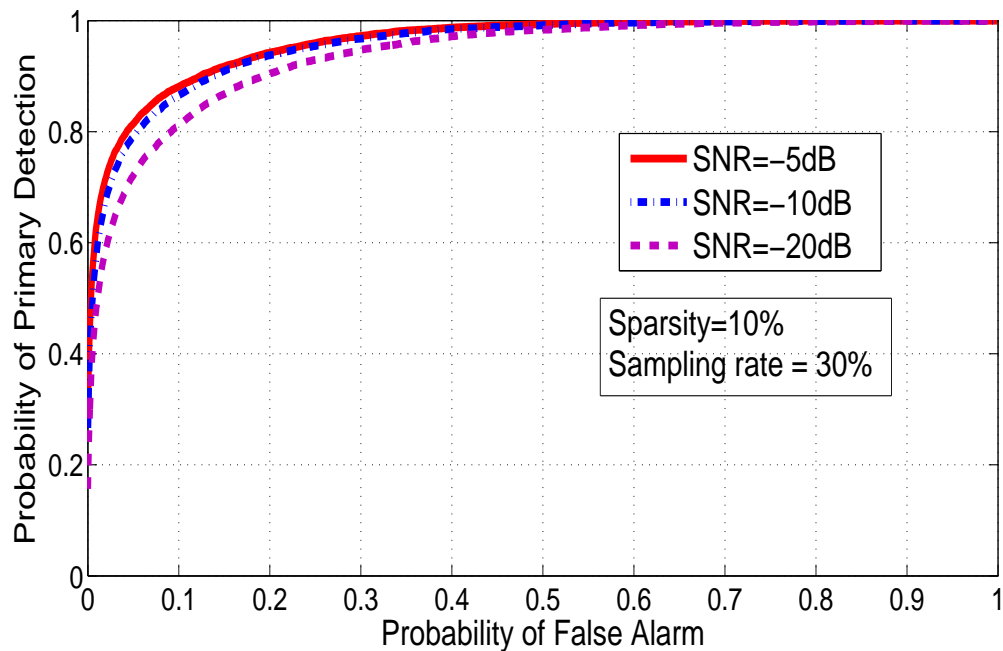


Figure 4.8: ROC performance for different SNR

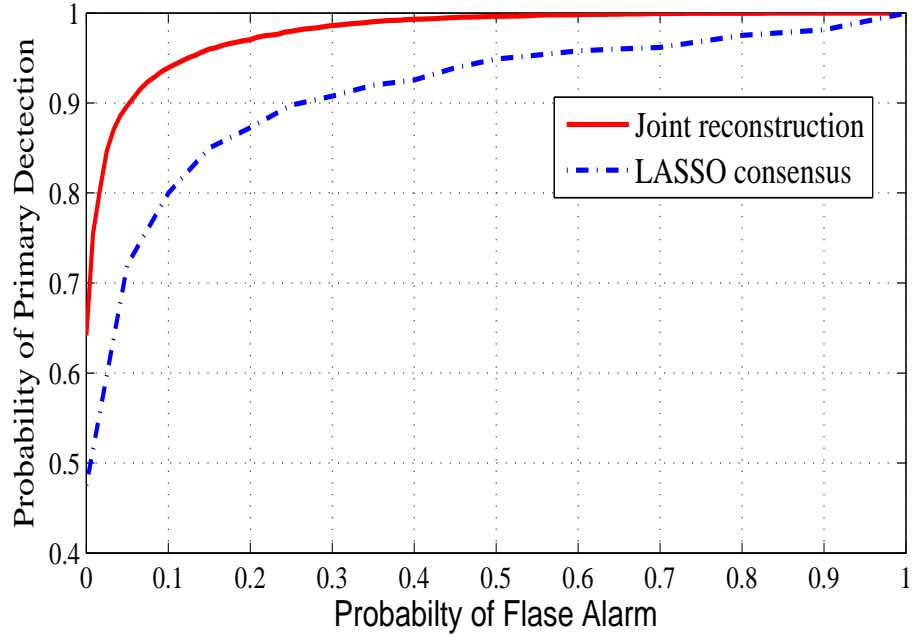


Figure 4.9: ROC performance comparison, For SNR=-5dB, S.R=0.6 and Sparsity=40%

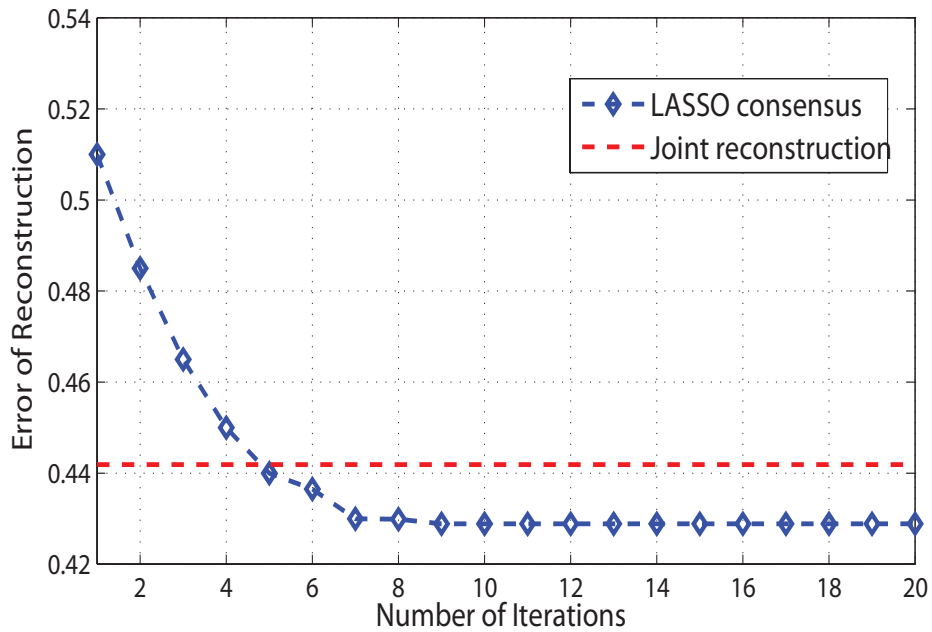


Figure 4.10: EOR comparison, For SNR=-5dB, S.R=0.6 and Sparsity=40%

We also reconstruct the original time domain signal using individual and joint

reconstruction methods in Figs. 4.11 and 4.12, respectively, at sampling rate of 32%. Comparing these figures, we observe that the signal reconstructed using the joint reconstruction matches more closely to the original signal.

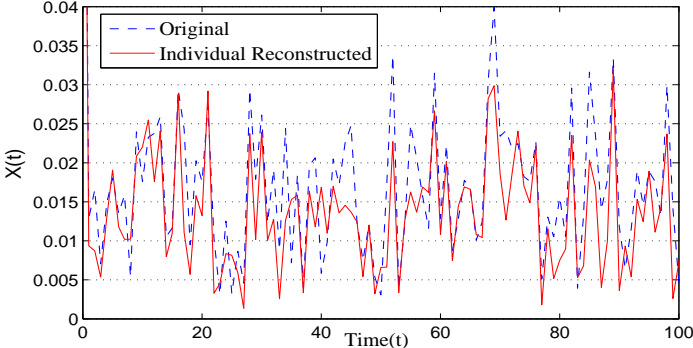


Figure 4.11: Original time domain signal and reconstructed using individual reconstruction method

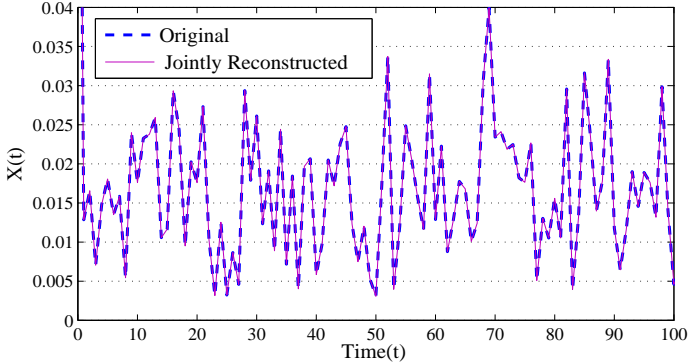


Figure 4.12: Original time domain signal and reconstructed using joint reconstruction method

#### 4.4 Conclusion

In this chapter, we proposed a novel wide band spectrum sensing for cognitive radios in the frequency overlapping networks using distributed compressive sensing and joint reconstruction. The concept have been demonstrated through the theoretical explanation and have been validated using the simulation results. A distributed com-

pressive sensing for cognitive radio network in the frequency overlapping system has been explored. Proposed joint reconstruction scheme for spectrum sensing exploits the joint sparsity in frequency overlapping networks and efficiently reduces the number of samples required. It is shown that the proposed scheme outperforms the individual reconstruction scheme and has better receiver operating characteristics compared to LASSO consensus algorithm. This is because the overlapping channels can be exploited to enhance the compressive decoding using joint reconstruction scheme.

## CHAPTER 5

### BINARY COMPRESSIVE SENSING

#### 5.1 Introduction

The paradigm of sparse sampling and reconstruction, called Compressive Sensing (CS) has been the state of art research in recent years. The gist of CS lies in determining the sparse solution of an under-determined system of linear equations. The solution of the under-determined system has been of particular research interest for a long time. However, the CS [30, 31] approach opened up many new research spaces in the field of under-determined system, ranging from theoretical formulations to many practical applications in image processing, wireless communication, genetic and molecular analysis, data-streaming, medical resonance imaging etc. Compressive sensing provides solution for the under-determined system of a sparse source. A vector,  $X \in \mathbb{R}^N$  is said to be  $K$  sparse if  $X$  contains  $K$  non-zero elements, i.e.  $\|X\|_{l_0} = K$ , where,  $\|X\|_{l_0}$  denotes zero norm of  $X$ . For illustration, let us consider a  $K$  sparse,  $N$  length source  $X$  be defined by  $M$  linear equations as in (5.1)

$$Y = \Phi X. \tag{5.1}$$

In terms of compressive sensing,  $\Phi \in \mathbb{R}^{M \times N}$ ,  $M \ll N$  is called sampling matrix or measurement matrix and  $Y \in \mathbb{R}^M$  is linear functionals of sparse source  $X$  and is called compressed measurements. In general, the system in (5.1) is ill-posed, but CS theory asserts that under the conditions, the source  $X$  is sparse and sampling matrix  $\Phi$  satisfies the Restricted Isometry Property (RIP) [32, 61], the solution can

be obtained by the following optimization problem,

$$\hat{X} = \underset{X}{\operatorname{argmin}} \|X\|_{l_0} \quad : Y = \Phi X. \quad (5.2)$$

Unfortunately, solving  $l_0$  is prohibitively computationally complex. However, the approximate solution to (5.1) is obtained by following  $l_1$  minimization.

$$\hat{X} = \underset{X}{\operatorname{argmin}} \|X\|_{l_1} \quad : Y = \Phi X. \quad (5.3)$$

Based on this general foundation, CS theory have been widely adopted and modified according to the signal characteristics. Many works have been carried out in designing the efficient sampling matrix  $\Phi$ , and decoding algorithms have been modified accordingly. CS decoding algorithm based on matching pursuit [62] and greedy algorithm, called Orthogonal Matching Pursuit and CoSaMP are developed in [33, 34, 36], respectively. Designing of sampling matrix  $\Phi$  according to signal and application is also of particular interest in CS. In [61], the RIP of random sampling matrices is proved. Systematic random sampling matrix based on linear error correcting codes for compressive sensing is designed in [63] and its RIP is proved. Similar sampling matrix related to linear codes and orthogonal optical codes is introduced in [64]. Model based compressive sensing for improved performance, and compressive sensing with prior partial information are explained in [37, 38, 39].

In this chapter, we introduce a novel compressive sensing approach for special class of signal with binary entries. We first design a sampling matrix for the binary signal, and then we present two different decoding algorithms for the binary sparse signal.

The rest of the chapter is organized as follows: In the Section 5.2, we formally define the binary compressive sensing problem and provide a quick review on existing works on binary compressive sensing and their pros and cons. In the Section 5.3, we introduce our new binary sampling matrix and the binary compressive decoding algorithm. Section 5.6 verifies our proposed scheme with numerical simulations



and comparison with the existing methods, and finally the Section 5.7 concludes the chapter.

## 5.2 Related Work and Contribution

In this chapter, we deal with the special class of the under-determined system in (5.1). Instead of considering the real valued signal, we have the prior information that the source signal  $X$  is binary. The system is thus redefined as:

$$Y = \Phi X. \quad (5.4)$$

where,  $X \in \mathbb{B}^N$  and  $\mathbb{B} = \{0, 1\}$ . Binary sparse signal can come into account in many practical applications such as event detection in wireless sensor networks, group testing, spectrum hole detection for cognitive radios etc [65, 66]. Linear programming based solution to (5.4) have already been proposed and discussed. In [67], the author modified the solution (5.3) for the binary system in (5.4) accordingly as in (5.5). The author has also provided the recovery threshold for  $l_1$  reconstruction of the binary signal.

$$\hat{X} = \underset{X}{\operatorname{argmin}} \|X\|_{l_1} \quad (5.5)$$

$$\text{subject to } Y = \Phi X,$$

$$0 \leq x_i \leq 1, \quad 1 \leq i \leq N.$$

In [68], the authors have developed reconstruction algorithm for binary sparse signal using  $l_q$  norm, where,  $0 \leq q \leq 1$ , which is based upon the re-weighted  $l_1$  minimization algorithm developed in [69]. Though these methods improve the performance for the binary sparse signal, the reconstructed signal  $\hat{x}_i \in [0, 1]$ ,  $i = 1, 2, 3 \dots N$ , whereas, the original  $x_i \in \{0, 1\}$ ,  $i = 1, 2, 3 \dots N$ . The mapping function for  $\hat{x}_i \in [0, 1]$  to the  $x_i \in \{0, 1\}$  is also undetermined. So, these solutions are not able to exactly reconstruct the original signal in  $X \in \mathbb{B}^N$ . In a very recent work [70], the authors

employ integer programming model to solve the the under-determined binary systems of linear equations. The work is basically the solution for the general binary systems of equations. In compressive sensing, we have an added advantage of having control over the sampling matrix  $\Phi$ , the elements of which are the coefficients of the linear equations. Implementation of bipartite graphs has also been interesting topic in CS. In [71], a mixed algorithm using two phase of encoding and reconstruction is proposed for CS using graph and matrix inversion. In [72, 73], the authors proposed use of bipartite graphs to represent the CS and have explained the rate distortion performance of binary CS based upon the edge evolution in low density parity check codes [74]. The authors have provided an interesting closed form solution for edge evolution using large deviation probability theory and the martingales [75]. However, the edge evolution process halts after some iterations and thus the reconstruction solution is incomplete. In this chapter, we first design a unique but universal sampling matrix  $\Phi$  for binary signal, suitable for graph based recovery. We then propose two recovery algorithms each of them having trade-offs in terms of computation and physical resource. We also provide analysis of our scheme and discuss the measurements required, error floor, and complexity and verify our scheme using both numerical analysis and simulations.

### 5.3 Binary Compressive Sensing

Let us represent the binary compressive sensing system in (5.4) by the bipartite graph as in the Fig. 5.1. The elements of the binary sparse signal  $X$  is represented by the circular nodes and the compressive sensing measurements, i.e. elements of  $Y$  are represented by the square nodes and are termed as Variable nodes ( $V$ -nodes) and the Check nodes ( $C$ -nodes), respectively as shown in the Fig. (5.1). The  $i^{th}$   $V$ -node and  $j^{th}$   $C$ -node are represented by  $v_i$  and  $c_j$  and their corresponding values are represented by  $x_i$  and  $y_j$ , respectively. The edge  $E_{ij}$  between  $v_i$  and  $c_j$ , represents

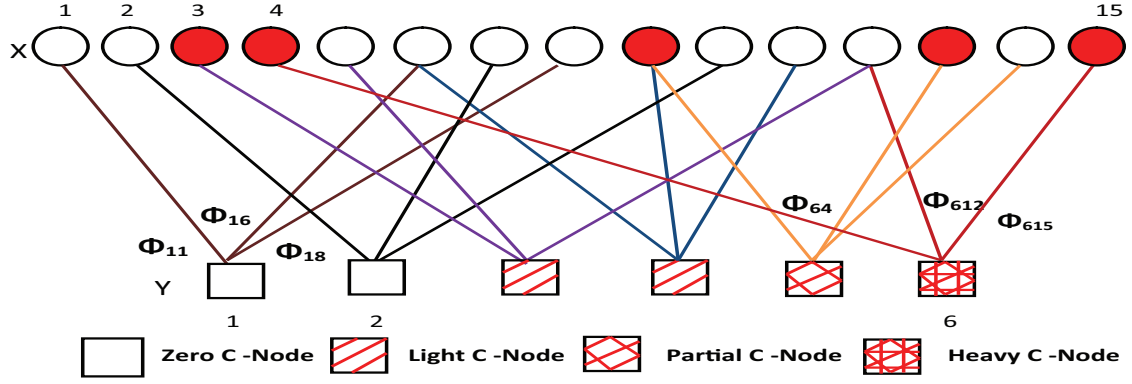


Figure 5.1: Representation of Compressive Sensing with Bipartite Graph

the  $j^{th}$  row and  $i^{th}$  column element of sampling matrix,  $(\Phi)_{ji}$ . The filled V-nodes represent  $x_i = 1$ ,  $x_i \in X$  and the empty V-nodes represent  $x_i = 0$ ,  $x_i \in X$ . Similarly, the  $C$  - nodes are divided into 4 different types as shown in the Fig.(5.1). We will discuss about these check nodes in the next section later. A  $V$  - node,  $v_i$  is said to be neighbor of  $C$  - node,  $c_j$ , if,  $\exists, E_{ji}$ , i.e.  $(\Phi)_{ji} \neq 0$ . In previous binary compressive sensing works using bipartite graph [72, 73], the sampling matrix  $\Phi$  is constant row weight binary matrix with row weight  $L$ . So in these approaches, the compressed measurements (C-nodes),  $y_i \in Y$  can be grouped in three groups,  $y_i = 0$  or  $y_i = L$  and rest all in one group.

Clearly, for decoding purpose,

$$\begin{aligned}
 \forall, v_k \in c_m, \quad & x_k = 0, \quad \text{if, } y_m = 0, & (5.6) \\
 & x_k = 1, \quad \text{if, } y_m = L, \\
 & x_k = \text{unknown}.
 \end{aligned}$$

This phase of recovering  $V$  - nodes associated with  $C$  - nodes with values  $y_i = 0$  and  $y_i = L$  is termed as *First Phase Recovery (FPR)*. After the first phase recovery, the edge recovery is performed by corresponding edge removal process. (For details in edge recovery please refer to [72, 73, 74]. But this approach has two major setbacks.

First, the edge recovery process does not recover all the  $V - nodes$  and the second, the work does not provides any explanation about the effect of row-weight  $L$  on overall recovery of the  $C - nodes$ . In the following section, we first design the sampling matrix  $\Phi$  and then discuss the consequence of row weight  $L$  on the FPR.

### 5.3.1 The Sampling Matrix, $\Phi$

Let us consider, the  $M \times N$  dimension sampling matrix  $\Phi$  of row weight  $L$ . Each row of  $\Phi$  contains  $L$  non-zero elements placed randomly. Let  $\Omega_i$  denotes the set of non-zero elements in  $i^{th}$  row and  $\Omega_{i1}$  and  $\Omega_{i2}$  are any two subsets :  $\Omega_{i1}, \Omega_{i2} \subseteq \Omega_i$  and  $\Omega_{i1} \neq \Omega_{i2} \quad i = 1, 2, \dots M$ . Let,  $\theta$  denotes the elements in  $\Omega_i$ , then, the following condition should be satisfied:

$$\sum_{j \in \Omega_{i1}} \theta_j \neq \sum_{j \in \Omega_{i2}} \theta_j. \quad (5.7)$$

In other words, all the possible sums of non-zero row elements of  $\Phi$  are unique. For a finite constant row-weight  $L$ , when the row-elements of  $\Phi$  are sampled from continuous random distributions such as Gaussian or Uniform, (5.7) is easily satisfied. Hence, the  $i^{th}$ ,  $i = 1, 1 \dots M$ , row of sampling matrix  $\Phi$  is given by following steps:

$$\Omega_i = f_r(i, L), \quad \Gamma_i = f_p(i, L, N), \quad (5.8)$$

For,  $k=1, 2, \dots N$

$$\begin{aligned} \Phi_{i,k} &= \Omega_i; \quad k \in \Gamma_i, \\ \text{else, } \Phi_{i,k} &= 0. \end{aligned} \quad (5.9)$$

$f_r(i, L)$  is a function that generates  $L$  random numbers from Gaussian or Uniform distribution, the function,  $f_p(i, L, N)$  generates  $L$  random positions from 1 to  $N$ , and  $\Gamma_i$  is the set of non-zero locations of the  $i^{th}$  row of  $\Phi$ . Hence, the sampling matrix in our method is sparse constant row weight matrix whose non-zero elements are drawn from the Gaussian or uniform distribution and each row of  $\Phi$  satisfies (5.7).

### 5.3.2 Compressed Measurements and the Check Nodes

The compressed measurements ( $C - nodes$ ) are the linear, scaled sums of the  $L$  random  $V - nodes$  as represented by (5.4) and the Fig.(5.1). The  $C - nodes$  are divided into 4 groups as followings:

**Definition 1:** A  $C - node$ ,  $c_j$  is said to be Zero  $C - node$ , if  $y_j = 0$ . This happens when all the neighbor  $v_i$ 's of  $c_j$  are zero elements.  $c_1, c_2$  are examples of Zero  $C - nodes$  in the Fig.(5.1).

**Definition 2:** A  $C - node$ ,  $c_j$  is said to be Light  $C - node$ , if,  $y_j = (\Phi)_{j,k}$ , where,  $k \in \Gamma_j$ . In other words, a  $C - node$ ,  $c_j$  is said to Light  $C - node$ , if,  $y_j$  is equal to any one non-zero element of  $j^{th}$  row of  $\Phi$ . This happens, when one of the neighbor  $v_i$ 's of  $c_j$  is one and all other are zeros.  $c_3, c_4$  are examples of Light  $C - nodes$  in the Fig. (5.1).

**Definition 3:**  $c_5$  is an example of Partial  $C - node$ . A  $C - node$ ,  $c_j$  is said to be Partial  $C - node$ , if,  $y_j \neq 0 \neq (\Phi)_{j,k}$  ;  $k \in \Gamma_j$  but, during edge recovery process, the node ultimately turns to be either Zero  $C - node$  or Light  $C - node$ .

**Definition 4:**  $c_6$  is an example of Heavy  $C - node$ . A Heavy  $C - node$ ,  $c_j$  occurs when for all the  $V - nodes$ ,  $v_i$ 's which are neighbors of  $c_j$ , there exists more than one  $v_i$  which is neighbor of only  $c_j$  and is not recovered by edge removal process.

### 5.3.3 Compressive Sensing Decoding

The node recovery or decoding is divided into two phases.

#### First Phase Recovery

In the First Phase Recovery (FPR), the  $V - nodes$  which are neighbors of Zero  $C - nodes$  and Light  $C - nodes$  are recovered. Let,  $\Lambda_j$  is set of neighbors  $v_i$ 's of  $C - node, c_j$ . The  $V - nodes$  which are neighbors of Zero  $C - nodes$  or Light  $C - nodes$

is recovered as follows:

$$\begin{aligned}
 & \text{if, } c_j \text{ is Zero } C - \text{node i.e. } y_j = 0, \\
 & \quad x_i = 0; \quad \forall v_i \in \Lambda_j
 \end{aligned} \tag{5.10}$$

$$\begin{aligned}
 & \text{elseif, } c_j \text{ is Light } C - \text{node ,i.e. } c_j = (\Phi)_{jk}, k \in \Gamma_j \\
 & \quad x_k = 1, \quad v_k \in \Lambda_j \\
 & \quad x_i = 0, \quad \forall v_i \in \Lambda_j, i \neq k.
 \end{aligned} \tag{5.11}$$

### Edge Removal, Check Nodes Update and Iteration

After, the variable nodes are recovered from Zero and Light  $C - nodes$ , edges associated with the corresponding  $V - nodes$  are removed from the graph, and subsequently the  $C - nodes$  are updated.

$$\begin{aligned}
 & \forall c_j, c_j \text{ is Zero or Light } C - \text{node,} \\
 & \forall v_i \in \Lambda_j,
 \end{aligned}$$

Remove  $E_{ji}$ ,

Remove  $E_{qi}$ , where,  $q \neq j, q = 1, 2 \dots M$

$$\begin{aligned}
 & \text{if, } x_i = 0, \\
 & \quad y_q = y_q.
 \end{aligned} \tag{5.12}$$

$$\begin{aligned}
 & \text{elseif, } x_i = 1, \\
 & \quad y_q = y_q - \Phi_{qi}.
 \end{aligned} \tag{5.13}$$

After, edge removal and check nodes update process, new Zero  $C - nodes$  and Light  $C - nodes$  will be created. Then the FPR process and the edge removal and check nodes update process is repeated until the generation of new new Zero  $C - nodes$  and Light  $C - nodes$  stops. The process of FPR and edge removal and check nodes update for the Fig.5.1 is illustrated graphically below.

For the graph in the Fig.5.1:

Zero  $C - node$  :  $c_1$ :  $\Gamma_1 = \{1, 6, 8\}$ ,  $\Lambda_1 = \{v_1, v_6, v_8\}$

$y_1 = 0$ ,  $\rightarrow x_1 = x_6 = x_8 = 0$ .

Edge Removal: Remove:  $E_{1,1}$ ,  $E_{1,6}$ ,  $E_{1,8}$

Remove:  $E_{4,6}$

Check Nodes Update:  $x_6 = 0$ ,  $\rightarrow y_4 = y_4$

Similar process is carried out for all Zero  $C - nodes$ .

For Light  $C - node$  :  $c_3$  :  $\Gamma_3 = \{3, 5, 12\}$ ,  $\Lambda_3 = \{v_3, v_5, v_{12}\}$

$y_3 = \Phi_{3,3}$ ,  $\rightarrow x_3 = 1$ ,  $x_5 = x_{12} = 0$ .

Edge Removal: Remove:  $E_{3,3}$ ,  $E_{3,5}$ ,  $E_{3,12}$

Remove:  $E_{6,12}$

Check Nodes Update:  $x_{12} = 0$ ,  $\rightarrow y_6 = y_6$

Similarly,

For Light  $C - node$  :  $c_4$  :  $\Gamma_4 = \{6, 9, 11\}$ ,  $\Lambda_4 = \{v_6, v_9, v_{11}\}$

$y_4 = \Phi_{4,9}$ ,  $\rightarrow x_9 = 1$ ,  $x_6 = x_{11} = 0$ .

Edge Removal: Remove:  $E_{4,6}$ ,  $E_{4,9}$ ,  $E_{4,11}$

Remove:  $E_{5,9}$

Check Nodes Update:  $x_9 = 1$ ,  $\rightarrow y_5 = y_5 - \Phi_{5,9}$

At this point, it should be noted that, the Partial  $C - node$ ,  $c_5$ , has changed to Light  $C - node$ . The reduced graph after these steps is shown in the Fig.5.2. The process of edge removal, check nodes update and Zero and Light  $C - nodes$  recovery is continued as long as there exist single Zero or Light  $C - node$ . However, all  $V - nodes$  cannot be recovered by these process. The  $V - nodes$  which are neighbor of Heavy  $C - nodes$  (e.g.  $c_6$ ) have to be yet recovered. These nodes are recovered by following method.

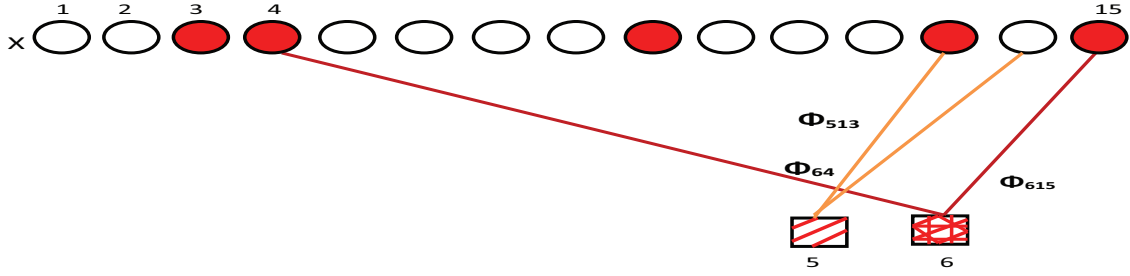


Figure 5.2: Reduced Graph after the First cycle of First Phase Recovery and Edge Removal and Check Nodes Update

### Check Sum Method for Heavy $C - nodes$

In the Section 5.3.1, we discussed about the non-zero elements of the sampling matrix  $\Phi$ . The condition for non-zero row elements of  $\Phi$  in (5.7) guarantees that any combinatorial sum of these elements is unique. We use this property the sampling matrix  $\Phi$  designed in the Section (5.3.1) to recover the Heavy nodes and  $V - nodes$ , which are neighbors of Heavy nodes. The Check Sum method is described by following steps.

---

#### Algorithm 1 Check Sum Method for Heavy Nodes Recovery

---

1.  $\forall$ , Heavy  $C - nodes$ ,  $c_j$ ,
  2. Find: Updated  $\Gamma_j$  and  $\Lambda_j$
  3. Find: The numbers of elements in  $\Gamma_j$ , i.e.  $|\Gamma_j| = \beta$
  4. Create: Vector,  $V_\phi = \Phi_{j,k}, \forall k \in \Gamma_j$ .
  5. Create: Binary Matrix ( $BT$ ) 0 to  $2^\beta - 1$ ,  
where, each row of table is corresponding binary representation of 0 to  $2^\beta - 1$ .
  6. Compute: Check-Sum ( $SUM$ ):  $SUM = BT \times V'_\phi$
  7. Find:  $y_j = SUM(l)$
  8. Assign:  $\forall, v_i \in \Lambda_j$ , Assign element wise  $l^{th}$  row of  $BT$  to  $v_i \in \Lambda_j$
- 

To illustrate this process for the Fig.5.1, we can see from the Fig:5.2 that the  $c_6$  is Heavy Check - node. Following the steps described above.

For Heavy Check - node,  $c_6$ ,



Updated:  $\Gamma_6 = \{4, 15\}$ ,  $\Lambda_6 = \{v_4, v_{15}\}$  and  $\beta = 2$ .

$$V_\phi = [\Phi_{6,4} \quad \Phi_{6,15}], \quad \text{Binary Table: } B.T = \begin{pmatrix} 0 & 0 \\ 0 & 1 \\ 1 & 0 \\ 1 & 1 \end{pmatrix}$$

$$SUM = [0 \quad \Phi_{6,4} \quad \Phi_{6,15} \quad (\Phi_{6,4} + \Phi_{6,15})]'$$

Clearly,  $y_6 = SUM(4) \rightarrow \Lambda_j \leftarrow (BT)_4$ .

Hence,  $x_4 = 1$  and  $x_{15} = 1$ .

In the following section, we present an alternative method of Binary CS based only on the Check Sum.

#### 5.4 An Alternative Approach

In this approach we modify the sampling matrix  $\Phi$ . The function  $f_r(i, L)$  is made independent of the row.

$$i.e. \quad \Omega_1 = \Omega_2 = \dots \Omega_M = f_r(L) = \Omega. \quad (5.14)$$

This suggests that the all the rows in sampling matrix  $\Phi$  contains same non zero elements from  $\Omega$ . Then, the sampling matrix  $\Phi$  is generated as:

For,  $k = 1, 2, \dots N$

$$\begin{aligned} \Phi_{i,k} &= \Omega; \quad k \in \Gamma_i \\ \text{else, } \Phi_{i,k} &= 0 \end{aligned} \quad (5.15)$$

All notations and functions have same meaning as described in the Section 5.3.1 unless stated otherwise and  $\Omega$  also satisfies the condition in (5.7).

### 5.4.1 Compressive Sensing Decoding

In this approach, the decoding center has a vector ( $SUM$ ) stored. A  $SUM$  vector is generated by following steps.

Create: Binary Matrix ( $BT$ ) 0 to  $2^L - 1$ ,

Compute: Check-Sum ( $SUM$ ):  $SUM = BT \times \Omega'$

It should be noted that the  $SUM$  vector is all possible combinatorial sum of elements in  $\Omega$ . Hence, the check nodes and their corresponding variable nodes are decoded by following algorithm.

---

**Algorithm 2** An Alternative Method

---

1.  $\forall, C - nodes, c_j$ ,
  2. Find:  $y_j = SUM(l)$
  3. Find: Vector,  $l_{binary} = f_B(l - 1, L)$ . where,  $f_B(l - 1, L)$  is a function that gives  $L$  bit binary representation of  $l - 1$  with least significant bit at right and left bits padded with zero whenever necessary.
  4. Assign:  $\forall, v_i \in \Lambda_j, x_i = l_{binary}(k), \quad k = 1 : L$
- 

## 5.5 Analysis and Discussion

The graph and check sum based compressive sensing for binary sparse signals is beneficial than the solution based on the  $l_1$  minimization approaches. In this section, we discuss the consequences of row weight  $L$  in performance, the encoding and decoding complexities, the measurement constraints and error probability of our scheme.

### 5.5.1 Choice of Row-Weight ( $L$ )

In our scheme, the first phase of recovery is based on the number of Zero and Light  $C - nodes$ . The number of Zero and Light  $C - nodes$  is a function of the row-weight  $L$  and the sparsity  $S$  of the binary sparse signal. The sparsity ( $S$ ) of signal  $X$ , with

$|X| = N$ , is defined as,  $S \equiv K/N$ , where  $K$  is the number of non zero elements in  $X$ . The recovery of *Zero* and *Light C – nodes* is crucial in our scheme for two broad purposes. Recovery of *Zero* and *Light C – nodes* requires only search operation and is faster than recovering *Heavy C – nodes*. Moreover, the edge recovery and check node update process during first phase recovery reduces the edges of *Partial* and *Heavy C – nodes* as illustrated in the Fig.5.2. The edge reduction decreases the size of  $\Gamma_j$  and  $\beta$ . Smaller is the  $\beta$ , lesser is the computations in the Check Sum method.

Let us consider,  $P_0$  and  $P_1$  denote the probability that the check node is *Zero – node* and *Light – node* respectively. Then,  $P_0$  is the probability the check node has all zero neighbors and  $P_1$  is the probability that the check node has only one non-zero ( $x_i = 1$ ) neighbor and all other are zero neighbors.  $P_0$  and  $P_1$  are given by:

$$P_0 = (1 - S)^L. \quad (5.16)$$

$$P_1 = (1 - S)^{L-1} \cdot S \cdot \binom{L}{1}. \quad (5.17)$$

It is clear that to maximize *Zero – nodes* and *Light – nodes* we need to maximize  $P_0$  and  $P_1$ . Let,  $F_P = P_0 + P_1$ . Then,

$$F_P = P_0 + P_1 \quad (5.18)$$

$$\frac{d(F_P)}{dL} = \frac{d(P_0 + P_1)}{dL} \quad (5.19)$$

$$= (1 - S)^L \cdot \ln(1 - S) + (1 - S)^{L-1} \cdot S + L \dot{S} \cdot (1 - S)^{L-1} \cdot \ln(1 - S). \quad (5.20)$$

To maximize  $F_P$  we equate (5.20) to 0 and approximating  $-\ln(1 - S) \approx S$ , we get  $L=1$ . From (5.16) we see that for  $L = 0$ ,  $P_0 = 1$ . However, taking row-weight  $L = 0$  or  $1$  do not make any sense in compressive sensing because, when  $L = 0$  we are not taking any samples and when  $L = 1$  we are taking only one sample in each measurement, it means in each measurement, we either sample only 0 or only 1. This violates the basic norm of compressive measurement that each measurement in compressive sensing is linear functionals of numbers of samples. So, taking  $L = 0$  or  $1$

is not feasible in compressive sensing. To illustrate this, in the Fig. 5.3 we show  $P_0$ ,  $P_1$  and  $F_P$  for  $S = 0.1$  and varying  $L$ . Hence, it is desirable to maximize *Light – nodes*.

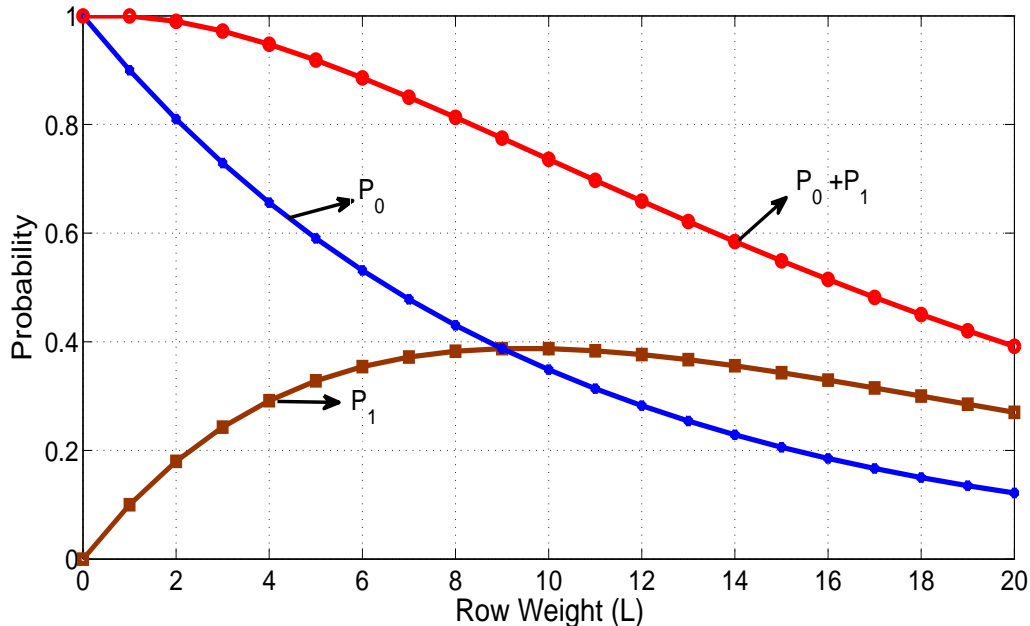


Figure 5.3: Probability of zero and light check nodes for different row-weight

Maximizing *Light C – nodes* has mainly two advantages:

- Light C-nodes reduce the edges of check nodes and makes the graph less denser.
- Light C-nodes after each iteration create new Light C-nodes. Every C-nodes which has two non-zero neighbors and one of the non-zero neighbors belongs to Light C-node turns into new Light C-node after edge removal and check node update process.

**Theorem 1** *The optimal row weight  $L$  for the maximum Light C – node is  $(1/S)$ .*

*Proof.* Let,  $P_1$  denote probability of C – node being Light C – node.

$$P_1 = (1 - S)^{L-1} \cdot S \cdot \binom{L}{1} \quad (5.21)$$

$$\begin{aligned}\frac{d}{dL}(P_1) &= 0, \\ (1-S)^{L-1} \cdot S + L \cdot S \cdot (1-S)^{L-1} \cdot \ln(1-S) &= 0, \\ L \cdot \ln(1-S) &= -1.\end{aligned}$$

Expanding,  $-\ln(1-S) = S + \frac{S^2}{2} + \frac{S^3}{3} + \dots$  and for small  $S$ ,  $-\ln(1-S) \approx S$

$$L \approx (1/S). \tag{5.22}$$

■

### 5.5.2 Encoding and Decoding Complexity

For encoding purposes in both, first approach and the alternative approach, each measurement requires  $L$ , measurements. We make  $M$  measurements. Hence, the encoding requires  $\mathcal{O}(ML)$  complexity.

The decoding complexity in the first approach depends upon the number of Heavy nodes and the  $\beta$  of the reduced graph. To decode Zero and Light  $C$  – nodes we need just one search operation. However, for each Heavy  $C$  – node, we need one matrix multiplication and a search operation. For this reason, it is very important to Zero and Light  $C$  – nodes first and reduce the graph by edge removal and check node update process. However, in an alternative approach, at the cost of physical memory to store check-sum vector ( $SUM$ ), the decoding complexity is greatly reduced. In alternative approach, to decode each  $C$  – node, we need only one search operation. Both of our decoding schemes are faster than the general compressive sensing decoding schemes for binary sparse signal in [67, 68] as shown in the Fig.5.11.

### 5.5.3 The Number of Measurements (M)

In our scheme, for successful decoding of all  $C$  – nodes and hence recover all  $V$  – nodes, two conditions have to be satisfied.

1. The non-zero elements of sampling matrix  $\Phi$  should satisfy (5.7).
2. Each of the  $V$  – node should be the neighbor of at least one  $C$  – node, i.e. Each of the variable node should be sampled at least once.

**Theorem 2** *For successful decoding of binary sparse source from compressed measurement using graph and sum based decoding algorithm, the number of measurements  $M$  is of  $\mathcal{O}(K \log(N))$ .*

*Proof.* For a bipartite graph with  $N$ ,  $V$  – nodes and  $M$ ,  $C$  – nodes with  $L$   $C$  – node degree, we need  $M \times L$  of order  $N \log(N)$  for all  $V$  – nodes to be sampled in the graph [76].

$$\text{Hence, } M = \mathcal{O}\left(\frac{N}{L} \log N\right)$$

$$\text{We have, } L = \mathcal{O}(1/S)$$

$$M = \mathcal{O}(K \log N)$$

■

**Lemma 1** *The encoding requires the computational complexity of  $\mathcal{O}(ML) = \mathcal{O}(N \log N)$*

#### 5.5.4 The Error Rate (E.R)

Let the error rate of the graph and sum based compressive sensing algorithm for binary sparse signals be defined as the ratio of numbers unrecovered variable nodes to the total number of variable nodes. Provided, (5.7) is satisfied, in our scheme, the variable nodes cannot be recovered only when it is not sampled in the check nodes (compressed measurements).

**Theorem 3** *Error rate (E.R) of Graph and Sum based scheme is given by:  $E.R = \left(1 - \frac{L}{N}\right)^M$*

*Proof.* The probability that a variable node is sampled in one measurement =  $\left(\frac{L}{N}\right)$   
The probability that a variable node is not sampled in one measurement =  $\left(1 - \frac{L}{N}\right)$   
The probability that a variable node is not sampled in  $M$  measurements =  $\left(1 - \frac{L}{N}\right)^M$   
The probability that a variable node is sampled in  $M$  measurements =  $\left[1 - \left(1 - \frac{L}{N}\right)^M\right]$   
 $\therefore$  For large  $N$ , average numbers of variable nodes sampled =  $N \times \left[1 - \left(1 - \frac{L}{N}\right)^M\right]$

$$\begin{aligned} \text{We have, } E.R &= \frac{N - N \left[1 - \left(1 - \frac{L}{N}\right)^M\right]}{N} \\ \therefore E.R &= \left(1 - \frac{L}{N}\right)^M \end{aligned} \quad (5.23)$$

■

## 5.6 Simulation and Results

For simulation purpose, following values are considered unless stated otherwise. We take the number of variable nodes  $N = 1000$ , the sparsity of the binary source  $S = 0.1$

In edge recovery, the number of check nodes recovered in the first phase is very important factor. More the numbers of  $C - nodes$  recovered in first phase, easier and quicker is the overall recovery scheme. The more numbers of  $C - nodes$  recovered in first phase phase has following advantages.

- The number of edges removed in each iteration increases with number of check nodes recovered in the iteration. The number of edges removed in each iteration is given by the *numbers of  $C - nodes$  recovered  $\times C - node$  degree*.
- It makes the overall *Variable Nodes* recovery process faster as the bipartite graph becomes less dense.
- Only few numbers of  $C - nodes$  will be remained for decoding using Check-Sum method.

In the Figs. 5.4 and 5.5 we compare the first iteration recovery of  $C$  – nodes in our scheme with that of in Binary Tree scheme in [72, 73].

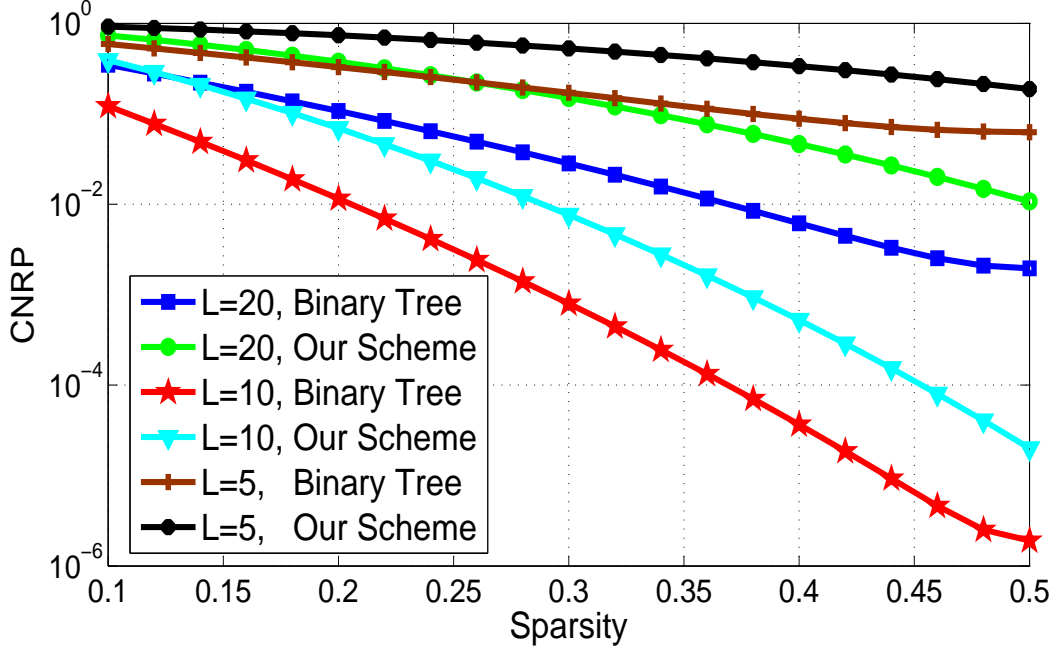


Figure 5.4: Probability of Check Nodes Recovered in First Iteration (CNRP)

Fig. 5.4 shows the probability of check nodes recovered (CNRP) in first iteration for different sparsity and different row weight ( $L$ ). We can clearly see that at each  $L$  and sparsity the CNRP is greater than that of in Binary Tree scheme. It also shows that for the given  $L$ , the CNRP decreases as the sparsity increases. So it is necessary to decrease the row weight in high sparsity signal to increase the CNRP. However, in all instances the CNRP in our scheme is greater than that of in the Binary Tree scheme.

To address the low CNRP for large sparsity is desirable to take the row weight  $L$  of the sampling matrix of the order  $\mathcal{O}\left(\frac{1}{s}\right)$  as discussed in 5.5.1. In the Fig. 5.5, we show the number of check nodes recovered in first iteration for different sparsity. The row weight  $L$  is taken to be  $\frac{1}{s}$  and the number of measurements (C-nodes) ( $M$ ) is taken as 300.



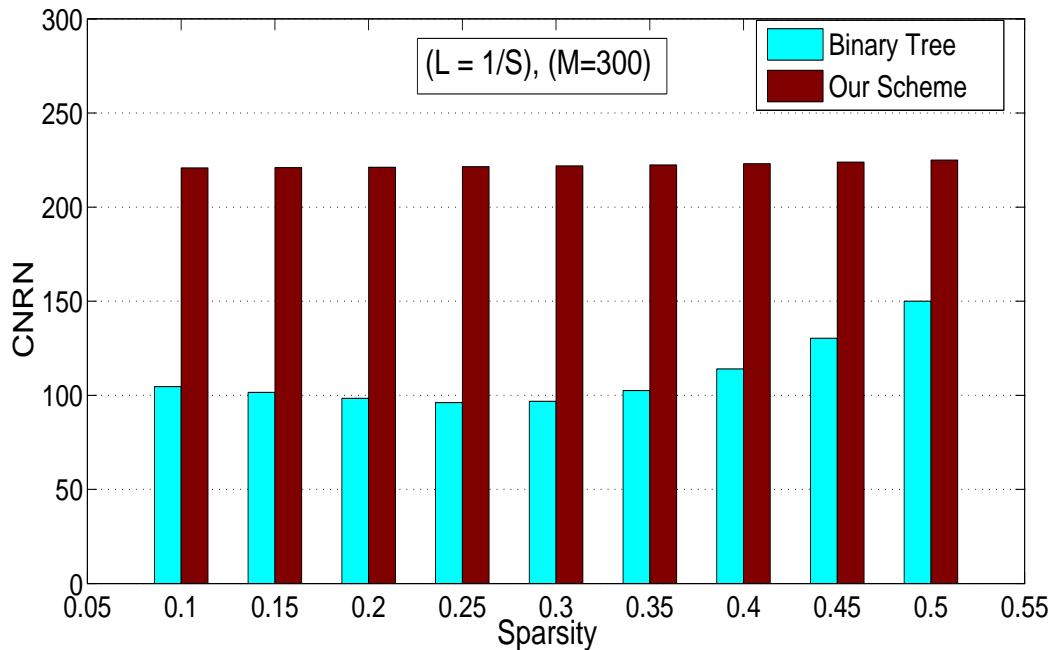


Figure 5.5: Numbers of Check Nodes Recovered in First Iteration (CNRN)

From the Fig. 5.5 we can clearly see that in our scheme, out of 300  $C - Nodes$ , about 225 are recovered in the first iteration itself whereas in Binary Tree scheme the number is as low as 100.

In our scheme, it is necessary that all the  $V - nodes$  be neighbor of at least one  $C - node$ . Whenever, a  $V - node$  is not a neighbor of any  $C - nodes$ , that particular  $V - nodes$  remains unrecovered and increases the Error Rate. In the Fig. 5.6, we can clearly see that for the given number of measurements, the Error Rate decreases as the row weight increases. However, this increase in performance is achieved by some cost in decoding time as shown in the Fig. 5.7.

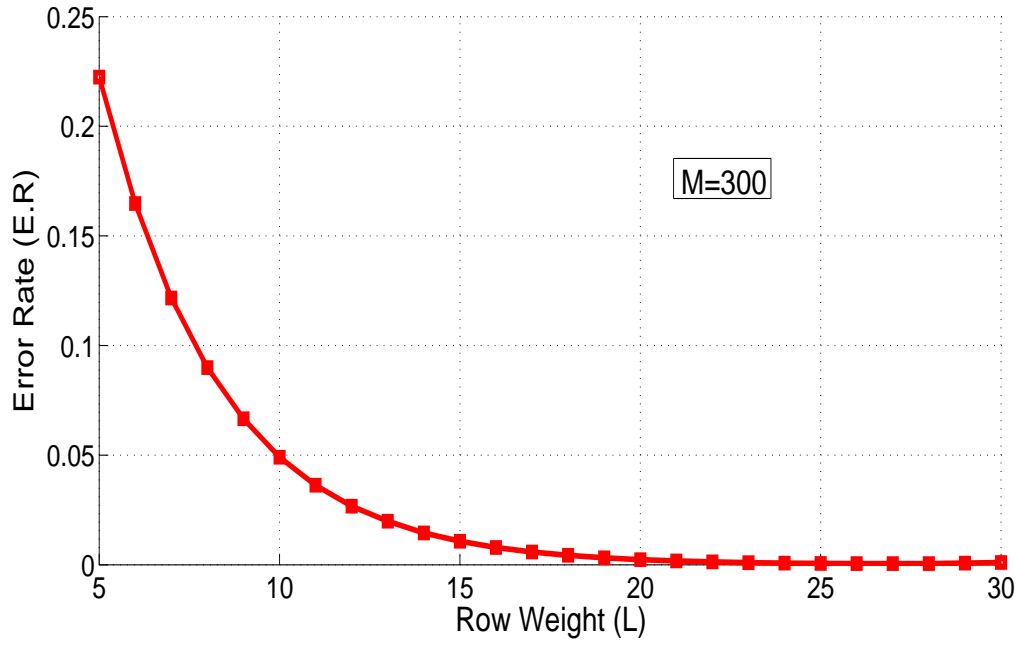


Figure 5.6: Error Rate for different Row Weight

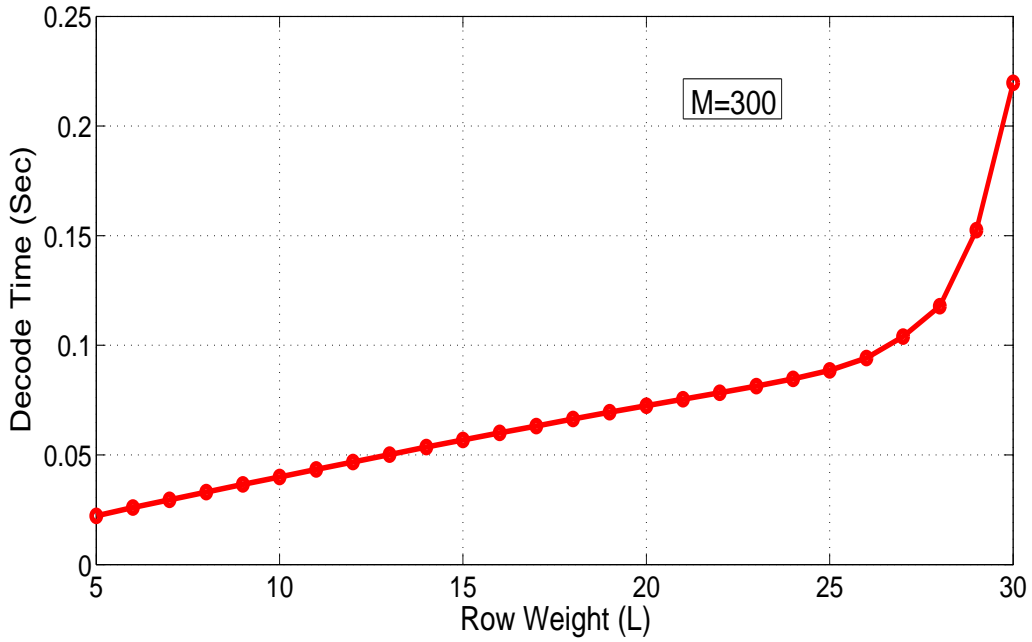


Figure 5.7: Row weight and Decode Time

Fig. 5.8 shows the performance of our scheme for various row weight and sampling rate. It is clearly seen that the Error Rate decreases as the sampling rate increases.

We can also see that for the same sampling rate, the error rate decreases as the row weight is increased.

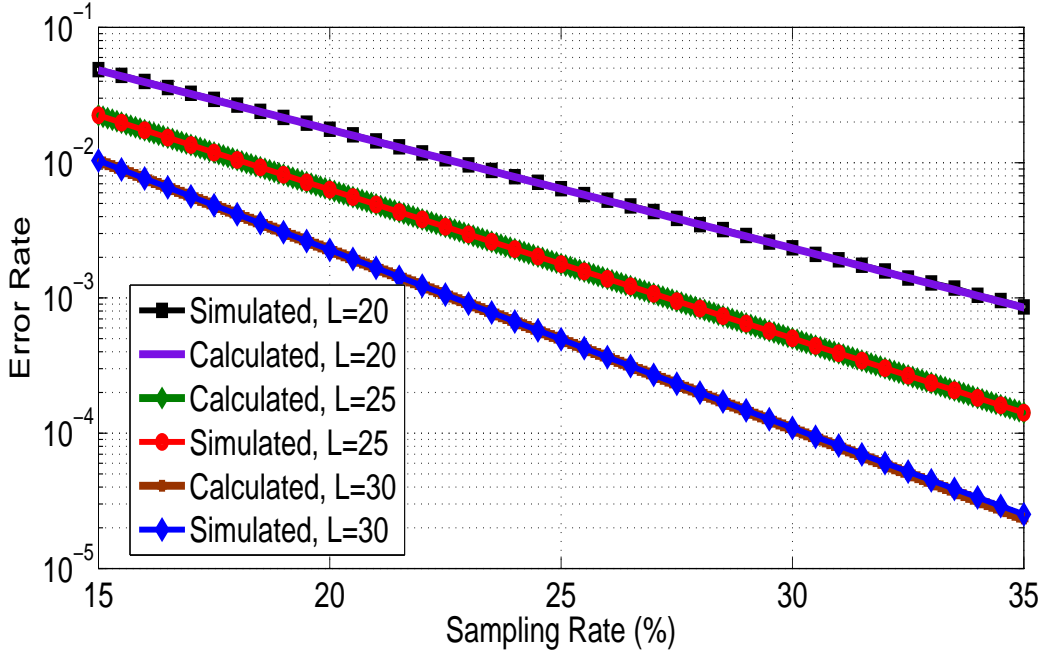


Figure 5.8: Error Rate for different Sampling Rate and Row weight

We can clearly see from the Fig. 5.8 that the simulated error rate is very close to the error rate calculated in the section 5.5.4. Hence, our calculated error rate (5.23) expression is validated through the experimental results as well.

In [67] and [68], the general  $l_1$  minimization method is modified for the Binary signal source. A new reconstruction constraint is used to bound the reconstructed signal values within,  $0 \leq \hat{x} \leq 1$ , in [67]. A similar approach is used in [68] where the optimization is iterated using the weight factor. These methods perform comparatively better than general  $l_1$  method for binary signal. However, in both of these schemes, the reconstructed binary signal values lie in the continuous range of  $0 \leq \hat{x} \leq 1$  instead of giving discrete values 0 or 1. In the Fig. 5.9 the original binary signal and reconstructed signal using the  $l_1$  binary and our scheme is shown. In the Fig. 5.9, (A) is the original Binary signal, (B) is the reconstructed signal using  $l_1$

binary method and (C) is reconstructed signal using our scheme.

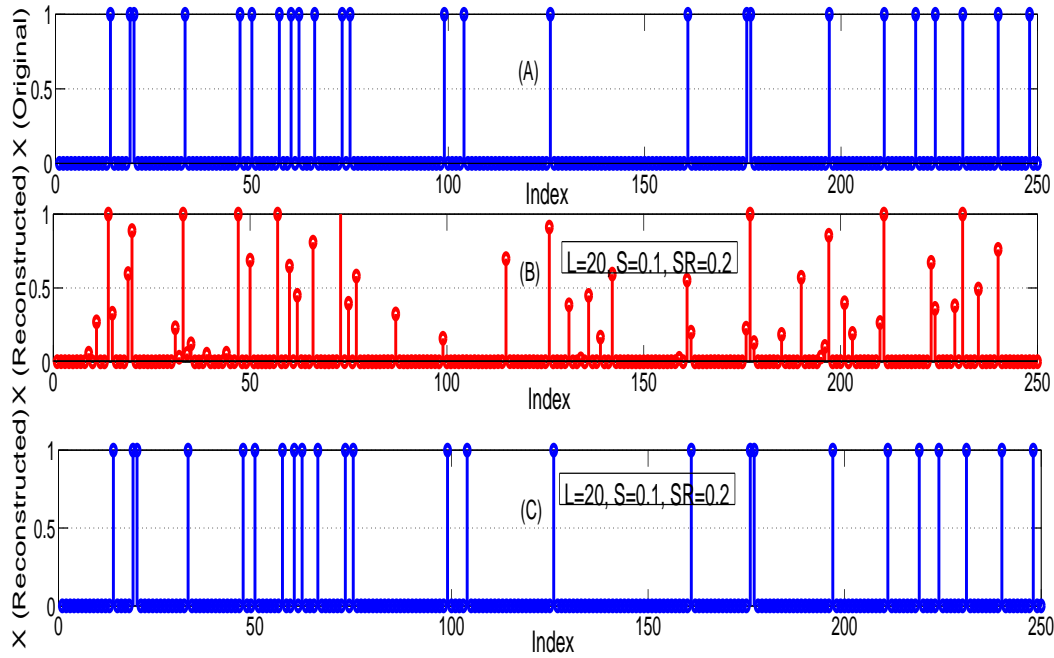


Figure 5.9: Original and Reconstructed Signal using Binary  $l_1$  and Our Scheme

For a better pictorial representation of the original and reconstructed signal in the Fig. 5.9, the simulation has been carried out for the binary signal of length ( $N = 250$ ), Sparsity ( $S = 0.1$ ) Row-weight ( $L = 20$ ) and Sampling Rate ( $S.R = 0.2$ ). We can clearly see that the scheme has better reconstruction than the  $l_1$  binary scheme. Besides, the reconstructed signal using  $l_1$  Binary method is continuously distributed over  $0 \leq \hat{x} \leq 1$ .

In Binary  $l_1$  scheme, the reconstructed signal values are in the range of  $0 \leq \hat{x} \leq 1$ . We modify this scheme slightly. We put the threshold 0.5 to make a decision if the reconstructed spike is 0 or 1. Fig. 5.10 shows the error rate comparison of our scheme and the Binary  $l_1$  scheme with threshold.

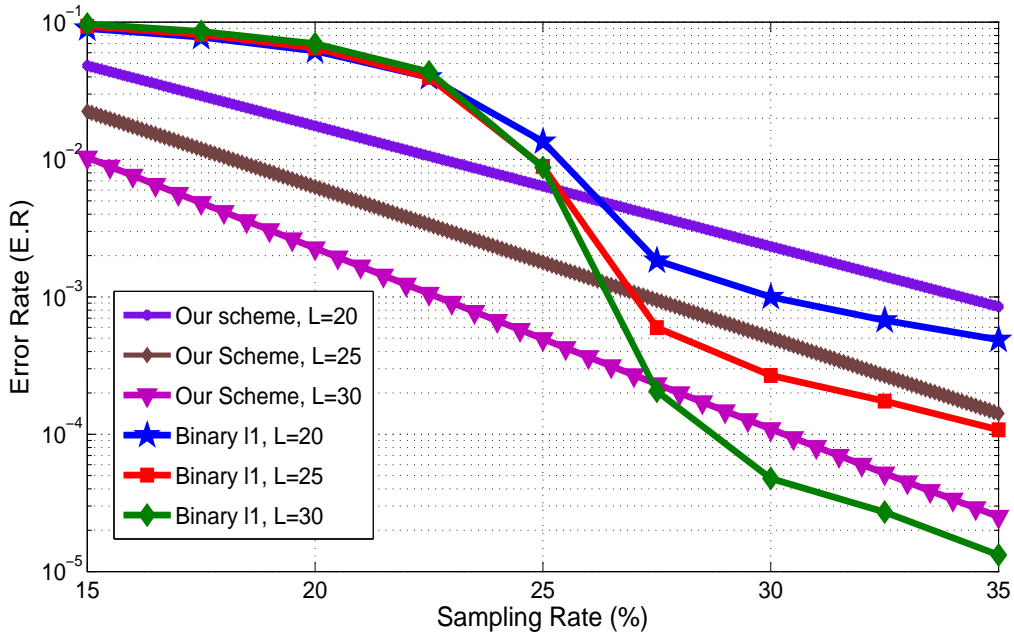


Figure 5.10: Error Rate Comparison with Binary  $l_1$  scheme with threshold

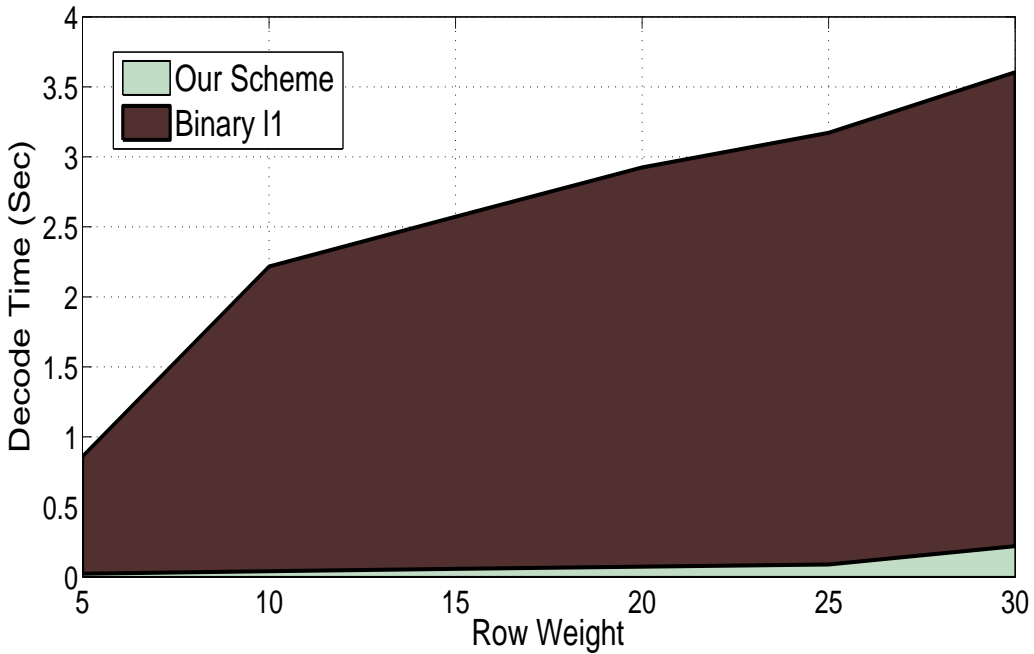


Figure 5.11: Decode Time comparison Binary  $l_1$  scheme with threshold

We can clearly see that for row weight of 30 at low sampling rate of 25%, the error rate of our scheme is in the order of  $10^{-4}$  whereas, the error rate in binary

$l_1$  method is in the order of  $10^{-2}$ . At very low sampling rate our scheme has very good performance rate compared to the binary  $l_1$  scheme. When the sampling rate is increased binary  $l_1$  has slightly better performance than our scheme, however, the error rate in both schemes are in the same order. It should be noted that the error rate in our scheme is solely because of the un-covered  $V - nodes$ . Moreover, Fig. 5.11 shows that our schemes takes comparatively very less time for decoding and small gain in error rate performance is achieved at very high cost of decode time in binary  $l_1$  method.

In the Section 5.3.3, we discussed about the check-sum method and heavy nodes degree  $\beta$ . Large values of  $\beta$ , makes the check sum method computationally complex. However, the iterative edge-recovery and check nodes update process make the heavy nodes degree very small. In the Fig.5.12 we show the maximum beta occurrence rate for  $S = 0.1$ ,  $L = 30$  and  $M = 300$ . The result provided is an average of 10,000 experiments.

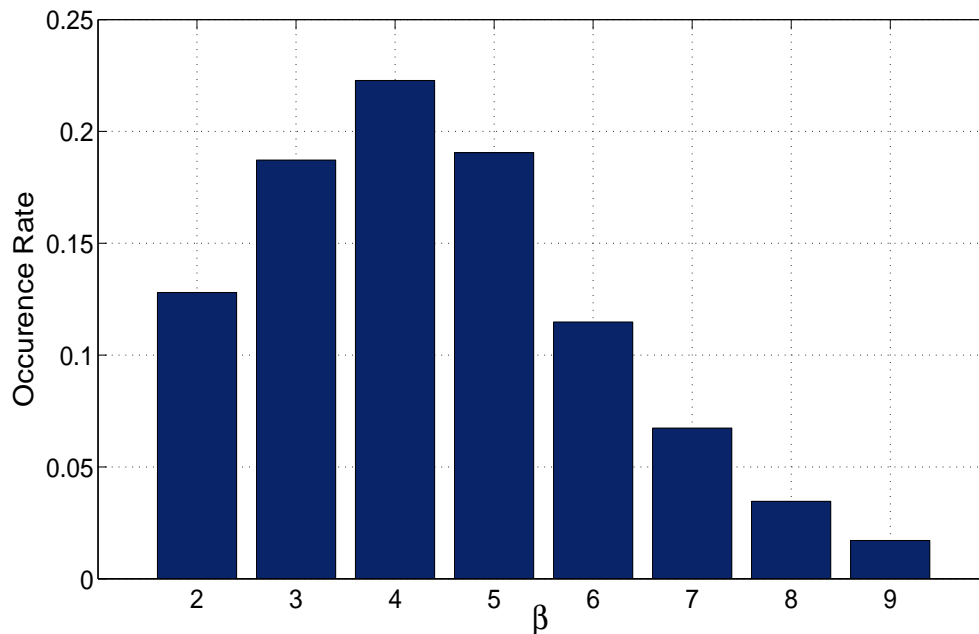


Figure 5.12: Maximum heavy node degree

We can clearly see the distribution of maximum  $\beta$  peaks around 3 – 5. This shows that the iterative edge removal and check nodes update process effectively reduces the heavy check nodes degree and makes check-sum method simple and feasible.

## 5.7 Conclusion

In this chapter, we presented a novel compressive sampling and decoding method for Binary Sparse Signal using Graph and Check-Sum method. We modeled the binary compressive sensing method as the Bipartite graph and implemented the edge recovery scheme. Edge recovery scheme in itself cannot guarantee the complete decoding. To overcome this drawback, we designed a unique sampling matrix for the binary sparse source. We showed that consequences of row weight of sampling matrix in edge recovery as well as overall recovery performance. We also formulated the error rate of our scheme for a given row weight and number of measurements. We compared our scheme with Binary tree recovery method and Binary  $l_1$  method. Binary sparse source is found in many real life applications. For instance, in event detection scheme in wireless sensor network, in spectrum occupancy decision and binary images, the source can be modeled as the binary signal. In these applications, our scheme can find appropriate applications.

## CHAPTER 6

### CONCLUSIONS AND FUTURE WORKS

In this thesis, we have proposed compressive sensing based spectrum sensing for wideband cognitive radio networks. In wideband cognitive radio networks conventional spectrum sensing is less feasible because of the data sampling and acquisition cost. A new paradigm in data sampling and acquisition, called compressive sensing is an effective approach for wideband data sampling. Compressive sensing possess an ability to reconstruct the certain class of compressible original signal from fewer numbers of samples than conventional point-to-point data sampling schemes. Unlike in traditional data compression, compressive sensing not only compresses sampled data, the compression process in itself is embedded in the sampling process. In this light, compressive sensing, in one hand reduces the number of samples and in the other hand it also relaxes the number of sensors and sensing points in the sampling process itself. These features make compressive sensing very feasible and attractive for data acquisition and sampling purposes.

In the Chapter 2, we briefly discussed about the spectrum scarcity and evolution of cognitive radio technique to address spectrum scarcity problem. Various challenges in implementation of cognitive radio such as power constraints, and spectrum sensing is briefly discussed. A brief introduction to spectrum sensing approaches and compressive sensing is discussed. In the chapter 3, we proposed compressive sensing based spectrum sensing for single network cognitive radio system. Proposed wideband compressive sensing based spectrum sensing method has good performance in terms of both detection probability and error in energy of reconstruction. We also investigated



various compressive sensing algorithms and their performance in spectrum sensing.

Compressive sensing based joint spectrum sensing in frequency overlapping networks is proposed in the Chapter 4. In many spectrum sensing schemes the geo-temporal diversity of spectrum occupancy is overseen and all CRs are assumed to be synchronized during sensing period. However, in large networks, this assumption is very optimistic and deviates far from the practical scenario. Frequency overlapping networks also comes into picture in multi-hop networks, multi-band operating devices. We proposed joint spectrum sensing using compressive sensing and developed joint reconstruction scheme for such frequency overlapping network. We exploit the joint sparsity of the overlapped region to have better spectrum sensing performance at minimal cost. Proposed joint spectrum sensing and reconstruction method have shown to perform better than the individual reconstruction and LASSO consensus scheme.

A novel compressive sensing scheme for Binary signals is proposed in the Chapter 5. Binary signals pictures into many practical applications such as detection problems, black and white images, group testing, binary classification etc. We implement the bipartite graphs to represent the binary compressive sensing process. A unique, but universal sampling matrix for binary signal is developed. We first implement edge evolution concept from error control coding to make the bipartite graph less dense and then implement check-sum method to completely decode all the variable nodes in the system. Our proposed scheme stands out from conventional optimization based compressive sensing scheme in terms of both, decoding accuracy and decoding time.

In totality, in this thesis, we have proposed compressive sensing based spectrum sensing for cognitive radio networks and also presented a novel binary compressive sensing scheme. However, there exists ample of space to improve and enhance in future work. Spectrum sensing in multiple Geo-Temporal-Frequency domains can be an interesting new research space to look into. Spectrum diversity can be modeled in

the Geo-Temporal-Frequency domain and their inter relation can be used to enhance the spectrum sensing performance. Our proposed compressive sensing for binary signals can be used in many practical applications such as even detection in wireless sensor networks, binary image sampling and reconstruction, small scale classification problems etc.

### 6.1 Future Works

Current works in spectrum sensing and our work in this area are bounded on the assumption that the spectrum occupancy state is static according to the Geo-temporal and frequency domain. It is considered that if a channel has some occupancy state busy or idle at any region or time, the occupancy state is same at any other location. Besides, the correlation between the channel occupancy state in geographical and temporal region is also not considered. If we model the channel occupancy state and their correlation in geo-temporal or even frequency region then we can exploit this prior correlation information in multi-dimensional spectrum sensing.

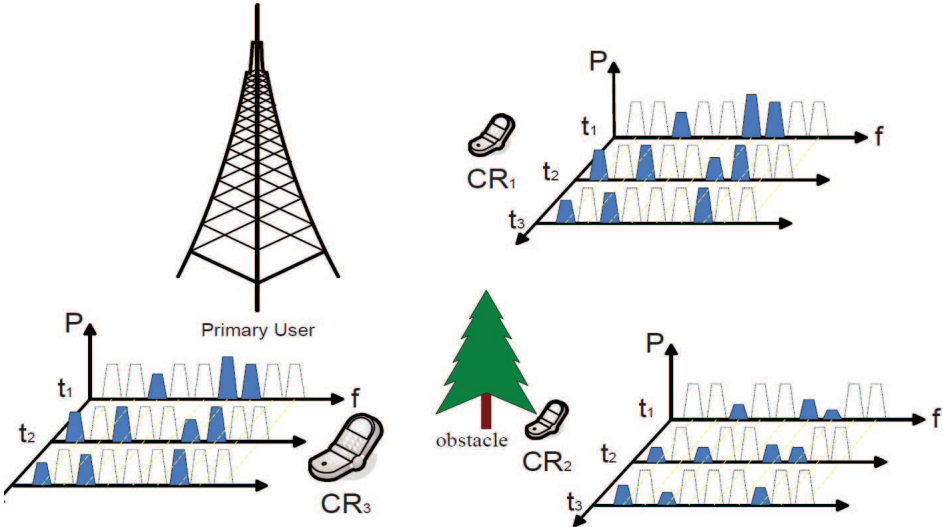


Figure 6.1: Spectrum occupancy state variation in spatio-temporal region

In the Fig. 6.1, we can see that the spectrum state variation according to the ge-

ographical and temporal region [77]. By modeling this correlation between the spatio-temporal spectrum occupancy distribution, multi-dimensional spectrum sensing can be carried out.

In the Chapter 5, we have developed a novel compressive sensing method for binary sparse signal. Binary sparse signal comes into application in many areas such as event detection in wireless sensor networks. In wireless sensor networks, an event is modeled as 1 whereas, no-event is modeled as 0 [65, 66]. In this case, the signal under consideration is Binary sparse signal so our approach can be used in this kind of network for sparse event detection.

The current compressive sensing algorithms based on  $l_1$  minimization process takes longer decoding time as discussed in the Chapter 5. Let us consider a dynamic wireless sensor network where the sensor events changes very rapidly with time as shown in the Fig. 6.2.

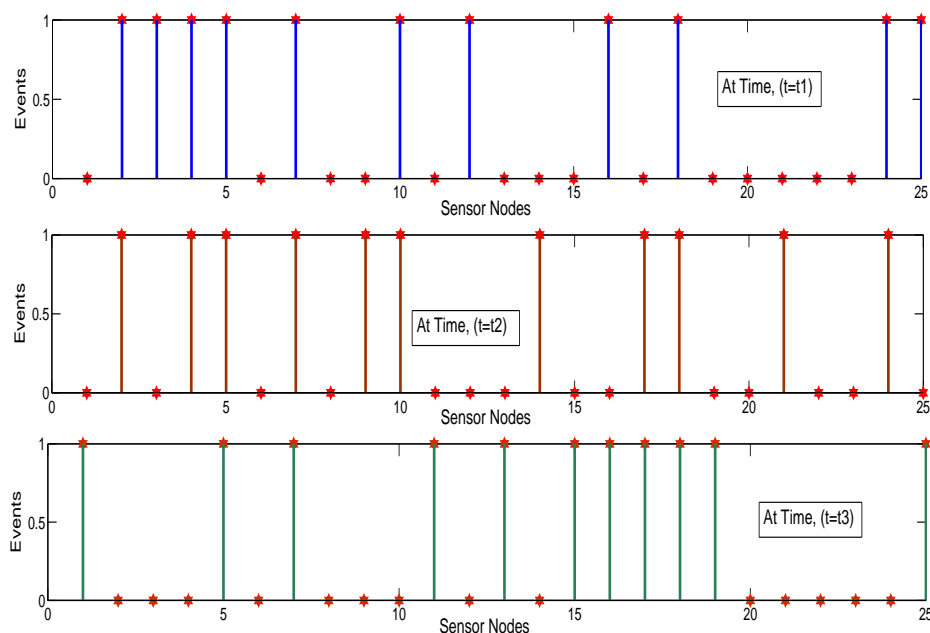


Figure 6.2: Wireless sensor network with dynamic and rapid event changes

When the time difference between the state change in the network is very short, i.e.

$(t_2 - t_1)$  is very short, there is high probability that the optimization based schemes, which takes longer decoding time fail to detect those changes. In these cases, we need very fast decoding approach. In the Chapter 5 we have already shown that our scheme takes comparatively very short decoding time compared to the optimization based schemes. Hence, our scheme can be very beneficial in such scenarios.

## BIBLIOGRAPHY

- [1] FCC, *Spectrum Policy Task Force Report, ET Docket No. 02-155*. Nov 2002.
- [2] S. S. Company, *Spectrum Occupancy Measurements*.
- [3] J. Mitola, *Cognitive radio: An Integrated Agent Architecture for Software Defined Radio*. Doctor of technology, Royal Inst. Technology. (KTH), Stockholm, Sweden, 2000.
- [4] D. Cabric, S. Mishra, and R. W. Brodersen, "Implementation issues in spectrum sensing," *Asilomar Conference on Signal, Systems and Computers*, November 2004.
- [5] A. Sahai, N. Hoven, S. Mishra, and R. Tandra, "Fundamental design tradeoffs in robust spectrum sensing for opportunistic frequency reuse," *Tech. Report*, 2006.
- [6] S. Haykin, "Cognitive radio: Brain empowered wireless communications," *IEEE Journal on selected areas in communications*, vol. 23, February 2005.
- [7] J. Mitola and G. Q. Maguire, "Cognitive radio: Making software radios more personal," *IEEE Personal communications*, pp. 13–18, August 1999.
- [8] J. Sonnenschein and P. M. Fishman, "Radiometric detection of spread spectrum signals in noise of uncertainty power," *IEEE Transactions on Aerospace and Electronic Systems*, vol. 28, no. 3, pp. 654–660, 1992.
- [9] R. Tandra and A. Sahai, "Fundamental limits on detection in low snr under noise uncertainty," *Proceedings of the International Conference on Wireless Networks, Communications and Mobile Computing*, vol. 1, pp. 464–469, 2005.

- [10] R. Tandra and A. Sahai, “snr’ walls for signal detection,” *Journal on Selected Topics in Signal Processing*, vol. 2, no. 1, pp. 4–17, 2008.
- [11] T. Yucek and H. Arslan, “A survey in spectrum sensing algorithms for cognitive radio applications,” *IEEE communications surveys and tutorials*, vol. 11, no. 1, pp. 116–130, 2009.
- [12] J. Proakis, *Digital communications*. McGraw Hill, 4 ed., 2001.
- [13] M. Davenport, M. Wakin, and R. Baraniuk, “Detection and estimation with compressive measurements,” TREE 0610, Rice ECE Department Technical Report, November 2006.
- [14] J. Haupt and R. Nowak, “Compressive sampling for signal detection,” *IEEE Int. Conf. on Acoustics, Speech, and Signal Processing (ICASSP)*, April 2007.
- [15] G. Giannakis, *Cyclostationary Signal Analysis*. Boca Raton: CRC Press LLC, 1999.
- [16] K. Kim, I. Akbar, K. Bae, T. Urn, C. Spooner, and J. Reed, “Cyclostationary approaches to signal detection and classification in cognitive radio,” *IEEE Int. Symposium on New Frontiers in Dynamic Spectrum Access Networks*, 2007.
- [17] C. M. da Silva, B. Choi, and K. Kim, “Distributed spectrum sensing for cognitive radio systems,” *Information Theory and Applications Workshop*, Oct 2007.
- [18] T. Farnham, G. Clemo, R. Haines, E. Seidel, A. Benamar, S. Billington, N. Greco, N. Drew, T. Le, B. Arram, and P. Mangold, “Ist-trust:a perspective on the reconfiguration of future mobile terminals using software download,” in *Proc. IEEE Int. Symposium on Personal, Indoor and Mobile Radio Communication*, pp. 1054–1059, Sept 2000.

- [19] M. Mehta, N. Drew, G. Vardoulas, N. Greco, and C. Niedermeier, "Reconfigurable terminals: an overview of architectural solutions," *IEEE Commun. Mag.*, no. 8, pp. 82–89, 2001.
- [20] G. Vardoulas, J. Faroughi-Esfahani, G. Clemo, and R. Haines, "Blind radio access technology discovery and monitoring for software defined radio communication systems: problems and techniques," *Int. Conf. 3G Mobile Communication Technologies*, pp. 306–310, March 2001.
- [21] Z. Wang, G. Arce, J. Paredes, and B. Sadler, "Compressed detection for ultra-wideband impulse radio," *SPAWC 2007*.
- [22] H. Tang, "Some physical layer issues of wideband cognitive radio systems," *Int. Symposium on New Frontiers in Dynamic Spectrum Access Network*, pp. 151–159, November 2005.
- [23] S. Geirhofer, L. Tong, and B. Sadler, "A measurement based model for dynamic spectrum access in wlan channels," *IEEE Military communication conference*, Oct 2006.
- [24] S. Geirhofer, B. Sadler, and L. Tong, "A measurement based model for dynamic spectrum access in wlan channels: empirical model and stochastic analysis," *Intl. Workshop on technology and policy for accessing spectrum*, Aug 2006.
- [25] D. Cabric, A. Tkachenko, and R. Broderick, "Spectrum sensing measurement of pilot, energy and collaborative detection," *IEEE Military communication conference*, Oct 2006.
- [26] F. Digham, M. Alouni, and M. Simon, "On the energy detection of unknown signal over fading channels," *IEEE conference on communication*, vol. 5, pp. 3575–3679, May 2003.

- [27] A. Ghasemi and E. Sousa, "Optimization of spectrum sensing for opportunistic spectrum access in cognitive radio network," *IEEE consumer communication and networking conference*, pp. 1022–1026, Jan 2007.
- [28] Y. Yuan, P. Bahl, R. Chandra, P. Chau, J. Ferrell, T. Moscibroda, S. Naralanka, and Y. Wu, "KNOWS: Cognitive radio network over white spaces," *IEEE Intl. Symposium on Dynamic Spectrum Access*, pp. 416–427, April 2007.
- [29] B. Nakarmi, "Study on cooperative spectrum sensing for the cognitive radio," Master's thesis, Harbin Engineering University, Harbin, China, June 2008.
- [30] D. Donoho, "Compressed sensing," *IEEE transaction on information theory*, vol. 52, pp. 1289–1306, April 2006.
- [31] R. Baraniuk, "Compressive sensing," *Lecture Notes in IEEE Signal Processing Magazine*, vol. 24, July 2007.
- [32] E. Candes, J. Romberg, and T. Tao, "Robust uncertainty principles: exact signal reconstruction from highly incomplete frequency information," *IEEE Transactions on Information Theory*, vol. 52, no. 2, pp. 489 – 509, 2006.
- [33] Y. Pati, R. Rezaifar, and P. Krishnaprasad, "Orthogonal matching pursuit: Recursive function approximation with application to wavelet decomposition," *In proc. of 27 Annual Asilomar Conference on Signals Systems and Computers*, pp. 1 – 5, Nov 1993.
- [34] J. A. Tropp and A. C. Gilbert, "Signal recovery from random measurements via orthogonal matching pursuit," *IEEE Transactions on Information Theory*, vol. 53, no. 12, pp. 4655 – 4666.
- [35] P. Huber, "Projection pursuit," *The annals of statistics*, vol. 13, pp. 1435–475, 1985.



- [36] D. Needell and J. A. Tropp, “Cosamp: iterative signal recovery from incomplete and inaccurate samples,” *Commun. ACM*, vol. 53, pp. 93–100, December 2010.
- [37] R. G. Baraniuk, V. Cevher, M. F. Duarte, and C. Hegde, “Model-based compressive sensing,” *IEEE Trans. Inf. Theor.*, vol. 56, pp. 1982–2001, April 2010.
- [38] D. Baron, S. Sarvotham, and R. G. Baraniuk, “Bayesian compressive sensing via belief propagation,” *to appear in IEEE Transactions on Signal Processing*, 2009.
- [39] N. Vaswani and W. Lu, “Modified-cs: modifying compressive sensing for problems with partially known support,” in *Proceedings of the 2009 IEEE international conference on Symposium on Information Theory - Volume 1*, (Piscataway, NJ, USA), pp. 488–492, IEEE Press, 2009.
- [40] FCC, “Spectrum policy task force report,” *In Procc. of the Federal communications comissions (FCC’02), Washigton, DC, USA*, Nov 2002.
- [41] M.H.Islam, C.L.Koh, and e. S.W.Oh, “Spectrum survey in singapore: occupancy measurements and analysis,” *Proc. of 3rd International Conference on Cognitive Radio Oriented Wireless Network and Communications (CROWNCOM’08), singapore*, May 2008.
- [42] Q. Zhao and B. Sadler, “A survey of dynamic spectrum access,” *Signal Processing Magazine, IEEE*, vol. 24, pp. 79–89, may 2007.
- [43] L. Grande, “Dynamic spectrum access policy standards work,” in *Military Communications Conference, 2009. MILCOM 2009. IEEE*, pp. 1–4, oct. 2009.
- [44] J. Mitola, *Cognitive radio: An Integrated Agent Architecture for Software Defined Radio*. Doctor of technology, Royal Inst. Technology. (KTH), Stockholm, Sweden, 2000.

- [45] F. Digham, M. Alouni, and M. Simon, "On the energy detection of unknown signal over fading channels," *IEEE conference on communication*, vol. 5, pp. 3575–3679, May 2003.
- [46] G. Vardoulas, J. Faroughi-Esfahani, G. Clemo, and R. Haines, "Blind radio access technology discovery and monitoring for software defined radio communication systems: problems and techniques," *Int. Conf. 3G Mobile Communication Technologies*, pp. 306–310, March 2001.
- [47] I. F. Akyildiz, W.-Y. Lee, M. C. Vuran, and S. Mohanty, "Next generation/dynamic spectrum access/cognitive radio wireless networks: A survey," *Computer Networks*, vol. 50, no. 13, pp. 2127 – 2159, 2006.
- [48] Z.Tian and G. Giannaskis, "Compressed sensing for wideband cognitive radios," *Proc. of International Conference on Acoustic Speech and Signal Processing*, pp. IV/1357–IV/1360, April 2007.
- [49] J.Meng, W.Yin, H.Li, and Z.Han, "Collaborative spectrum sensing for sparse observation using matrix completion for for cognitive radio network," *The 35th International conference on acoustic, speech, and signal processing, (ICASSP)*, 2010.
- [50] Z. Yu, X. Chen, S. Hoyos, B. M. Sadler, J. Gong, and C. Qian, "Mixed-signal parallel compressive spectrum sensing for cognitive radios," *International Journal of Digital Multimedia Broadcasting*, 2010.
- [51] S. Kirolos, J. Laska, M. Wakin, M. Duarte, D. Baron, T. Ragheb, Y. Massoud, and R. Baraniuk, "Analog-to-information conversion via random demodulation," 2006.

- [52] F. Digham, M. Alouni, and M. Simon, "On the energy detection of unknown signal over fading channels," *IEEE conference on communication*, vol. 5, pp. 3575–3679, May 2003.
- [53] E. J. Candes, M. B. Wakin, and S. P. Boyd, "Enhancing sparsity by reweighted l1 minimization," *J Fourier Anal Appl*, vol. 14, pp. 877–905, 2008.
- [54] Z. Zhang, S. Chan, Y. Zhou, and Y. Hu, "Robust linear estimation using estimation and weighted l1 regularization: Model selection and recursive implementation," in *Circuits and Systems, 2009. ISCAS 2009. IEEE International Symposium on*, pp. 1193–1196, may 2009.
- [55] "<http://www.ntia.doc.gov/osmhome/allochrt.pdf>,"
- [56] F. Zeng, C. Li, and Z. Tian, "Distributed compressive spectrum sensing in cooperative multihop cognitive networks," *IEEE Journal of Selected Topics in Signal Processing*, vol. 5, pp. 37–48, Feb 2011.
- [57] U. Nakarmi and N. Rahnavard, "A new approach to spectrum management in cognitive radio networks," *In proc. of International conference on smart technologies for materials, communications, controls, computing and Energy, (ICST)*, pp. 3–7, Jan 2011.
- [58] M. F. Duarte, S. Sarvotham, M. B. Wakin, D. Baron, and R. G. Baraniuk, "Joint sparsity models for distributed compressed sensing," *Online Proceedings of the Workshop on Signal Processing with Adaptive Sparse Structured Representations (SPARS)*, 2005.
- [59] M. F. Duarte, S. Sarvotham, D. Baron, M. B. Wakin, and R. G. Baraniuk, "Distributed compressed sensing of jointly sparse signals," in *Proceedings of the 39th Asilomar Conference on Signals, Systems and Computation*, (Pacific Grove, CA), pp. 1537–1541, Nov. 2005.

- [60] C. Dossal, M.-L. Chabanol, G. Peyré, and J. Fadili, “Sharp support recovery from noisy random measurements by l1 minimization,” *CoRR*, vol. abs/1101.1577, 2011.
- [61] R. Baraniuk, M. Davenport, R. Devore, and M. Wakin, “A simple proof of the restricted isometry property for random matrices,” *Constr. Approx.*, vol. 2008, 2007.
- [62] S. Mallat and Z. Zhang, “Matching pursuit with time-frequency dictionaries,” *IEEE Transactions on Signal Processing*, vol. 41, pp. 3397–3415, 1993.
- [63] Z. Li, F. Wu, and J. Wright, “On the systematic measurement matrix for compressed sensing in the presence of gross errors,” in *Proceedings of the 2010 Data Compression Conference*, (Washington, DC, USA), pp. 356–365, IEEE Computer Society, 2010.
- [64] A. Amini and F. Marvasti, “Deterministic construction of binary, bipolar and ternary compressed sensing matrices,” *CoRR*, vol. abs/0908.2676, 2009.
- [65] J. Meng, H. Li, and Z. Han, “Sparse event detection in wireless sensor networks using compressive sensing,” in *43rd Annual Conference on Information Sciences and Systems, 2009. CISS 2009.*, pp. 181 –185, march 2009.
- [66] J. Meng, W. Yin, H. Li, E. Houssain, and Z. Han, “Collaborative spectrum sensing from sparse observations using matrix completion for cognitive radio networks,” in *2010 IEEE International Conference on Acoustics Speech and Signal Processing (ICASSP)*, pp. 3114 –3117, march 2010.
- [67] M. Stojnic, “Recovery thresholds for l1 optimization in binary compressed sensing,” *International symposium in information technology (ISIT).*, pp. 1593–1596, June 13-18 2010.

- [68] J. Wen, Z. Chen, S. Yang, Y. Han, and J. D. Villasenor, “Reconstruction of sparse binary signals using compressive sensing,” in *Proceedings of the 2010 Data Compression Conference, DCC '10*, (Washington, DC, USA), pp. 556–, IEEE Computer Society, 2010.
- [69] E. J. Candes, M. B. Wakin, and S. P. Boyd, “Enhancing sparsity by reweighted  $\ell_1$  minimization,” *J Fourier Anal Appl (2008)*., pp. 877–905, 2008.
- [70] O. L. Mangasarian and B. Recht, “Probability of unique integer solution to a system of linear equations,” *European Journal of Operational Research*, doi:10.1016/j.ejor.2011.04.010, 2011.
- [71] S. Sarvotham, D. Baron, and R. G. Baraniuk, “Sudocodes – fast measurement and reconstruction of sparse signals,” in *IEEE International Symposium on Information Theory – ISIT*, (Seattle), Jul. 2006.
- [72] F. Wu, J. Fu, Z. Lin, and B. Zeng, “Analysis on rate-distortion performance of compressive sensing for binary sparse source,” in *Proceedings of the 2009 Data Compression Conference*, (Washington, DC, USA), pp. 113–122, IEEE Computer Society, 2009.
- [73] J. Fu, Z. Lin, B. Zeng, and F. Wu, “Tree structure based analyses on compressive sensing for binary sparse sources,” in *Proceedings of the 2010 Data Compression Conference, DCC '10*, (Washington, DC, USA), pp. 530–, IEEE Computer Society, 2010.
- [74] M. Luby, M. Mitzenmacher, M. Shokrollahi, and D. Spielman, “Efficient erasure correcting codes,” *IEEE Transactions on Information Theory*., vol. 47, pp. 569–584, feb 2001.
- [75] N. C. Wormald, “Differential equations for random processes and random graphs,” *The Annals of Applied Probability*, vol. 5, pp. 1217–1235, Nov 1995.

- [76] A. Shokrollahi, “Raptor codes,” *IEEE Transactions on Information Theory*, vol. 52, pp. 2551–2567, June 2006.
- [77] Z. Zhang, H. Li, D. Yang, and C. Pei, “Space-time bayesian compressed spectrum sensing for wideband cognitive radio networks,” pp. 1–11, april 2010.

## VITA

Ukash Nakarmi

Candidate for the Degree of

Master of Science

Thesis: COMPRESSIVE SPECTRUM SENSING FOR COGNITIVE RADIO NETWORKS

Major Field: Electrical Engineering

Biographical:

Personal Data: Born in Kathmandu, Bagmati, Nepal on August 26, 1985.

Education:

Received the B.E. degree from Tribhuwan University, Kathmandu, Bagmati, Nepal, 2008, in Electronics and Communication

Completed the requirements for the degree of Master of Science with a major in Electrical Engineering Oklahoma State University in Dec, 2011.

Experience:

- Graduate Research Assistant, Communications and Wireless Networks Lab, OSU, USA
- Lecturer, National College of Engineering, Tribhuwan University, Nepal
- Design Engineer, Dream and Devise, Kathmandu, Nepal

Name: Ukash Nakarmi

Date of Degree: Dec, 2011

Institution: Oklahoma State University

Location: Stillwater, Oklahoma

Title of Study: COMPRESSIVE SPECTRUM SENSING FOR COGNITIVE RADIO NETWORKS

Pages in Study: 94

Candidate for the Degree of Master of Science

Major Field: Electrical Engineering

Spectrum sensing is the most important part in cognitive radios. Wideband spectrum sensing requires high speed and large data samples. It makes sampling process challenging and expensive. In this thesis, we propose wideband spectrum sensing for cognitive radio using compressive sensing to address challenges in sampling and data acquisition during spectrum sensing. Compressive sensing based spectrum sensing for a single network is extended to large frequency overlapping networks and joint reconstruction scheme is developed to enhance the performance at minimal cost. The joint sparsity in large networks is used to improve the compressive sensing reconstruction in large networks. Further, a novel compressive sensing method for binary signal is proposed. Unlike general compressive sensing solution based on optimization process, a simple, reliable and quick compressive sensing method for binary signal using bipartite graph, edge recovery and check-sum method is developed. The proposed models and methods have been verified, proved and compared with existing approaches through numerical analysis and simulations.

ADVISOR'S APPROVAL: \_\_\_\_\_